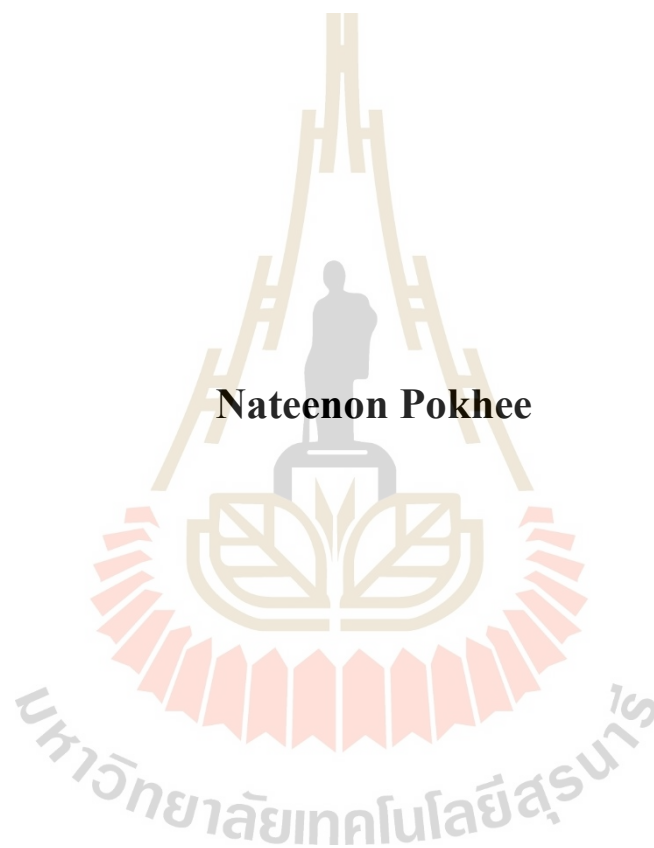


**MECHANICAL PERFORMANCES OF CONSOLIDATED
SLUDGE-CRUSHED SALT MIXTURES AS BACKFILL
MATERIALS IN SALT MINE**



Nateenon Pokhee

**A Thesis Submitted in Partial Fulfillment of the Requirements for the
Degree of Doctor of Philosophy of Engineering in Civil,
Transportation and Geo-Resources Engineering
Suranaree University of Technology
Academic Year 2020**

ศักราชเชิงกลของดินตะกอนประปาสมเกลือบดภายใต้การอัดตัวคายน้ำ
สำหรับเป็นวัสดุอุดในเหมืองเกลือ



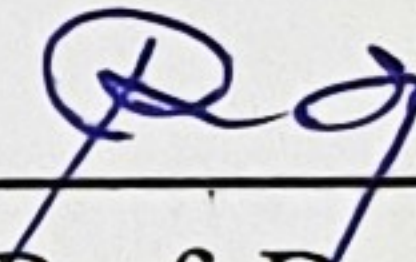
นายณรินทร์ โพธิ์จี

วิทยานิพนธ์นี้เป็นส่วนหนึ่งของการศึกษาตามหลักสูตรปริญญาวิศวกรรมศาสตรดุษฎีบัณฑิต
สาขาวิชาวิศวกรรมโยธา ขนส่ง และทรัพยากรธรณี
มหาวิทยาลัยเทคโนโลยีสุรนารี
ปีการศึกษา 2563

**MECHANICAL PERFORMANCES OF CONSOLIDATED
SLUDGE-CRUSHED SALT MIXTURES AS BACKFILL
MATERIALS IN SALT MINE**

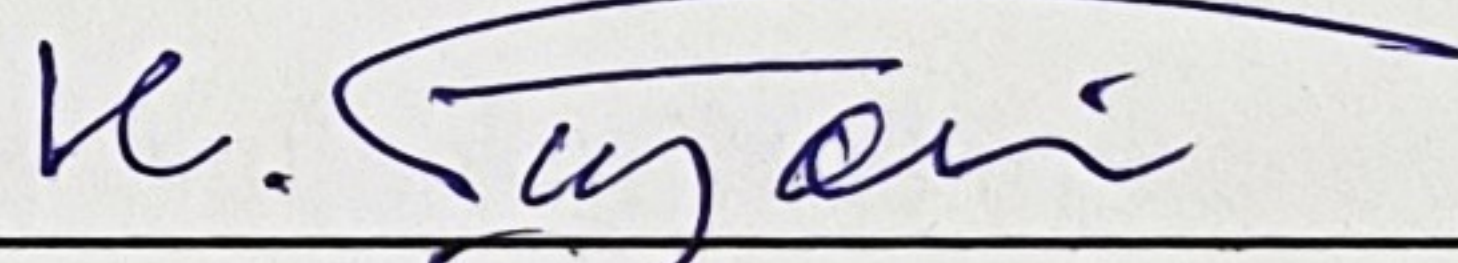
Suranaree University of Technology has approved this thesis submitted in partial fulfillment of the requirements for the Degree of Doctor of Philosophy.

Thesis Examining Committee



(Assoc. Prof. Dr. Pornkasem Jongpradist)

Chairperson



(Prof. Dr. Kittitep Fuenkajorn)

Member (Thesis Advisor)



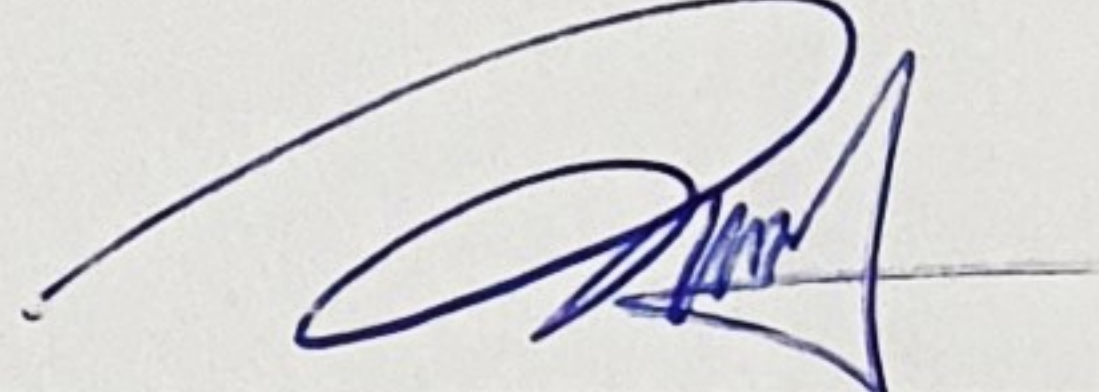
(Asst. Prof. Dr. Prachya Tepnarong)

Member



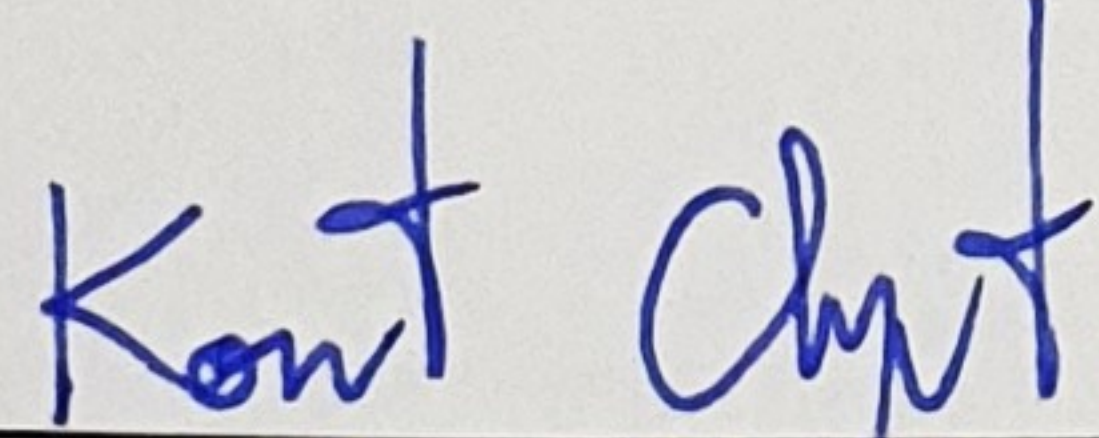
(Asst. Prof. Dr. Decho Phueakphum)

Member

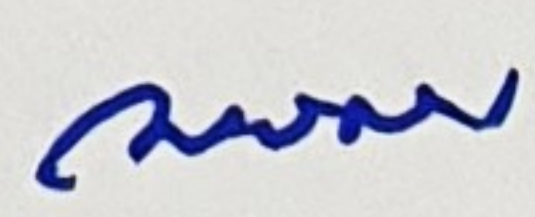


(Asst. Prof. Dr. Akkhapun Wannakomol)

Member



(Assoc. Prof. Flt. Lt. Dr. Kontorn Chamniprasart)



(Assoc. Prof. Dr. Pornsiri Jongkol)

Vice Rector for Academic Affairs
and Innovation

Dean of Institute of Engineering

ณรินทร์ โพธิ์ : ศักยภาพเชิงกลของดินตะกอนประปาผสมเกลืออบภายใต้การอัดตัวคาย
น้ำสำหรับเป็นวัสดุถมในเหมืองเกลือ (MECHANICAL PERFORMANCES OF
CONSOLIDATED SLUDGE-CRUSHED SALT MIXTURES AS BACKFILL
MATERIALS IN SALT MINE) อาจารย์ที่ปรึกษา : ศาสตราจารย์ ดร.กิตติเทพ เฟื่องขจร,
96 หน้า.

ศักยภาพเชิงกลของส่วนผสมดินตะกอนประปาและเกลืออบภายใต้การอัดตัวคายน้ำได้ถูก
หาเพื่อใช้เป็นวัสดุถมกลับในเหมืองแร่เกลือ ส่วนผสมของดินตะกอนประปาต่อเกลือบดชุดหิน
มหาสารคามที่มีอัตราส่วนเชิงน้ำหนักจาก 30:70 ถึง 70:30 ได้ถูกบดอัดเพื่อหาปริมาณน้ำเกลือที่
เหมาะสม จากนั้นตัวอย่างที่ถูกบดอัดได้ถูกอัดตัวคายน้ำภายใต้ความเค้นคงที่จาก 2.5 ถึง 10 เมกะ
ปาสกาล เป็นระยะเวลา 30 วัน ผลการศึกษาชี้ให้เห็นว่าอัตราความเครียดของส่วนผสมที่มีดิน
ตะกอนประปาร้อยละ 70 มีแนวโน้มที่ไม่ขึ้นกับเวลา ส่วนผสมของเกลือบดกับดินตะกอนประปา
สามารถลดอัตราการอัดตัวคายน้ำในระยะยาวได้ ค่าความหนาแน่น กำลังรับแรงกด สัมประสิทธิ์
ความยืดหยุ่นและอัตราส่วนปัวส์ซองของส่วนผสมมีค่าลดลงเมื่อเพิ่มปริมาณดินตะกอนประปา
และเพิ่มขึ้นตามความเค้นกดและระยะเวลาในการอัดตัวคายน้ำที่เพิ่มขึ้น ชุดสมการเชิงประจักษ์ที่
สัมพันธ์กับคุณสมบัติของส่วนผสมดินตะกอนประปาและเกลือบด กับค่าความหนาแน่นพลังงาน
ความเครียดเฉลี่ยได้ถูกพัฒนาเพื่อใช้คาดคะเนคุณสมบัติเชิงกลของส่วนผสมภายหลังการติดตั้งใน
ช่องเปิดภายใต้ความเค้นในที่ (ความลึก) ความลึกของการติดตั้ง และระยะเวลาได้รับการพิสูจน์ว่า
เป็นปัจจัยสำคัญที่ควบคุมความหนาแน่น กำลังรับแรงกดและสัมประสิทธิ์ความยืดหยุ่นในระยะยาว
ของวัสดุถมกลับ

สาขาวิชา เทคโนโลยีธรณี
ปีการศึกษา 2563

ลายมือชื่อนักศึกษา Natton
ลายมือชื่ออาจารย์ที่ปรึกษา K. Sorn

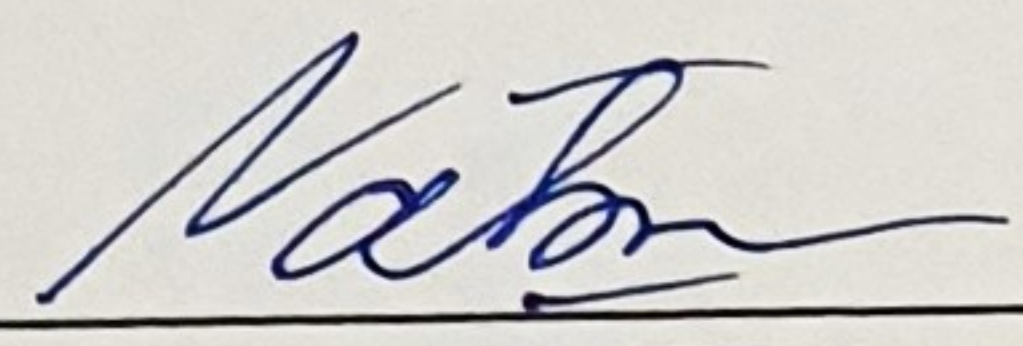
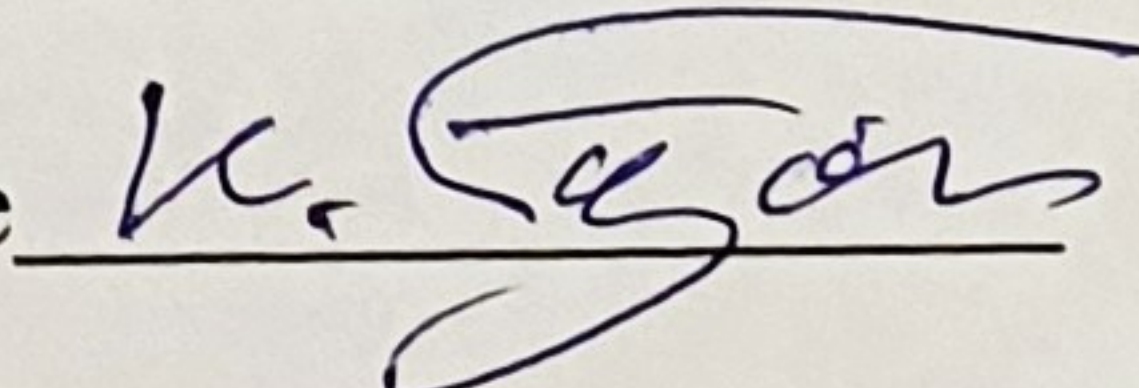
NATEENON POKHEE : MECHANICAL PERFORMANCES OF
CONSOLIDATED SLUDGE-CRUSHED SALT MIXTURES AS
BACKFILL MATERIALS IN SALT MINE . THESIS ADVISOR :
PROF. KITTITEP FUENKAJORN, Ph.D., 96 PP.

ROCK SALT/BRINE/COMPACTION/STRAIN ENERGY/STRENGTH

Mechanical performance of consolidated sludge-crushed salt mixtures is determined for use as backfilling material in salt mine. The sludge-to-Maha Sarakham crushed salt mixtures having weight ratios from 30:70 to 70:30 are compacted to determine their optimum brine contents. The compacted specimens are then consolidated under constant stresses from 2.5 to 10.0 MPa for up to 30 days. The results indicate that strain rates of 70% sludge mixtures have a tendency of time independent. Mixing crushed-salt with sludge can reduce long-term consolidation rate of the mixtures. The density, compressive strengths, elastic moduli and Poisson's ratios of the mixtures decrease with increasing sludge contents and increase with consolidation stress and period. A set of empirical equations relating the sludge-crushed salt properties with applied mean strain energy density is developed to predict the mechanical properties of mixture after installation in the openings under various in-situ stresses (depths). The installation depth and the time are proved to be significant factors controlling long-term density, strength and elasticity of sludge-crushed salt backfill.

School of Geotechnology

Academic Year 2020

Student's Signature 
Advisor's Signature 

ACKNOWLEDGMENTS

I would like to express my deep gratitude to my advisor, Prof. Dr. Kittitep Fuenkajorn, for his motivation and encouragement throughout of my graduate education. I have received a lot of academic advice and valuable experiences from him. In addition, he guided me with meaningful attitude for learning and living. My appreciation also extends to Assoc. Prof. Dr. Pornkasem Jongpradist, Asst. Prof. Dr. Akkhapun Wannakomol, Asst. Prof. Dr. Prachya Tepnarong and Asst. Prof. Dr. Decho Phueakphum for their constructive advice, insightful suggestions, and comments on my research as thesis committee members.

I would like to acknowledge Suranaree University of Technology (SUT) for financial support that giving me an opportunity in engineering study and for providing workplaces with facilities. I wish to thank all lectures of School of Geotechnology for a warm learning atmosphere that make me be a better and more confident learner.

I thank all staffs of Geomechanics Research Unit, Institute of Engineering who always supported my work experiments in laboratory.

Last, the grateful thank are also extended to my parents, my brother and other family members for their unconditional love and spiritual support on all situation in my life.

Nateenon Pokhee

TABLE OF CONTENTS

	Page
ABSTRACT (THAI).....	I
ABSTRACT (ENGLISH)	II
ACKNOWLEDGMENTS	III
TABLE OF CONTENTS.....	IV
LIST OF TABLES.....	VIII
LIST OF FIGURES	IX
SYMBOLS AND ABBREVIATIONS.....	XIV
CHAPTER	
I INTRODUCTION.....	1
1.1 Background.....	1
1.2 Objectives	2
1.3 Scope.....	3
1.4 Research methodology.....	4
1.4.1 Literature review	4
1.4.2 Sludge-crushed salt preparation.....	4
1.4.3 Compaction test	5
1.4.4 Consolidation test.....	5
1.4.5 Direct shear test.....	6
1.4.6 Uniaxial compression test.....	6
1.4.7 Physical measurements	6

TABLE OF CONTENTS (Continued)

	Page
1.4.8 Scanning electron microscope investigation.....	6
1.4.9 Empirical equations derivation	7
1.4.10 Analytical solutions	7
1.4.11 Discussions and conclusions.....	7
1.4.12 Thesis writing.....	7
1.5 Thesis contents.....	8
II LITERATURE REVIEW.....	9
2.1 Introduction.....	9
2.2 Basic properties of sludge.....	9
2.3 Mechanical properties of crushed salt.....	14
2.4 Compaction test	18
2.5 Direct shear test.....	23
2.6 Mechanical properties of consolidation backfill material	26
III SAMPLE PREPARATION.....	32
3.1 Introduction.....	32
3.2 Test materials	32
3.2.1 Sludge	32
3.2.2 Crushed salt.....	33
3.2.3 Saturated brine	33
3.3 Sludge-crushed salt mixture preparation	37

TABLE OF CONTENTS (Continued)

	Page
IV LABORATORY TESTING	38
4.1 Introduction.....	38
4.2 Compaction test	38
4.2.1 Test method.....	38
4.2.2 Compaction test results	39
4.3 Direct shear test.....	40
4.3.1 Test method.....	40
4.3.2 Direct shear test results	42
4.4 Consolidation test.....	44
4.4.1 Test method.....	44
4.4.2 Consolidation test and results	45
4.5 Uniaxial compressive strength test	47
4.5.1 Test method.....	47
4.5.2 Uniaxial compression test results.....	48
4.6 Scanning electron microscopy analysis	55
4.6.1 Test method.....	55
4.6.2 Test results	56
V DEVELOPMENT OF EMPIRICAL EQUATIONS	60
5.1 Introduction.....	60
5.2 Mean strain energy density of sludge-crushed salt mixtures.....	60

TABLE OF CONTENTS (Continued)

	Page
5.2.1 Sludge-crushed salt density.....	60
5.2.2 Sludge-crushed salt strength	62
5.2.3 Elastic modulus of sludge-crushed salt.....	62
5.2.4 Sludge-crushed salt poisson's ratio.....	63
VI PREDICTION OF BACKFILL PROPERTIES AFTER EMPLACEMENT	70
6.1 Introduction.....	70
6.2 Circular opening in salt and potash media under uniform external pressure.....	70
6.3 Sludge-crushed salt properties after emplacement	76
VII DISCUSSIONS AND CONCLUSIONS	88
7.1 Discussions	88
7.2 Conclusions.....	93
7.3 Recommendations for futures studies.....	96
REFERENCES	97
BIOGRAPHY	110

LIST OF TABLES

Table		Page
3.1	Chemical compositions of the tested sludge and crushed salt.....	34
3.2	Particle shape identification for aggregates given by Powers (1982).....	36
4.1	Results of compaction test.....	40
4.2	Direct shear test results.....	44
4.3	Uniaxial compressive test results.....	54
4.4	SEM images of specimen under different consolidation stresses (σ_{cons}) at consolidation time (t) 30 days.....	58
5.1	Parameters of density relationship ($S_{\%}$ = Sludge content by weight).....	61
5.2	Parameters of equation (5.4) ($S_{\%}$ = Sludge content by weight).....	63
5.3	Parameters of elastic modulus, time and energy relationship ($S_{\%}$ = Sludge content by weight).....	64
5.4	Parameters of Poisson's ratio relationship ($S_{\%}$ = Sludge content by weight).....	65
6.1	Material parameters of Maha Sarakham salt with different carnallite contents (Wilalak and Fuenkajorn, 2016; Luangthip et al., 2016).....	73

LIST OF FIGURES

Figure		Page
1.1	Research methodology	5
2.1	Shear consolidations at $\sigma_1 = 5$ MPa and $\sigma_3 = 1$ MPa (Hansen, 1997).....	16
2.2	Shear consolidations at $\sigma_1 = 6$ MPa and $\sigma_3 = 2$ MPa (Hansen, 1997).....	16
2.3	Volumetric strain and brine flow as function of time (Hansen and Mellegard, 2002).....	17
2.4	Compaction as a function of water content and particle size gradation (Ran and Deamen, 1995).....	19
2.5	Effect of cation valance on the maximum dry density and optimum water content (Shariatmadari et al., 2011).....	20
2.6	Three-ring compaction mold (Sonsakul and Fuengkajorn, 2013).....	21
2.7	SEM on are dried samples at magnification factors of 75x; a) sand 100%, b) bentonite 5% and c) bentonite 50% (Proia et al., 2016).....	23
2.8	Compaction test results (Sonsakul et al., 2013).....	24
2.9	Reduction in porosity of crushed salt due to creep consolidation at various seal lacion-permain basin repository (Kelsall et al., 1984).....	27
2.10	The volumetric strains vs. time. (O'kelly, 2004).....	29
2.11	Consolidation crushed salt with NaCl solution (a) (Khamrat et al., 2017) and with MgCl ₂ solution (b) (Suwannabut et al., 2020).....	31
3.1	Particle size distributions of sludge and crushed salt.....	34

LIST OF FIGURES (Continued)

Figure	Page
3.2	Examples of salt grains for various size ranges..... 35
3.3	Standard chart for roundness and sphericity of sedimentary particles (Powers, 1982)..... 36
4.1	Dry density as a function of brine content (W_b)..... 40
4.2	Direct shear test frame for three-ring mold (Sonsakul and Fuenkajorn, 2013)..... 42
4.3	Shear stress (a) and normal displacement (b) for different shear displacement..... 43
4.4	Shear strength as a function of normal stress..... 44
4.5	Test arrangement for consolidation testing..... 45
4.6	Axial (consolidation) strain (ϵ_{cons}) as a function of time (t) for different consolidation stresses (σ_{cons}). Dash lines indicate time at which each specimen is removed from three-ring mold..... 46
4.7	Sludge-crushed salt mixture specimens after consolidation..... 47
4.8	Uniaxial compressive strength device..... 48
4.9	Some post-tested sludge-crushed salt mixture specimens after uniaxial compressive strength testing..... 49
4.10	Uniaxial stress-strain curves of specimens after consolidation time (t) for consolidation stresses (σ_{cons}) 2.5 MPa..... 50

LIST OF FIGURES (Continued)

Figure	Page
4.11 Uniaxial stress-strain curves of specimens after consolidation time (t) for consolidation stresses (σ_{cons}) 5.0 MPa.....	50
4.12 Uniaxial stress-strain curves of specimens after consolidation time (t) for consolidation stresses (σ_{cons}) 7.5 MPa.....	51
4.13 Uniaxial stress-strain curves of specimens after consolidation time (t) for consolidation stresses (σ_{cons}) 10.0 MPa.....	51
4.14 Density (ρ) as a function of consolidation time (t) for different consolidation stresses (σ_{cons}).....	52
4.15 Uniaxial compressive strengths (σ_c) as a function of consolidation time (t) for different consolidation stresses (σ_{cons}).....	52
4.16 Elastic modulus (E) as a function of consolidation time (t) for different consolidation stresses (σ_{cons}).....	53
4.17 Poisson's ratio (ν) as a function of consolidation time (t) for different consolidation stresses (σ_{cons}).....	53
4.18 JEOL JSM-6010LV scanning electron microscope used in this study.....	56
4.19 Some specimens prepared for scanning electron microscope (SEM).....	56
5.1 Density (ρ) in terms of mean strain energy (W_m) for different consolidation time (t).....	66

LIST OF FIGURES (Continued)

Figure	Page
5.2	Uniaxial compressive strengths (σ_c) increases with increasing mean strain energy (W_m) for different consolidation time (t)..... 67
5.3	Elastic modulus (E) increases with increasing mean strain energy (W_m) for different consolidation periods (t)..... 68
5.4	Poisson's ratio (ν) decreases with increasing mean strain energy (W_m) for different consolidation periods (t)..... 69
6.1	Mean strain energy density (W_m) released from time-dependent deformation of pure salt openings under different external pressures (P_o)..... 75
6.2	Mean strain energy density (W_m) released from time-dependent deformation of openings in potash with different carnallite contents (C%)..... 75
6.3	Remaining strain energy density (ΔW_m) as a function of time after backfill emplacement in salt (a) and potash (b) at year 3..... 79
6.4	Density of different sludge content backfill as a function of time after emplacement..... 80
6.5	Density of different sludge content backfill as a function of time after emplacement in salt mass with different carnallite contents..... 81
6.6	Uniaxial compressive strength of different sludge content backfill as a function of time after emplacement in salt opening..... 82

LIST OF FIGURES (Continued)

Figure	Page
6.7 Uniaxial compressive strength of different sludge content backfill as a function of time after emplacement in salt with different carnallite contents	83
6.8 Elastic modulus of different sludge content backfill as a function of time after emplacement in salt openings	84
6.9 Elastic modulus of different sludge content backfill as a function of time after emplacement in salt with for different carnallite contents	85
6.10 Poisson's ratios of different sludge content backfill in terms of time which install after emplacement in salt openings	86
6.11 Poisson's ratios of different sludge content backfill as a function of time after emplacement in salt with different carnallite contents	87

SYMBOLS AND ABBREVIATIONS

ε_r^c	=	the radial strain in creep mode caused by the time-dependent closure of the opening wall
ε_r^e	=	the radial strain in elastic mode
β	=	Material constant for equation (5.2)
φ	=	Material constant for equation (5.6)
γ	=	Material constant for equation (5.6)
ω	=	Material constant for equation (5.8)
δ	=	Material constant for equation (5.4)
ν	=	Poisson's ratio
ρ	=	Density
α	=	Material constant for equation (5.2)
χ	=	Material constant for equation (5.4)
ρ_{Brine}	=	Density of saturated brine
σ_c	=	Uniaxial compressive strengths
σ_{cons}	=	Consolidation stresses
ρ_{dry}	=	Dry density
ΔE_{cons}	=	The increase of elastic modulus during consolidation
$\rho_{\text{H}_2\text{O}}$	=	Density of water
ΔL	=	length change overtime
ρ_{max}	=	Maximum density

SYMBOLS AND ABBREVIATIONS (Continued)

ρ_{wet}	=	Wet density
Δv_{cons}	=	Decrease of Poisson's ratio caused by the strain energy
$\Delta \rho_{\text{cons}}$	=	Reduction of density caused by the increase of strain energy
$\Delta \sigma_{\text{cons}}$	=	Strength increase due to consolidation
$\Delta W_{m,s}$	=	Released strain energy as a function of time after excavation.
A	=	Area of sample for equation (4.4)
a	=	Material constant for equation (5.2)
a	=	Radius for equation (6.2-6.3)
b	=	Material constants for equation (5.4)
c	=	Cohesion
c	=	Material constants for equation (5.6)
C%	=	Carnallite contents
CBR	=	California bearing ratio
c_u	=	Coefficient of Uniformity
d	=	Material constants for equation (5.8)
d_n	=	Normal displacement
d_s	=	Shearing displacement
E, E_{sec}	=	Elastic modulus
EDS	=	Energy-dispersive X-ray spectroscopy analysis
E_{initial}	=	Initial elastic modulus
F	=	Sheared force for equation (4.4)
FS	=	fine sand

SYMBOLS AND ABBREVIATIONS (Continued)

GIM	=	Electrical grounding improvement material
J	=	Compaction energy per unit volume for equation (4.1)
L	=	Height of hammer drop for equation (4.1)
L	=	Initial length
LL	=	Liquid limit
MgCl ₂	=	Magnesium chloride
MH	=	High-plasticity silt
ML	=	Low-plasticity silt
MS	=	Medium sand
MWA	=	Metropolitan Waterworks Authority of Thailand
n	=	Number of blows per layer for equation (4.1)
NaCl	=	Sodium chloride
P	=	Normal load for equation (4.5)
P _i	=	Constant internal pressures
PI	=	Plasticity index
PL	=	Plastic Limit
P _o	=	Constant external pressures
q _u	=	Unconfined compressive strength
r	=	Radial distance from the opening center
S%	=	Sludge content by weight
S:C	=	Ratios of sludge-crushed salt mixtures
SB	=	Solubility of salt in dissolved water
SEM	=	Scanning electron microscope Analysis

SYMBOLS AND ABBREVIATIONS (Continued)

SG	=	Specific gravity
SG _{brine}	=	Specific gravity of saturated brine
SL	=	Shrinkage limit
SP	=	Poorly graded sand
S _r	=	Radial stress deviation
SS	=	Municipal sewage sludge
t	=	Number of layers for equation (4.1)
t	=	Consolidation time
t ₀	=	Time at which loading is applied
t ₁	=	Time at which the strains are calculated.
t _B	=	Time at which the backfill is installed
t _i	=	Any selected period
UCS	=	Unconfined compressive strength
V	=	Volume of mold for equation (4.1)
W	=	Weight of hammer for equation (4.1)
W ₁	=	Weight of wet soil and container
W ₂	=	Weight of dry soil and container
W _b	=	NaCl Brine content
W _{can}	=	Weight of container
W _i	=	Initial water content
WIPP	=	Waste Isolation Pilot Plant
W _m	=	Mean strain energy density

SYMBOLS AND ABBREVIATIONS (Continued)

$W_{m,l}$	=	Energy lost due to time-dependent deformation before backfill installation
$W_{m,s}$	=	Strain energy released by the creep closure
XRD	=	X-Ray diffraction
XRF	=	X-ray fluorescence
ϑ	=	Material constant for equation (5.8)
Δt	=	Duration for consolidation
$\Delta W_{m,s}$	=	Remaining strain energy
β'	=	Material constants of the potential creep law
ϵ_{cons}	=	Consolidation strain
$\epsilon_{ax}, \epsilon_{axial}$	=	Axial strain of consolidated sludge-crushed salt mixture
ϵ_r	=	Radial strain
ϵ_z	=	Axial strain
ϵ_θ	=	Tangential strain
ϕ	=	Internal friction angle
γ'	=	Material constant of the potential creep law
κ'	=	Material constant of the potential creep law
ν	=	Possion's ratio
$\nu_{initial}$	=	Initial Possion's ratio
$\rho_{initial}$	=	Initial density before apply mean strain energy
σ^*	=	Equivalent (effective) stress

SYMBOLS AND ABBREVIATIONS (Continued)

v_{initial}	=	Initial Poisson's ratio
ρ_{initial}	=	Initial density before apply mean strain energy
σ^*	=	Equivalent (effective) stress
σ_{cons}	=	Consolidation stresses
σ_{initial}	=	Initial strength before applying the mean strain energy
σ_r	=	Radial stresses
σ_z	=	Axial stresses
σ, σ_n	=	Normal stress
σ_θ	=	Tangential stresses
τ	=	Shear stress

CHAPTER I

INTRODUCTION

1.1 Background

Underground salt and potash mines can cause severe environment impact such as initiate surface subsidence and sinkholes owing to creep deformation of support pillars and mine roof. The problem may have adverse effects on engineering structures and natural resources on ground surface. While the mining industry produces several types of waste, such as mill tailing, waste salt, and sludge (Aubertin et al., 2002). One of the remediation methods is to return the waste salt to the mined-out openings to reduce roof and pillar deformations. The placement of waste crushed salt as backfill in salt and potash mines has two environmental purposes: avoidance of surface tailing piles and reduction of ground control and subsidence problems. Crushed salt has been widely recognized as one of the most suitable materials in salt and potash mines (Case and Kelsall, 1987; Holcomb and Hannum, 1982; Wang, et al., 1996; Holcomb and Shields, 1987; Hansen et al., 1993). Its primary advantages are the availability, low cost and chemical compatibility with host rock (Stormont and Finley, 1996). The volumetric strain and density of crushed salt can increase with consolidation periods and stresses (Somtong, et al., 2015). Over prolonged periods, crushed salt is expected to gradually reconsolidate into a material comparable to intact rock salt (Salzerk et al., 2007). Backfilling with crushed salt may however lead to large time-dependent deformation of the openings because it can consolidate significantly under applied load induced by opening convergence (Miao et al., 1995). One of the solutions used internationally in

mining industry is to mix bentonite and crushed salt as a backfill material. The bentonite is, however, expensive and can be highly consolidated even under low loading. Additional geologic materials, such as sand, gravel or sludge, have been considered to mix with crushed salt to form a more rigid and time-independent backfill. Sludge in Thailand is a waste material obtained from water treatment plant, classified as elastic silt and cohesionless material (Bumrungsuk and Fuenkajorn, 2015), which tends to be time-independent. The particle sizes of sludge are exceedingly small, it can fill and reduce voids between crushed salt grains, and hence the fluid flows through the mixture with lower velocity (Shor et al., 1981). Mixing of the crushed salt with a more rigid granular material can reduce its consolidation ability. In addition, the amount of crushed-salt obtained from processing plant is not adequate to backfill the mine openings. Sludge is being considered in the crushed-salt mixtures because it is a waste product obtained from water purification plant. It composes mainly of quartz (Wetchasat and Fuenkajorn, 2013) which tends to be chemically stable under underground environment.

1.2 Objectives

This study aims to investigate the mechanical performance of sludge-to-crushed salt mixtures for use as backfill in salt and potash mine openings. The task involves performing consolidation test on compacted specimens with various weight ratios of sludge-to-crushed salt mixtures. Saturated NaCl brine is used as mixing fluid. The compaction test result can be used as initial installation parameters of the backfill. The results from the consolidation test under various periods and stresses can be used to develop a set of empirical equations to design the initial installation parameters in terms of the physical and mechanical properties of the sludge-crushed salt backfill.

The mean strain energy released by creep closure of opening is calculated. Potential applications of the strain energy criterion involve predicting long-term mechanical properties of sludge-crushed salt backfill emplaced in opening. The findings can be useful to design the backfill material for different depths and installation periods for the openings of salt and potash mines.

1.3 Scope

Given below are the scope and limitations of this study:

1. Crushed salt samples with grain sizes ranging from 0.075 to 2.35 mm are prepared from Lower member of Maha Sarakham formation, northeast of Thailand. This size range is equivalent to those expected to be obtained as waste product from the mines.
2. Sludge is obtained from the Metropolitan Waterworks Authority of Thailand (MWA). It is sieved through mesh no. 40. The grain sizes range from 0.001 to 0.475 mm.
3. Saturated brine is prepared from sodium chloride powder (NaCl).
4. Three-ring device (Sonsakul and Fuenkajorn, 2013) is used in the compaction and direct shear tests.
5. Compaction test is performed to determine suitable brine content
6. The ratios of sludge-crushed salt mixtures (S:C) vary from 30:70, 50:50 to 70:30 by weight.
7. Consolidation tests use constant axial stresses from 2.5 to 10 MPa.
8. The consolidation periods are 0, 7, 15 and 30 days.
9. Basic characterization tests are determined from the specimens after removing from the three-ring mold, including the uniaxial compression test and

scanning electron microscope (SEM). The sample preparation and test method follow the relevant ASTM (D4543 - 19) practices.

10. All tests are conducted under ambient temperature.

1.4 Research methodology

The research methodology includes literature review, sludge-crushed salt preparation, laboratory testing, scanning electron microscope investigation, empirical equations development, sludge-crushed salt properties after emplacement in mine opening analytical solution, discussions and conclusions and finally thesis writing as shown in Figure 1.1.

1.4.1 Literature Review

Related research topics including the basic properties of sludge, mechanical properties of crushed salt, compaction testing, consolidation testing, physical and mechanical properties of sludge-crushed salt mixtures. The sources of information are from conference papers, technical reports, journals and textbooks.

1.4.2 Sludge-crushed salt preparation

Sludge is collected from the Metropolitan Waterworks Authority in Bangkok. The dried sludge is sieved through a mesh no. 40. The grain sizes of sludge range from 0.001 to 0.475 mm. Rock salt blocks are obtained from Lower member of Maha Sarakham formation. They are crushed in milling machine until they can pass sieve number 4 to provide particles ranging from 0.075 to 2.35 mm. Saturated brine is obtained by mixing pure salt powder (NaCl) with distilled water. The preparation is set in plastic tank by continuous stirring with plastic stick for 20 minutes. The brine proportion is more than 39% weight of salt in water.

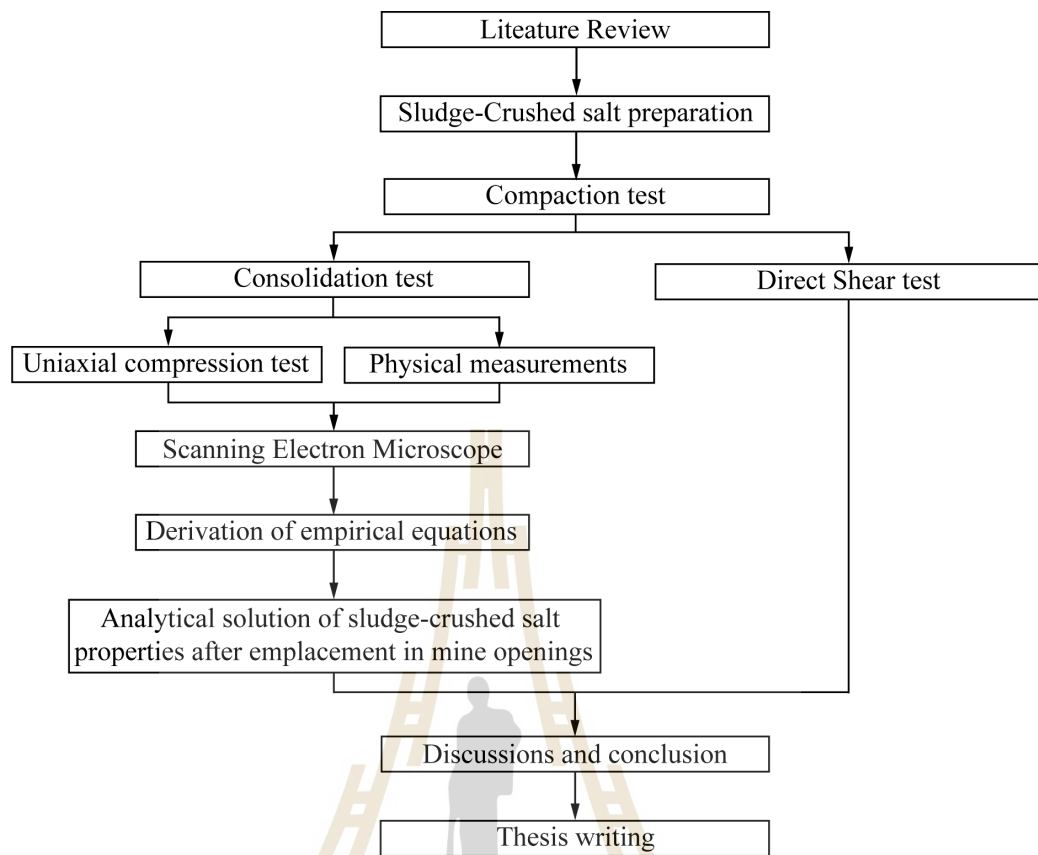


Figure 1.1 Research methodology

1.4.3 Compaction Test

The ratios of sludge-crushed salt mixtures vary from 30:70, 50:50 to 70:30 by weight. The ratios of 0, 5, 10, 15, 20, 25, 30, 35 and 40% by weight of saturated brine is added to the sludge-crushed salt mixtures. The relationship between optimum brine content and maximum dry density are determined by compacting mixtures in the three-ring mold. The sludge-crushed salt mixtures under their optimum brine content are used for the subsequent consolidation tests.

1.4.4 Consolidation Test

The consolidation tests are performed on the sludge-crushed salt mixtures installed in three-ring mold after compaction with optimum brine content for

each sample by applying constant stresses. The stresses range from 2.5, 5, 7.5 to 10 MPa, for periods of 0, 7, 15 and 30 days. Axial displacements are monitored using high precision dial gages (± 0.001 mm). The measurements are used to determine axial strain, density and void ratio. All tests are conducted under ambient temperature.

1.4.5 Direct Shear Test

The shear strengths of the compacted specimens are determined. The normal and shear force are applied by the hydraulic load cell. Normal stresses used here are 0.05, 0.1, 0.2, 0.4 and 0.6 MPa. Shear strength measurements are made after compaction. The friction angle and cohesion are calculated based on the Mohr-Coulomb criterion. The test method and calculation follow the ASTM D3080-11.

1.4.6 Uniaxial Compression Test

Compressive strength of the consolidated mixtures is determined by axially loading the sludge-crushed salts samples (after removing from the three-ring mold). The test procedure follows the ASTM (D7012-14e1) standard practice. The nominal diameters are 101.6 mm with length-to-diameter ratios ranging from 2 to 3. The density of specimen is determined before compression testing. Axial and lateral deformations are used to calculate elastic properties of the specimens.

1.4.7 Physical Measurements

Both before and after the consolidation tests. The density of the consolidated specimens is determined as a function of consolidation period. It is used to compare with the mechanical properties above.

1.4.8 Scanning Electron Microscope investigation

The scanning electron microscope (SEM) is used to examine the microstructures of compacted sludge-crushed salt mixtures under optimum NaCl

brine contents. Each sample is scanned both before and after the consolidation tests. Changes of the microscopic structures are made as a function of consolidation period and stress.

1.4.9 Empirical Equations Derivation

The physical and mechanical properties of the sludge-crushed salt mixtures are used to develop a set of empirical equations as a function of mean strain energy and consolidation period by SPSS statistical software. The equations correlate between the applied stresses and consolidation period with densities, uniaxial compressive strengths, Poisson's ratio and elastic parameters of the consolidated mixtures. The relations are used to predict the sludge-crushed salt mixtures properties installed in mine openings under various in-situ stresses and placement periods.

1.4.10 Analytical solutions

The strain energy density principle is applied to evaluate the energy required to consolidate the sludge-crushed salt specimens with different stresses and periods. The mean strain energy released by creep closure of mine openings in infinite mass subjected to in-situ stress is determined and used to predict the changes of the mixture properties after installation.

1.4.11 Discussions and Conclusions

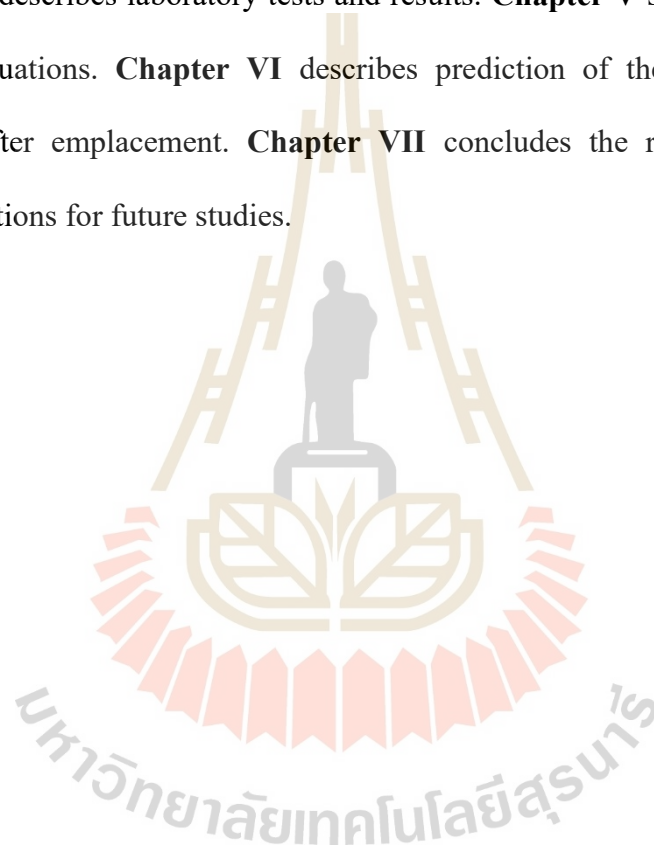
Discussions are made on the reliability and adequacies of the test data and the correctness of the interpretation and analysis. Future research needs to identify.

1.4.12 Thesis Writing

The methods and results are documented and compiled in the thesis. This research is application to design mine backfill which mixture strength, Poisson's ratio and elastic parameter of the consolidated sludge-crushed salt mixtures.

1.5 Thesis contents

The thesis comprises eight chapters. **Chapter I** introduces the thesis by briefly describing the background of problems and significance, research objectives, research methodology and scope and limitations of the study. **Chapter II** summarizes the literature review. **Chapter III** describes sludge-crushed salt mixture preparation. **Chapter IV** describes laboratory tests and results. **Chapter V** shows development of empirical equations. **Chapter VI** describes prediction of the sludge-crushed salt properties after emplacement. **Chapter VII** concludes the research findings and recommendations for future studies.



CHAPTER II

LITERATURE REVIEW

2.1 Introduction

Relative topics and previous researches are reviewed for an enhancement of the comprehension in basic characteristics of sludge, mechanical properties of crushed salt, compaction test, consolidation test, direct shear test and numerical model. The significant results of the literature review are described below, including the consequences of moisture, duration, consolidation stresses, initial density, particle size density, porosity, compressive strengths and elastic parameters of sludge-crushed salt mixtures that affected by stress and consolidation time.

2.2 Basic properties of Sludge

Laothong (2003) study the sludge cake obtained from the process of water treatment at Wang Noi power station. The results indicate that the sludge is a nonhazardous waste. It produces 300 tons of the sludge per month, costing 2.48 baht/kg or 460,000 baht per month in total for disposal step. The use of the sludge cake can reduce an operation cost of the power plant. The sludge is found to be loamy sand. Alternative utilizations of sludge cake are explored, including cement replacement in mortar, laterite replacement in an interlocking block, clay replacement in baked clay brick and ceramic wares. The results indicated that the most effective alternative way is laterite replacement in interlocking block with the proportion of cement: sludge: laterite is 2:2:5 by weight. The assembly cost of this material is 3.83

baht/kg which higher than the disposal cost (1.35 baht/kg). However, the product can be sold at the worth of about 6 to 8 baht/kg. In consequence, the utilization of sludge cake in making interlocking block is being considered as a workable alternative process.

Suriyachat et al. (2004) studied the basic properties of sludge from water treatment. The results showed the values of plastic and liquid limits, plasticity index, and shrinkage limit are 50.76%, 77.96%, 27.20% and 11.15%, respectively. Therefore, the maximum density is 1.33 g/cm³. The correlation between moisture content and permeability coefficient is provided in the condition that the moisture content is low with high permeability coefficient.

Valls et al. (2004) studied the additional of sludge into concrete with Portland cement. They mixed different amounts of sludge. The mechanical and physical properties are studied. The experiments indicate that when sludge content increases, the deformability of concrete also increases. In addition, the concrete density decreases with increasing sludge content and curing time. Moreover, the increasement of absorption coefficient and porosity is obtained when the sludge content decreases as the curing time increase.

Bunjongsiri and Bunjongsiri (2005) studied the content of sludge from community wastewater treatment for brick production by mixing with clay. There are six ratios of sludge and clay including 1:3, 3:7, 3.5:6.5, 2:3, 4.5:5.5 and 7:3. The experiment of leachate extraction procedure is used to indicate the quantity of the heavy metal contained in brick (mg/kg) of 1:3 and 7:3 ratios. The quantities in mg/kg for copper were 490.07 and 240.84, for lead were 59.16 and 17.66, for cadmium were 0.96 and 0.636, for manganese were 973.28 and 667.87, for chromium were 157.45 and

167.44 and for zinc were 337.75 and 136.82. However, all the bricks could not achieve the industrial standard of TIS 77-2531. The ratio of 1:3 revealed the best value that close to standard as the compressive strength was 15.05 kg/cm². The density was 1.10 g/cm³. Tolerance of length, wide, and thickness was 5.24, 6.16, and 9.35%, respectively. The weight was 388.60 g and the absorption were 36.23%.

Poonsawat and Lertpocasombut (2006) studied sludge from Bang Khen and Mahasawat water treatment plants as a raw material for producing clay plan roofing tile. Various properties of tile bodies are investigated based on the containing of 70 to 100% of the sludge and 0 to 30% of quartz and feldspar. When the materials are heated 1,000, 1,050 and 1,100°C. The obtained results imply that the plasticity index of the sludge from Bang Khen is higher than those from Mahasawat. High temperature increases the strength, shrinkage and bulk density of the material while it decreases their water absorption and porosity. At 1,100°C, the ratios of sludge: quartz: feldspar of 90:5:5 from Bang Khen and 85:5:10 from Mahasawat are suitable proportions for making clay plan roofing tile.

Kongthong and Lertpocasombut (2006) studied an adsorption property of sludge from Bang Khen water treatment plant. This research aimed to reduce color remaining in effluent wastewater from dye industries. An initial concentration of three solutions (basic, reactive, and disperse dyes) as 50 mg/l is used. The sludge is burned at 500°C before using as an adsorbent. The effect of pH study replied that no adsorption of the basic and re-active dyes while the dispersion of dye at pH 4 is effectively adsorbed. From the determination of equilibrium and adsorption isotherm, the results showed that the dried sludge provided better behavior compared to the sludge ash in basic dye adsorption. In contrast, the results of the disperse dye adsorption exhibited no action of

re-active dye adsorption either using dried sludge or sludge ash.

Sangiumsak and Cheerarot (2008) determined the properties of artificial aggregates produced by using sludge from water treatment. The aggregates contained various proportions between the sludge and clay of 100:0, 80:20, 60:40, 40:60, 20:80 and 0:100 by weight. They were prepared by molding and firing at 800, 1,000, and 1,200°C for 24 hours. Then the artificial aggregate is tested by compressive strength. In addition, abrasion test, stability in sodium sulfate and water adsorption are studied in some of them. The results showed that the compressive strength of the artificial aggregates increases with increasing amount of sludge and firing temperature. The aggregates with the ratio of sludge to clay of 60:40 fired at 1,200°C provided the highest compressive strength of 490 ksc while the aggregate fired at 800 and 1,000°C presented similar compressive strengths. In terms of the water absorption, abrasion, and stability in sodium sulfate, all of them decreased when the amount of the sludge increased. Comparing with natural aggregates, the artificial aggregates of all ratios had a higher water absorption and lower abrasion and stability in sodium sulfate than that of the natural ones. In conclusion, containing the artificial aggregates in concrete provided higher compressive strength than that of natural aggregates containing.

Wetchasat and Fuenkajorn (2013) studied the performance of sludge from Bang Khen water treatment plant mixed with a commercial grade of Portland cement type I. The sludge contained quartz with more than 80% by grain size less than 75 μm . The bentonite-mixed cement in terms of the mechanical properties. Three sludge: cement mixtures are 1:10, 3:10 and 5:10 which were contained closely similar mechanical properties.

Zbar et al. (2013) investigated the effect of organic matter (sludge) on the behavior of compacted clay soil. The different percentages of sludge (2.5, 5, 7.5 and

10%) were added to the natural clay soil. Increasing of sludge content enhanced both liquid and plastic limits. In compaction test, they found that optimum moisture and maximum dry density slightly decreased then incline to increase with an increasing of sludge. In case of shear strength test results, the q_u and c_u had similar behavior to the density water relation in compaction test which increased with sludge content and tend to decrease afterward. The compressibility of organic soils depends on various parameters including organic content, water content, void ratio and arrangement of soil particles. The compression behavior can be varied based on two roles, the first is the compression of organic soils and the second is the compression of creep.

Siyuan et al. (2020) studied the consolidation and permeability characteristics of the sludge to enhance the capability of dehydration process. The sludge was treated with $FeCl_3$ and Fenton reagent through consolidation test. After 15% $FeCl_3$ was added, the sludge exhibited ultra-high compressibility with an increasing of the consolidation coefficient by 5~8 times comparing to untreated sludge ($10^{-7} \sim 10^{-6} \text{ cm}^2/\text{s}$). In addition, the consolidation coefficient of the sludge reached $10^{-6} \sim 10^{-5} \text{ cm}^2/\text{s}$ after the progress with Fenton reaction.

Taki et al. (2020) studies the geotechnical properties of municipal sewage sludge (SS) for utilizing as sustainable engineering construction material. The SS samples were mixed with 0 to 8% of lime (CaO) by weight then keep for 7, 14 and 28 day. An increasing of unconfined compressive strength (UCS) from 207 kPa to 1102 kPa is obtained after 28 day of curing with 6% lime. The improvement of UCS is contributed from pozzolanic reactions which provided a formation of cementing compounds. They concluded that SS showed the behavior of expansion from the high containing of Montmorillonite. Moreover, the treatment by lime enhanced the

strength, swelling and plasticity characteristics of SS. Lately, many researchers have been utilized SS in geotechnical process. For instance, Ayininuola and Ayodeji (2016) used 7% of sludge ash to improve the shear strength of soil. The enhancement is obtained from the cementitious binding among product particles. Ayodele et al. (2016) reported an increasement of soil strength after using SS from 2 to 16%. De Figueirêdo et al. (2013) proposed the application of lime-stabilized mixtures of soil and SS as back filling and road base material.

2.3 Mechanical Properties of Crushed Salt

Fuenkajorn and Daemen (1988) select rock salt from New Mexico to study the property of compressive strength. The salt seems to act as brittle material (strain-softening) when using high strain rates whereas applying lower strain rates, it tends to behave as ductile material (strain-hardening). In the beginning of loading, the tendency of sample volume decreased then it shortly increased before the reaching of peak stress. The mechanical behavior of salt is described by the rheological models. However, the actual mechanisms of deformation are ignored. The assumption of deformation characteristics is controlled by spring elasticity and viscosity. The combination of these two elements is used to model the mechanical behavior of salt. As the rheological model structure is not involved to any specific test, the model can be used to solve time-dependent behavior of general problems with no requirement of additional assumptions.

Miao et al. (1995) used the constitutive models for material healing with an application of crushed rock salt compaction. The crushed rock salt provided a capability healing with time. The healing reduced the size of micro cracks and voids according to the increase of strength.

Stormont and Finley (1996) reported the productive sealing penetration (borehole) in geological materials. The formation of nature rock salt contains low permeability that provided a suitable location for sealing. Moreover, the important properties and behaviors (healing, creep and reconsolidation) of rock salt allow an effective construction seals in a long time. The advantages of rock salt are its availability, low cost, low permeability and distinct compatibility with the host rock.

Hansen (1997) investigated the mechanical characteristics in term of dynamically compacted crushed salt. The creep strains occur for sample RS/DCCS/1 at a mean stress of 2.33 MPa (Figure 2.1). The consolidation results for sample RS/DCCS/3 at a mean stress of 2.33 MPa (Figure 2.2). RS/DCCS/3 exhibits more volumetric strain than RS/DCCS/1. This observation is consistent with predictions of the constitutive model.

Hansen and Mellegard (2002) study the dynamic compacted crushed salt specimens with a diameter of 100 mm and lengths up to 200 mm. were derived from the full-scale compaction demonstration and from a laboratory scale dynamic compaction studied. Starting material was wetted to moisture contents of nominally 1.6% by weight. Figure 2.3 plots volumetric strain as a function of time on the primary axis and brine flow as a function of time on the secondary axis. Shear consolidation creep test results were added to a database of similar results for the purpose of estimating parameter in a creep model that represents the behavior of crushed salt. Current testing was performed at higher initial fractional densities (0.9) and stresses (1 to 5 MPa) than were used in previous programs to give better coverage of the range of conditions likely to be experienced by salt seal element at the WIPP.

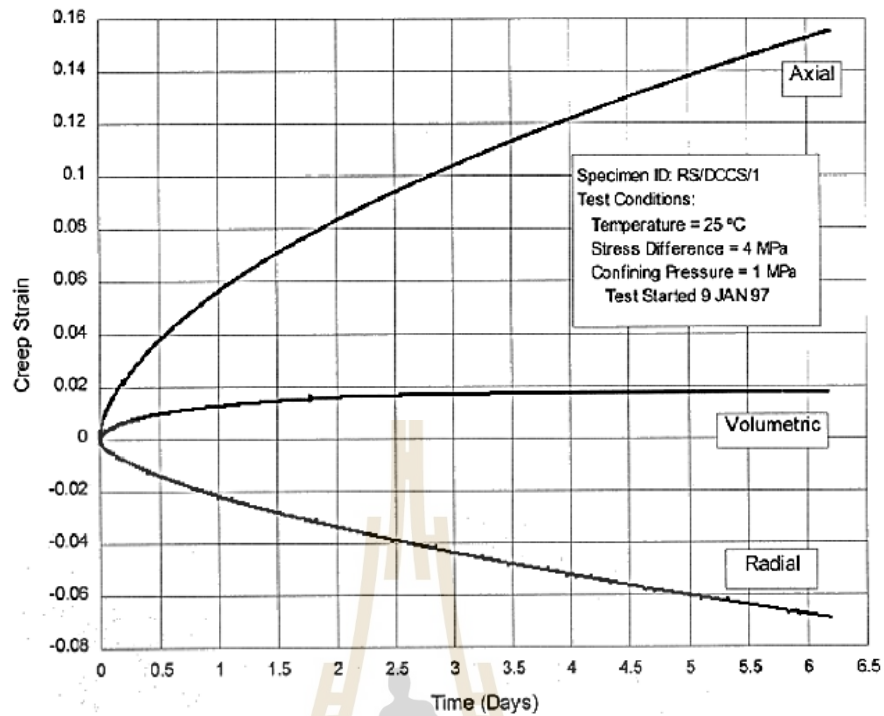


Figure 2.1 Shear consolidations at $\sigma_1 = 5$ MPa and $\sigma_3 = 1$ MPa (Hansen, 1997).

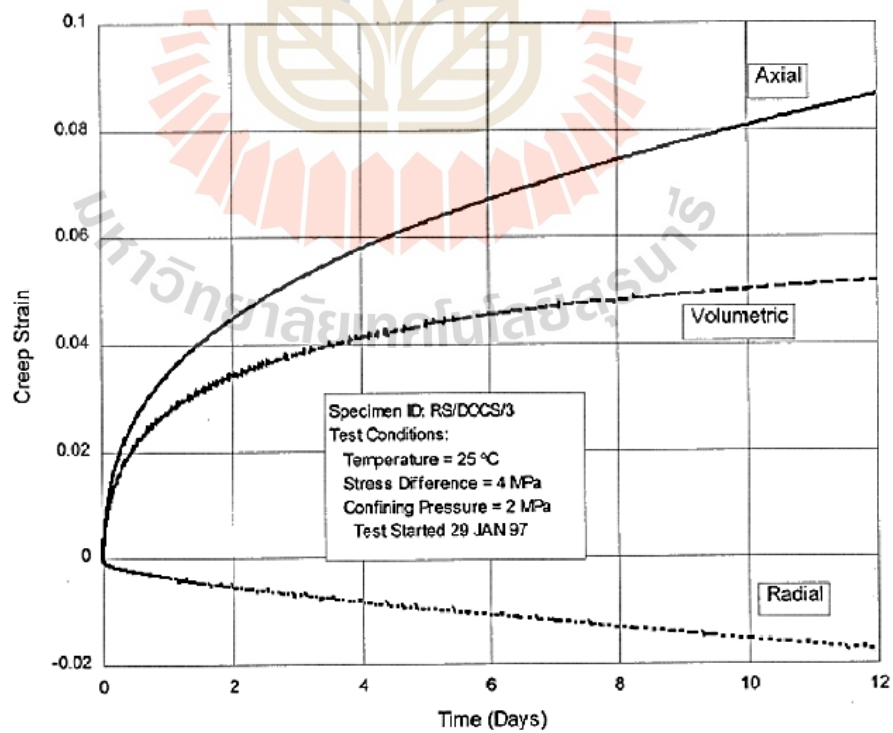


Figure 2.2 Shear consolidations at $\sigma_1 = 6$ MPa and $\sigma_3 = 2$ MPa (Hansen, 1997).

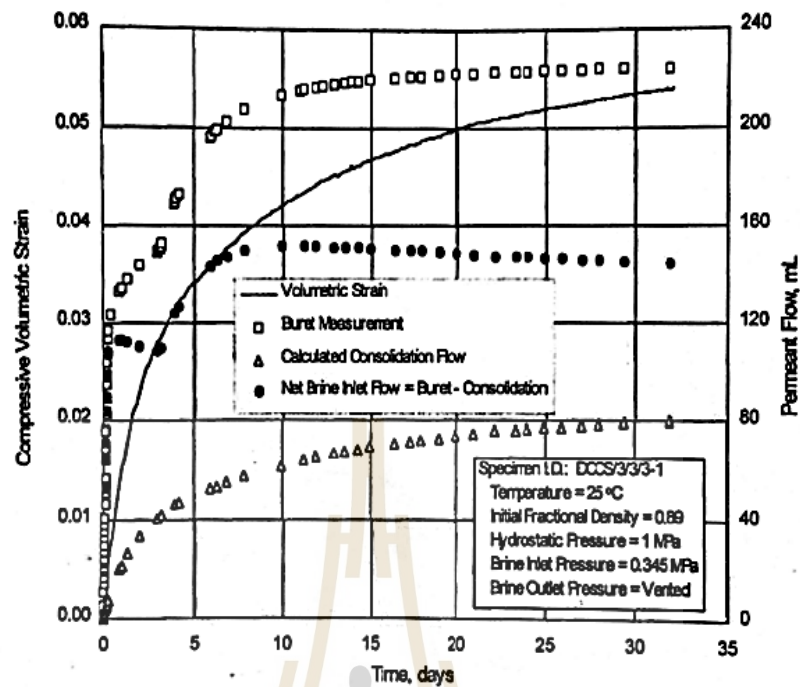


Figure 2.3 Volumetric strain and brine flow as function of time (Hansen and Mellegard, 2002).

Mills et al. (2018) studied micromechanics of consolidated granular salt samples by varying various conditions of stress, temperature and moisture. They found that increasing of confining pressure induced plastic deformation with only grain rearrangement and cataclastic process are generated as revealed from SEM observation. While with only 1% weight added moisture effectively enhanced the consolidation. In addition, elevated temperature also improved the cohesion degree along grain boundaries.

Kang et al. (2021) evaluated the performance of granular salt reconsolidation by the orthogonal test with the studied factors of temperature, compressive stress, moisture content and compression time. The results showed that the adding of moisture and increasing of compressive stress significantly reduced the porosity of the samples. While the impact of stress during the creep stage on volumetric strain was relatively

small. In case of temperature effect, they found that higher temperature provided more volumetric strain rate which led to the decreasing of porosity. In the granular salt compaction process, the porosity decreased drastically then formed a denser layer from the applying stress at the transient loading stage. The event is occurred throughout the particle rearrangement and cataclastic flow. However, additional mechanisms that explained the porosity reduction in the constant-load creep stage are dislocation creep, pressure-solution creep and recrystallization.

2.4 Compaction Test

Ran and Daemen (1995) investigated the dynamic compaction tests of crushed rock salt in bentonite-based materials by the relation between moisture content and particle size gradation. The result from Figure 2.4 indicated that compaction strain increases with larger particle size of crushed salt. In addition, compaction energy varied significantly with moisture which provided optimum value of 5% water content then decreased with further moisture increment.

Charlemyanont and Arrykul (2005) studied a compaction test to investigate the optimum condition of the compacted sand-bentonite mixture in term of water content and maximum dry density. The optimum water contents with maximum dry unit weights are obtained from the peak of compaction graphs. The results indicated that the increasing of water content provided the increment of dry unit weight as expected. After reaching optimum water content, the dry unit weight decreases with further increase water capacity especially at high amount of bentonite. This occurrence was similar to those from Kaya and Durukan (2004) and Zhang et al. (2012).

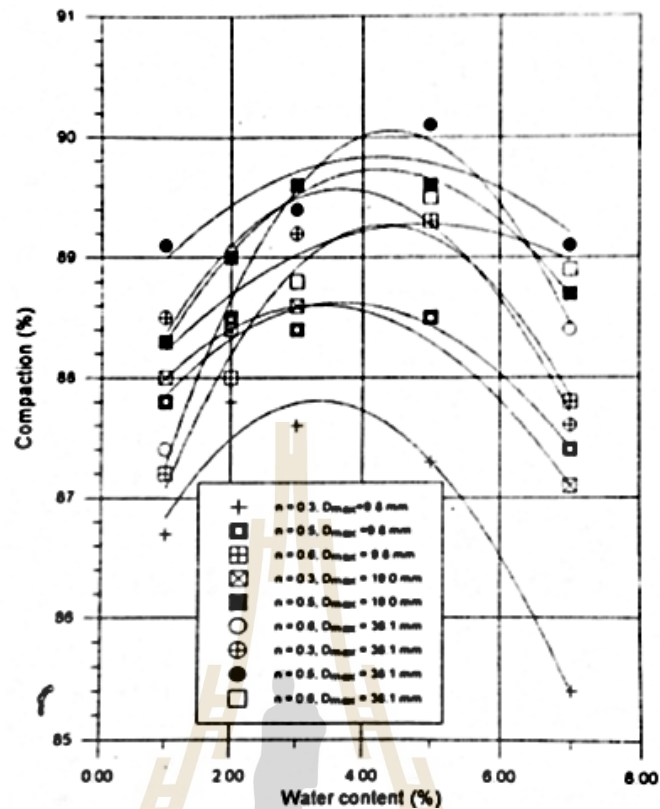


Figure 2.4 Compaction as a function of water content and particle size gradation (Ran and Deamen, 1995).

Shariatmadari et al. (2011) studied the compaction test of the mixture of two proportion of clay-bentonite (10% and 20% by weight) combined with three different inorganic salt solutions including sodium chloride, calcium chloride and magnesium chloride. In this work, distilled water and salt solutions are used as reference and permeant liquids, respectively. From the results of Figure 2.5, comparing to reference, all three salt solutions showed the higher in maximum dry density and lower optimum water content. Those phenomena are attributed from adding salt leads to the filling of pore fluid then the decrement of diffuse double layer thickness. Hence, the particles are packed better even using the same energy of compaction along with the increase of dry density.

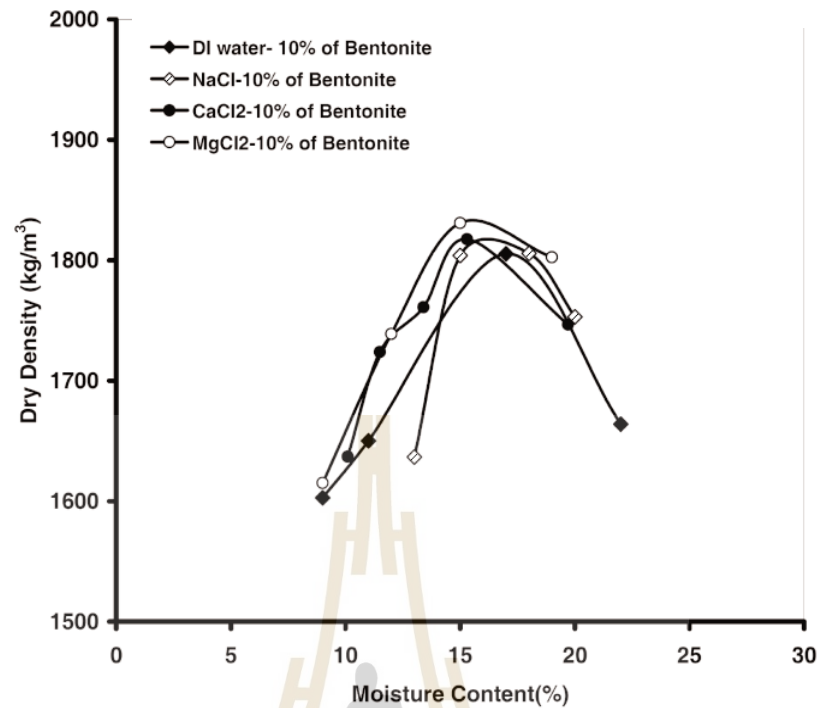


Figure 2.5 Effect of cation valence on the maximum dry density and optimum water content (Shariatmadari et al., 2011).

Lim et al. (2013) studied and compared the functionality as electrical grounding improvement material (GIM) of sodium bentonite and calcium bentonite. They found that sodium form is superior than calcium since it contains higher swelling capacity and lower hydraulic conductivity to water.

Sonsakul and Fuenkajorn (2013) developed the direct shear testing tool and three-ring compaction to investigate the shear strength, maximum dry density and optimum water content of bentonite samples. The three-ring mold compaction test is dynamically releasing from 10 pounds weight steel hammer for 27 times per each layer in total of 6 layers. The whole energy of the compaction mold is $2,700 \text{ kN/m}^3$. The overall features of three-ring mold are shown in Figure 2.6. The maximum particle size of tested soil up to 10 mm is allowed for this three-ring mold device.

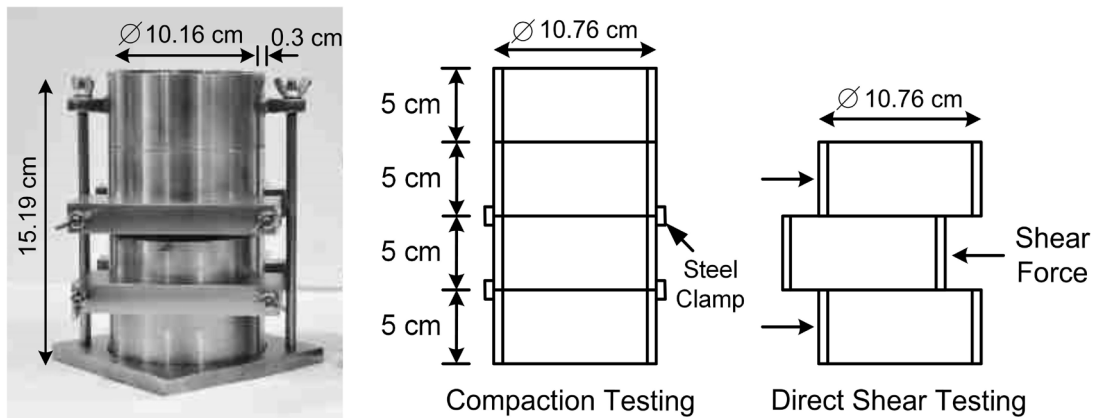


Figure 2.6 Three-ring compaction mold (Sonsakul and Fuengkajorn, 2013).

Gullu and Giriskan (2013) utilized the locally available industrial wastewater sludge as a soil stabilizer to improve geotechnical characteristics of fine-grained soil (ML). The main advantage of using locally sludge related to environment concern of recycling and sustainability issues. In this work, they studied the sludge proportions with 0, 5, 10, 20, 30, 40, 50, 60, 70, and 80 % by dry weight of the mixture. The results showed that sludge dosages significantly enhanced the internal friction of untreated soil. Moreover, they found that the geotechnical properties of compaction, shear strength, CBR, and UCS of treated fine-grained soil were improved by the rate of sludge dosage. The overall results of 50 % sludge dosage indicated that the soil quality was good rating for using as base layers for road stabilization. The addition of sludge also contributed the ductility behavior of the mixture from the stress-strain responses. The results also implied that the sludge can be potentially employed as a soil conditioner agent.

Hashimoto et al. (2016) investigated the compaction and consolidation performance of two mixed waste materials: sludge ($D < 2.0$ mm) + crushed concrete (2.0 mm $< D < 9.5$ mm) and sludge + incineration ash ($D < 2.0$ mm). Various

parameters were studied with different mixing proportions. The initial maximum dry density of sludge, crushed concrete, and incineration ash were 0.76 g/m^3 , 1.45 g/m^3 , and 1.51 g/m^3 , respectively. After mixing with an increment of sludge, the maximum dry density of two mixture decreased distinctly. In case of compression coefficient, the value of sludge and incineration ash mixture slightly decreased with an increasing of incineration ash proportion. Meanwhile, the compression coefficient of sludge and crushed concrete mixture decreased rapidly with an increasing of crushed concrete proportion. As a result, different consolidation characteristics of two mixture between sludge and crushed concrete or incineration ash were obtained that agree with the report of Iqbal et al. (2019). They also varied the proportions of tested materials then studied a series of laboratory tests including compaction, California bearing ratio (CBR), undrained triaxial compression and consolidation.

Proia et al. (2016) prepare bentonite-sand mixture with various proportions of components for analyzing the effect of bentonite content for compaction test. As can be seen in Figure 2.7, the images from scanning electron microscope (SEM) displayed the appearance of the mixture surface with different amounts of bentonite and sand. The micrographs show that the increment of bentonite content resulting in the higher interaction of sand grains surface. It can be assumed as bridges connect each coarse particle.

Srikanth and Mishra (2016) studied the behavior of sand-bentonite mixture on different sand contents with a particular size containing. Two type of sands are selected to study comprising of fine sand (FS) and medium sand (MS) mixed with bentonite. Various proportions of sand content from 50 to 90 % by dry weight are used. Comparing in the same proportion, the mixture of FS-bentonite and MS-bentonite

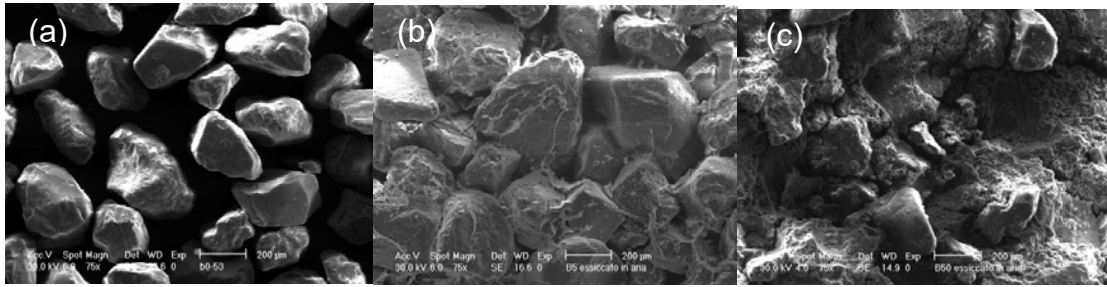


Figure 2.7 SEM on are dried samples at magnification factors of 75x; a) sand 100%, b) bentonite 5% and c) bentonite 50% (Proia et al., 2016).

displayed differences in optimum moisture and maximum dry density. The results indicated that particle size of sand possibly affected the compaction characters of the whole mixture. The mixture of MS-bentonite provided a lower moisture content and higher dry density. That attributed from the productive filling of bentonite particle inside the void spaces existed between sand particles.

2.5 Direct Shear Test

Crosby (2007) investigated the geomechanical test and geotechnical properties of Maha Sarakham Formation rock type. The main components of overburden are the Middle Clastic comprising of mudstone, siltstone and sandstone along with the Loer clastic consist of claystone and mudstone. As the dipping of fractures regularly less than 30° , and seldom at 70° . The results indicate extensive fractures of the halite and anhydrite-filled and bands with 2-5 cm thickness typically. The direct shear tests of Middle Clastic siltstone provided cohesion yield of 0.30 MPa with friction angle of 27° by smooth saw-cut surfaces preparation.

Sonsakul et al. (2013) improved three-ring compaction and direct shear mold to provide the optimum tool for 10 mm in grain size of soil samples. They verified the

method by using commercial grade bentonite then compared with the results of ASTM standard testing devices. The results from three-ring mold and the standard mold were similar as presented in Figure 2.8. While the cohesion and friction angles from the three-ring device are greater than those from ASTM standard approximately 10%. Pongpeng et al. (2017) also obtain similar data from the compaction study of bentonite-crushed salt and bentonite-gravel materials.

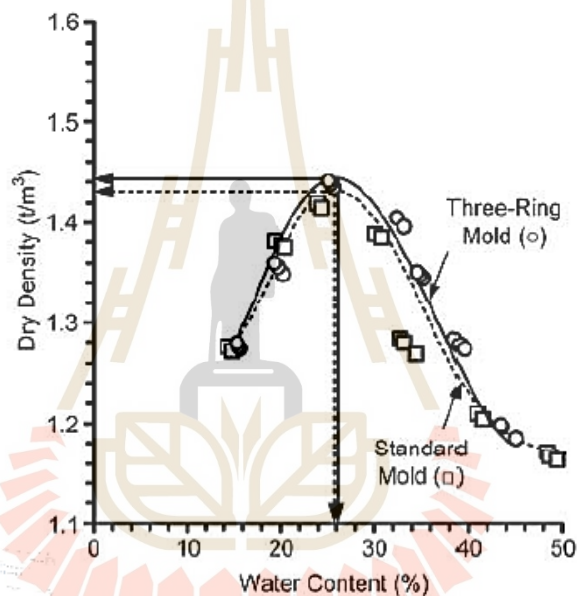


Figure 2.8 Compaction test results (Sonsakul et al., 2013).

Sattra and Fuenkajorn (2015) studied and focused on shear strength tests of compacted sludge-crushed salt. The direct shear tests have been investigated to provide the mechanical property of compacted sludge-crushed salt seals for the holes in mines i.e. salt and potash. Crushed salt with diameters at 0.075-2.35 mm is sorted and mixed with the sludge from water treatment plant. The ratios of sludge to crushed salt specimens are varied from 10:90 to 100:0. The results provide optimum brine with maximum dry densities of 4% to 34% and 12.5 to 17.5 kN/m³. The shear

strengths peak of 10:90 ratio (sludge: crushed salt) show the cohesion of 0.167 MPa with friction angle 46° . The cohesion and friction angle decrease to 0.068 MPa and 32° with an increasing of sludge content of 100%. This investigation is useful for defining the mixture parameters of initial installation in the salt and potash mines opening.

Neiwphueng and Fuenkajorn (2015) use compacted bentonite-crushed salt mixtures as sealants for rock salt and potash openings. The direct shear tests were evaluated to explain mechanical performances of sealing materials. The crushed salt with grain size range of 0.075 to 2.35 mm is used to mix with commercial grade bentonite. The ratios of bentonite to crushed salt that selected to study are from 10:90 to 100:0 (by weight). The optimum brine content from compaction tests results are 2.2% to 20% with the corresponding maximum dry densities of 15.9 to 19.0 kN/m³. The higher crushed salt content increased the shear strength and friction angles of the mixtures. All ratios of the mixture obtained the cohesion ranges from 0.20 to 0.28 MPa. The properties of 30:70 ratio was suitable for using as a sealing material.

Zhang et al. (2016) assess the concentration effect of salt solution on the shear strength of bentonite-sand mixture. The results show that the shear strength or shear resistance improves remarkably with an increase of salt solution concentration. The friction angle increases moderately with the concentration while cohesion is unchanged.

Bagherzadeh-Khalkhali and Mirghasemi (2009); Soltani-Jigheh and Jafari, (2012), Kim and Ha (2014) also studied the relationship between shear strength and particle size. Soil particles with larger size provided the shear strengths with larger values. It can be concluded that the shear parameter depends on the grain size of as the friction angle value increases with an increasing of grain size.

Sitthimongkol et al. (2020) investigated the mechanical properties of mixing ratios from 30:70 and 100:0 by weight of compacted bentonite-aggregate mixture with saturated sodium chloride (NaCl) and magnesium chloride (MgCl₂). They found that particle size of the aggregate and bentonite content played important roles in maximum dry densities and optimum brine content. Moreover, an increasing of aggregate content and angularity led to an increasing of the cohesion and friction angles. In addition, the specimens mixed with NaCl brine provided higher dry density and strength than that of MgCl₂ brine.

2.6 Mechanical Properties of Consolidation Backfill Material

Kelsall et al. (1984) investigated the properties of crushed salt and the nature of fracture healing. They also presented analytical methods for predicting the rates at which the processes will occur in a repository. The grain size of the crushed material is ranged from 75 mm to about 0.05 mm. The results explained that consolidation to low porosities should occur within hundred years at most candidate repository sites for locations within the repository close to the waste (Figure 2.9). Fracture healing should occur relatively speedily, within ten to hundred years, as the confining stress across the fracture approaches lithostatic levels. Healing of fractures caused by excavation may be enhanced by placing relatively rigid concrete plugs in the tunnel openings.

Pfeifle (1991) studies consolidation and compressive strength of bentonite-crushed salt mixtures. Each mixture contained bentonite and crushed salt in 30% and 70% of total dry weight. The proportion of water content to bentonite-crushed salt mixtures is therefore determined as 5 or 10% by weight. The tests of consolidation are performed in hydrostatic stresses between 3.45 and 14 MPa. The volumetric strains

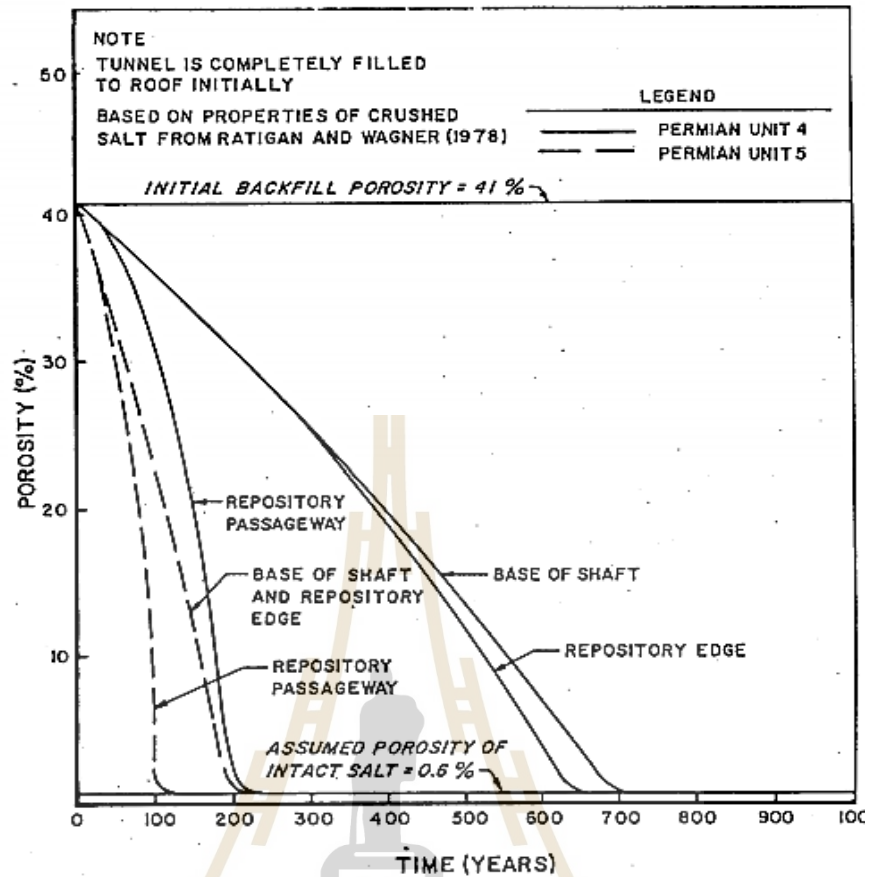


Figure 2.9 Reduction in porosity of crushed salt due to creep consolidation at various seal location-permain basin repository (Kelsall et al., 1984).

increase between 0.2 and 0.3 with increasing hydrostatic stress and consolidation time. The unconfined compressive strength is ranging from 0.5 to 8.1 MPa. The higher strengths are measured at higher densities.

Butcher (1991) presented the advantage of a salt-bentonite backfill from WIIP. The author explained that a 70% and 30% by weight of salt and bentonite in the mixture is superior backfill material comparing with pure crushed salt. The mixture of salt-bentonite is low porosity and chemical stability. In addition, it potentially adsorbed brine and radionuclides. The bentonite swelling pressure is between 2.3 to 3.5 MPa.

Aydilek et al. (1999) studied large-scale and small-scale consolidation test of wastewater treatment sludge are investigated using laboratory and field test. The specimen has 50 mm of inside diameter. The small-scale consolidation tests (ASTM D2435) has 12 mm height and the large-scale consolidation tests has 48 mm height. As a result of the volumetric strains of large-scale test are much higher than small-scale tests because of high initial water contents and void ratio.

O'Kelly (2004) works on mechanical performance of dewatered, anaerobically digested sewage sludge. The component of sludge is mainly organic clay. The specific gravity of sludge was 1.55. The maximum dry density value is 0.56 tones/m³ for the dried sludge material. It was monitored by the standard proctor compaction with moisture content of around 85% (solids content of 54%). The value of ϕ for moderately and strong digested sludge increased to 32° and 37°, respectively. The effective cohesion of sludge material stayed zero throughout the whole process. The sample sets are then consolidated until effective confining pressures of 30, 60 and 140 kPa. The volumetric strains increased with an increasing of consolidation time as displayed in Figure 2.10.

Somtong et al (2015) evaluate the mechanical properties of consolidated crushed salt mixed with brine content of 5% by weight. The samples were packed in the cylinders with 54 mm diameter. Then the application of constant axial stresses of 2.5, 5, 7.5 and 10 MPa were used for 3, 5, 7, 10 and 15 days. The consolidation amplitude and density increased with the applied axial stress. Along with consolidation period, the uniaxial compressive strength and porosity increased and decreased, respectively.

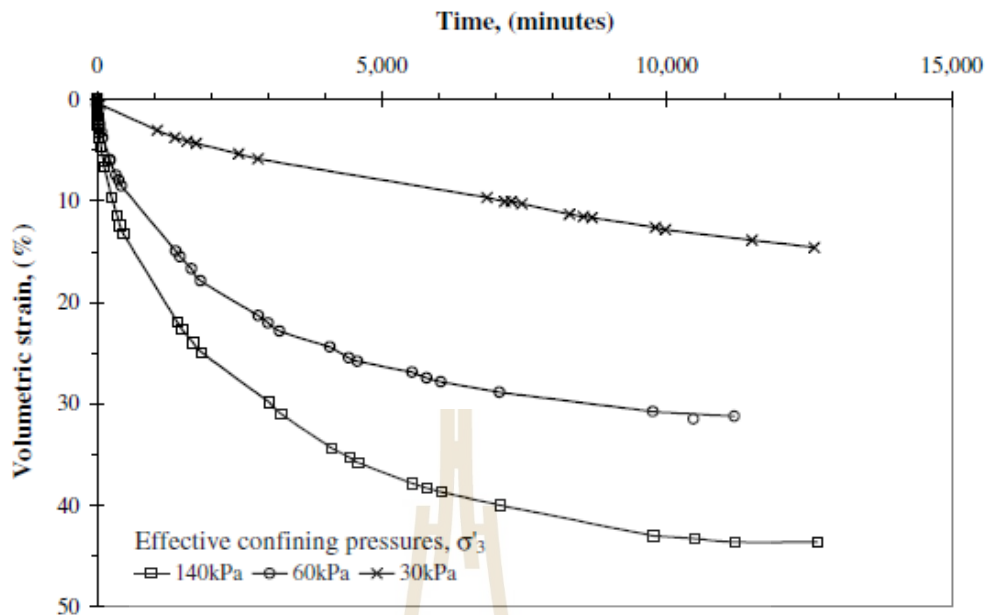


Figure 2.10 The volumetric strains vs. time. (O'Kelly, 2004)

Bumrungrasuk and Fuenkajorn (2015) investigate the mechanical performance of sludge-crushed salt mixture for using as a backfill material in salt and potash mines. The various series of sludge-to-crushed salt ratios were tested in consolidation experiments to determine the effects of different component amounts on the mechanical properties. The sludge-to-crushed salt were varied in the ratios of 0:100, 25:75, 50:50, 75:25 to 100:0 by weight. The applied constant axial stresses were 2.5 MPa for 2, 7, and 15 days. The intrinsic permeability of sludge-crushed salt is determined by the flow testing during the consolidation experiment. The evaluation of uniaxial compressive strength is studied after the sample was consolidated. It can be concluded from the results that the density, strength and elastic modulus increased with increasing consolidation time.

Khamrat et al. (2017) study consolidation of crushed salt mix with 5% saturated NaCl brine solution for sealing the borehole of potash mines, and

Suwannabut et al. (2020) there are similar tests. But there is a replacement of the solution by used to $MgCl_2$. The consolidation tests are carried out to determine the mechanical performance of crushed salt from the application of stresses and consolidation duration time. The crushed salt ranges from 0.075 to 4.76 mm mixed with 5% saturated brine through the stresses of 2.5 to 10 MPa for 3-180 days (Figure 2.11). In the same solution, the consolidation curves showed instantaneity and temporary strains. The results showed that the application of higher consolidation stress (σ_{cons}) provided a larger strain. The strain rates decreased with time and lean toward to stay relatively constant after 30 days. The uniaxial compression tests with greater consolidation duration and stress show greater strength and elasticity. while Poisson's ratio decreases slightly. NaCl solution tends to higher uniaxial compressive strength than those the $MgCl_2$ solution due to $MgCl_2$ solution does not have recrystallization of the salt particles. The strength and stiff of crushed salt mass contained 2 important mechanisms; (1) The changes of volumetric consolidation owing to the rearrangement and cracking of particle, and (2) the process of recrystallization and healing.

Akgün and Koçkar (2018) studied the mechanical and hydrological properties of compacted mixtures between sand and bentonite. The mixtures with 5 to 40% of bentonite containing were investigated to provide an optimum proportion for using as a waste isolation material. They found that the mixture with 30% of bentonite was suitable since it contributed the highest maximum dry density and lowest optimum water content. Hence the cohesive behavior of bentonite could strengthen the skeletal structure of the sand particles as supported by Komine (2010). While the mixture with bentonite content > 30% lowered the maximum dry density and increased the optimum

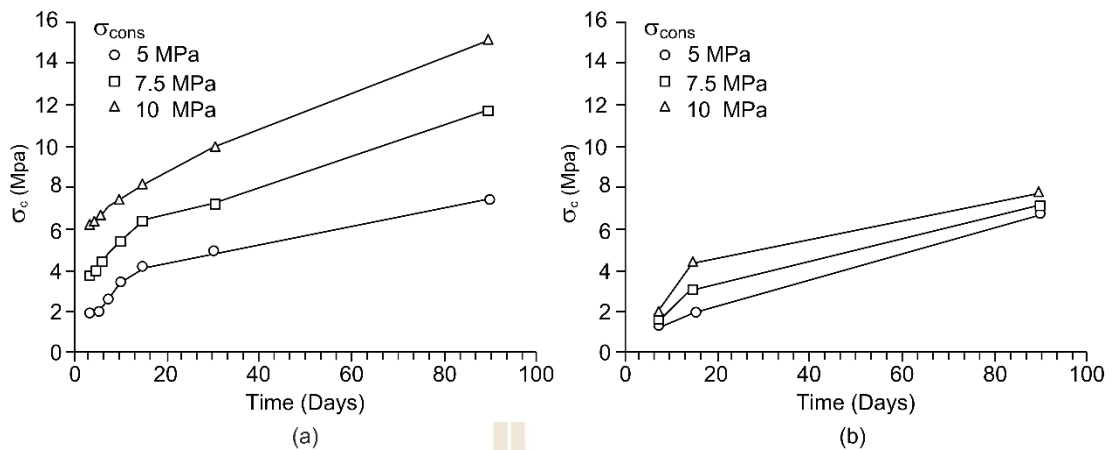


Figure 2.11 Consolidation crushed salt with NaCl solution (a) (Khamrat et al., 2017) and with MgCl₂ solution (b) (Suwannabut et al., 2020).

water content. Since the increasing of bentonite content contributed the increase of cohesion and the decrease of the angle of internal friction. For the mixtures with bentonite containing less than 30%, the higher increasing rate of unconfined compressive strength and Young's modulus and the lower decreasing rate of internal friction angle were obtained. Since the mixture represented as sand rather than cohesive agent because it contained small content of bentonite. In term of hydrological tests, they found that the increment of bentonite in compacted mixture provided the decreasing of hydraulic conductivity. This behavior was agreed well with the reports of Chapuis (1990, 2002), Kenney et al. (1992), Komine (2004), Tashiro et al. (1998) and Kaoser et al. (2006) since bentonite itself has a very low permeability, in the order of 10^{-10} and 10^{-12} m/s.

CHAPTER III

SAMPLE PREPARATION

3.1 Introduction

Presented in this chapter are basic properties of testing materials and sample preparation for use in the compaction test, direct shear test and consolidation test in this study. Materials used in the experiment consist of sludge and crushed salt.

3.2 Test materials

3.2.1 Sludge

Sludge was obtained from dewatering plant of Bang Khen Water Treatment Plant found in Bangkok Metropolis. Dried sludge is taken out and dehydrated by drying under sunlight. It is oven-dried at 105°C for 24 hours or until its weight remains constant. The dried sludge is sieved by using the mesh no.40 to obtain the range of particle sizes between 0.001 to 0.475 mm (Figure 3.1). Based on Atterberg's limits testing, it is classified as silt with over 80% silica. It has liquid limit = 59%, plastic limit = 31%, plastic index = 28%, and specific gravity = 2.56. The sludge sample is classified by the Unified Soil Classification System (50% or more passes the no.200 sieve) as high-plasticity silt (MH). Table 3.1 lists the chemical compositions of the sludge sample obtained from the X-Ray diffraction (XRD) identification.

3.2.2 Crushed salt

Salt blocks are obtained from the lower member of the Maha Sarakham formation. It is virtually pure halite. They are crushed by milling machine (2HP-4 POLES, Spec jis c-4004) until their grain sizes are in the range of 0.075 to 2.35 mm (Figure 3.1). This range is equal to expected size of the obtained waste product from potash mines processing plant. Table 3.1 provides chemical compositions of the specimens discriminated from X-ray fluorescence (XRF) spectrometer. The specific gravity of salt is 2.160. The crushed salt is classified by ASTM (D2487 - 17e1). The uniformity coefficient (C_u) = 3.48 and the coefficient of curvature (C_c) = 0.94. The crushed salt is poorly graded sand (SP). The roughness and sphericity are defined from individual particles under an optical microscope (Olympus BX51M), as shown in Figure 3.2. Based on the widely known systematic classification (Figure 3.3) of Powers (1982), crushed salt is classified as angular to sub-angular with spherical shape. The averages of the roughness and sphericity for each material are shown in Table 3.2.

3.2.3 Saturated brine

Saturated brine is obtained by dissolving pure salt powder (NaCl) with distilled water in a plastic tank then stirred continuously by a plastic stick for 20 minutes. The portion of NaCl and water is more than 39% by weight. The specific gravity of saturated brine (SG_{brine}) can be calculated from an equation: $SG_{\text{brine}} = \rho_{\text{brine}}/\rho_{\text{H}_2\text{O}}$, where ρ_{brine} is density of saturated brine (measured by a hydrometer (kg/m^3)) and $\rho_{\text{H}_2\text{O}}$ is density of water (kg/m^3) equal $1,000 \text{ kg}/\text{m}^3$. The SG value of saturated brine in this work is 1.211 at 21°C .

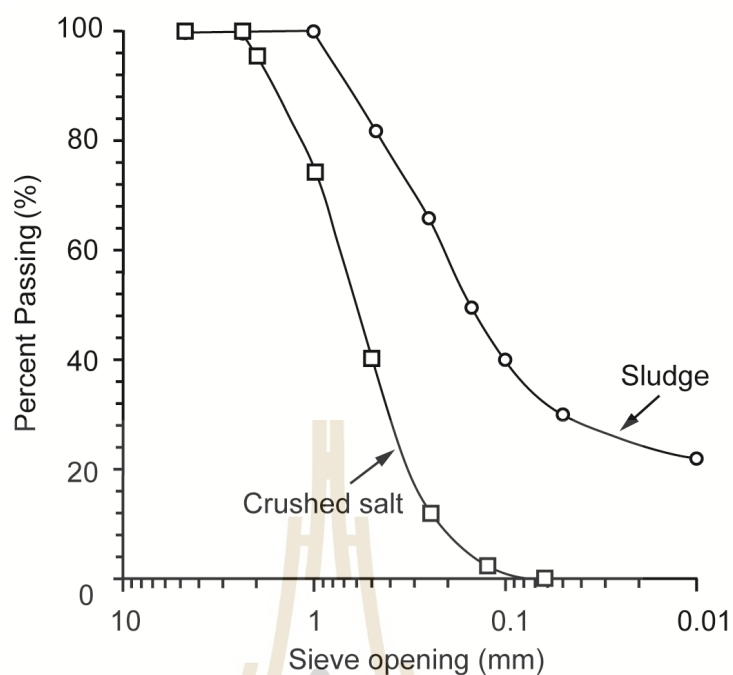


Figure 3.1 Particle size distributions of sludge and crushed salt

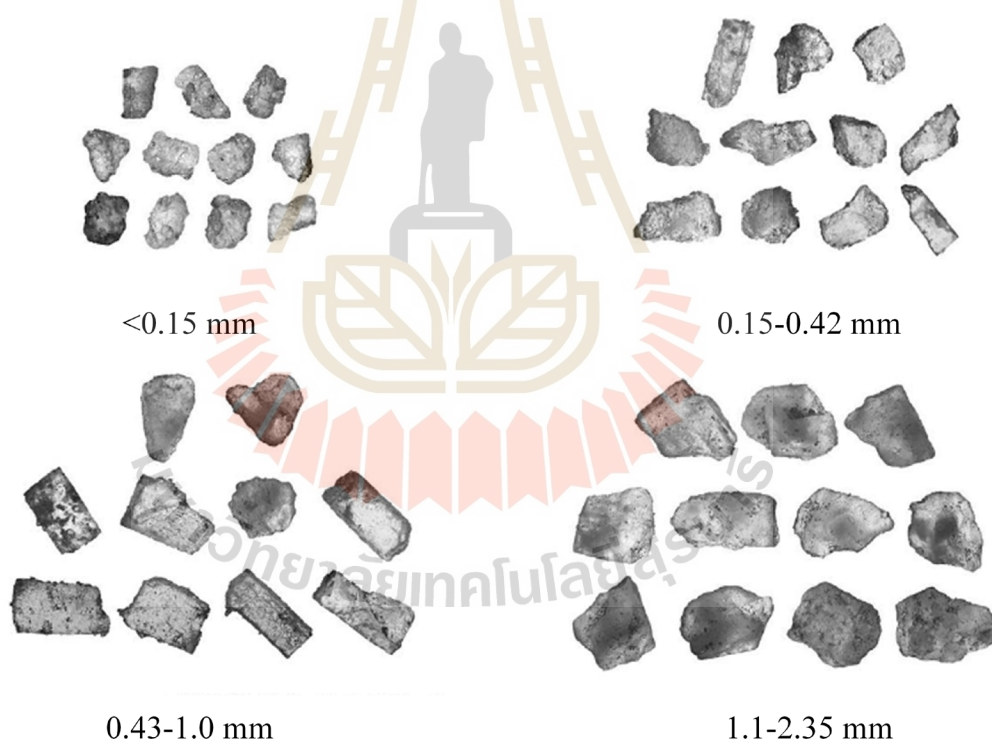
Table 3.1 Chemical compositions of the tested sludge and crushed salt.

Compositions	Weight (%)	
	Sludge	Crushed salt
SiO ₂	88.877	0.03
K ₂ O	4.932	6.40
CaO	3.113	0.26
TiO ₂	0.993	-
Cr ₂ O ₃	0.157	-
MnO ₂	1.547	-
CuO	0.038	-
ZnO	0.097	-
Ga ₂ O ₃	0.022	-
Rb ₂ O	0.073	-
ZrO ₂	0.075	-
PbO	0.076	-

Table 3.1 (continued) Chemical compositions of the tested sludge and crushed salt.

Compositions	Weight (%)	
	Sludge	Crushed salt
Na ₂ O	-	20.70
MgO	-	4.39
SO ₃	-	0.05
Cl ₂ O	-	68.03
Br ₂ O	-	0.16
Total	100	100

N/D = not detected

**Figure 3.2** Examples of salt grains for various size ranges.

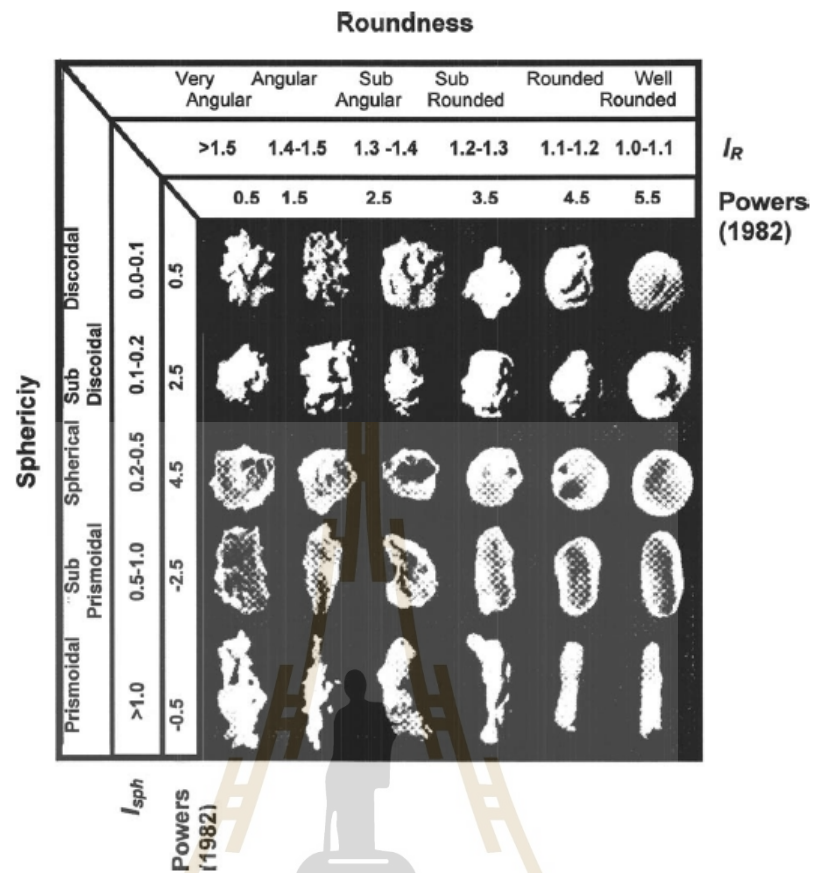


Figure 3.3 Standard chart for roundness and sphericity of sedimentary particles (Powers, 1982).

Table 3.2 Particle shape identification for aggregates given by Powers (1982).

Particle size range (mm)	Roundness Classification		Sphericity Classification	
	I_R	Roundness	I_{sph}	Sphericity
<0.15	1.5 - 2.5	Angular-Sub Angular	-2.5	Sub-Prismatic
0.15-0.42	1.5 - 2.5	Angular-Sub Angular	-2.5	Sub-Prismatic
0.43-1.0	1.5 - 2.5	Angular-Sub Angular	-2.5	Sub-Prismatic
1.1-2.35	1.5 - 2.5	Angular-Sub Angular	4.5	Spherical

3.4 Sludge-crushed salt mixture preparation

The sludge-crushed salt mixture weight ratios are 70:30, 50:50 and 30:70. The mixtures are prepared in a plastic tray with total weight in 2.7 kilograms of the mixture. Then, the prepared saturated brine (from section 3.2.3) is added by spaying the mixture with brine until a desired content is reached. They are mixed thoroughly using a plastic spatula.



CHAPTER IV

LABORATORY TESTING

4.1 Introduction

This chapter describes equipment, methods and results of the compaction, direct shear, consolidation and uniaxial compression testing. The microstructures of specimen before and after consolidation process are observed using scanning electron microscope (SEM).

4.2 Compaction test

4.2.1 Test method

The three-ring compaction mold (Sonsakul and Fuenkajorn, 2013) is an apparatus for testing the compaction. Sludge (S) and crushed salt (C) mixture with ratios by weight of 70:30, 50:50 and 30:70 are combined with NaCl brine at 0, 5, 10, 15, 20, 25, 30, 35 and 40% by weight of the mixtures to investigate the optimum brine content. The mixtures are compressed dynamically by 10 pounds weight steel hammer for 27 times per layer for 6 layers. The total energy of the compaction mold is 2,700 kN/m³. Energy of compaction (J) can be calculated by Proctor (1933):

$$J = \frac{n \times W \times L \times t}{V} \quad (4.1)$$

which J is compaction energy per unit volume, W is weight of hammer, L is height of hammer drop, t is number of layers, n is number of blows per layer and V is volume of mold.

After compaction process, the specimens are dried at $105\pm 5^{\circ}\text{C}$ for 24 hours in an oven. The determination of maximum dry density and optimum brine content is obtained from the plot between dry densities and brine contents. Equation 4.2 (Fuenkajorn and Daemen, 1988) is used to calculate the NaCl brine content (W_b):

$$W_b = \frac{[100 + SB] \times \left[W_1 - W_2 - \left(\frac{W_i}{100} \right) (W_2 - W_{\text{can}}) \right] \times 100}{100(W_2 - W_{\text{can}}) - SB(W_1 - W_2)} \quad (4.2)$$

which W_b is brine content (% by weight), W_i is initial water content of specimen (% by weight), W_{can} is weight of container (g), W_1 is weight of wet soil and container (g), W_2 is weight dry soil and container (g) and SB (solubility of salt in dissolved water) is 176.3% by weight of NaCl in water. Equation 4.3 is used to calculate the dry density (ρ_{dry}) of the compacted mixtures:

$$\rho_{\text{dry}} = \left[\rho_{\text{wet}} / (W_b + 100) \right] \times 100 \quad (4.3)$$

which ρ_{dry} is dry density of specimen (g/cc), ρ_{wet} is wet density (g/cc), W_b is NaCl brine content of specimen (% by weight).

4.2.2 Compaction test results

The samples of 15 specimens has been tested. The relationship between dry densities and brine contents are plotted to evaluate the maximum and optimum value, respectively (Figure 4.1). The results show that the increasing of sludge percentages provides the decreasing of maximum dry density the increasing of optimum brine content. Table 4.1 exhibits the summarized results of the compaction test. These data agree reasonably well with the results obtained by Kaya and Durakan

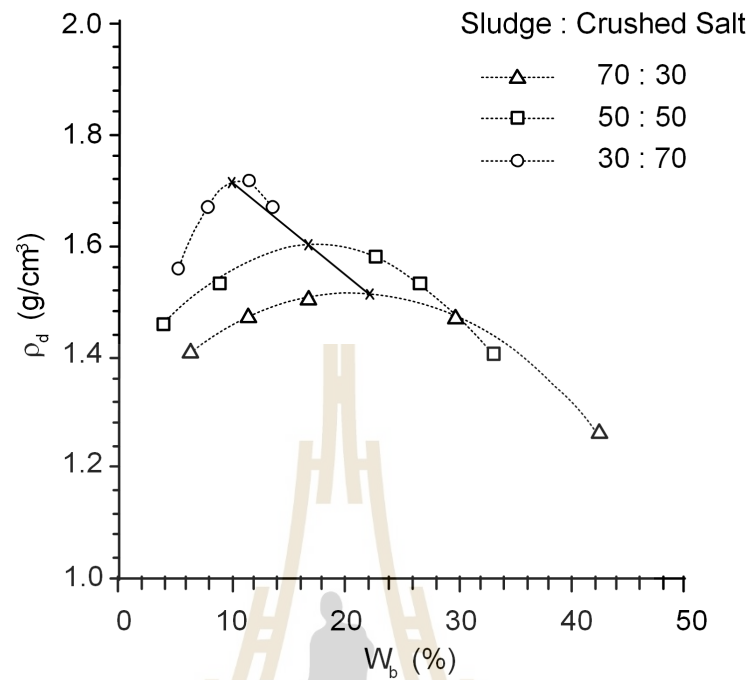


Figure 4.1 Dry density as a function of brine content (W_b)

Table 4.1 Results of compaction test.

Sludge (S) : Crushed salt (C)	Optimum brine content (%)	Maximum dry density (ton/m ³)
70:30	22.9	1.51
50:50	18.0	1.59
30:70	9.1	1.73

(2004), Charlermyanont and Arrykul (2005), Soltani-Jigheh and Jafari (2012) and Zhang et al. (2012).

4.3 Direct shear test

4.3.1 Test method

The direct shear test is operated to investigate maximum shear strengths of the sludge and crushed salt mixtures with the optimum brine after the

compaction in the three-ring mold. Figure 4.2 displays the direct shear test frame improved for the three-ring mold. The main parts for the shear test frame are the system of lateral load and vertical load for pushing the middle ring and applying a constant normal load on the compacted sample, respectively. After compaction process, the clamps of the three-ring mold are displaced, and the mold is put into a direct shear load frame. A hydraulic load cell is used for applying normal and shear force. The used normal stresses are 0.2, 0.4, 0.6 and 0.8 MPa. The shear stress is applied. The shear displacement and dilation are read for every 0.1 mm. Equations (4.4) and (4.5) are used to calculate normal stress and shear stress in order:

$$\tau = F/2A \quad (4.4)$$

$$\sigma_n = P/A \quad (4.5)$$

which τ is the shear stress, F is sheared force, A is area of sample, σ_n is normal stress and P is normal load.

The cohesions and friction angles of the compacted mixtures under their optimum NaCl brine content are shown in the form of the Coulomb's criterion. It can be demonstrated as Equation (4.6):

$$\tau = c + \sigma \tan \phi \quad (4.6)$$

which τ and σ are the shear stress and normal stress, ϕ is the angle of internal friction, and c is cohesion.

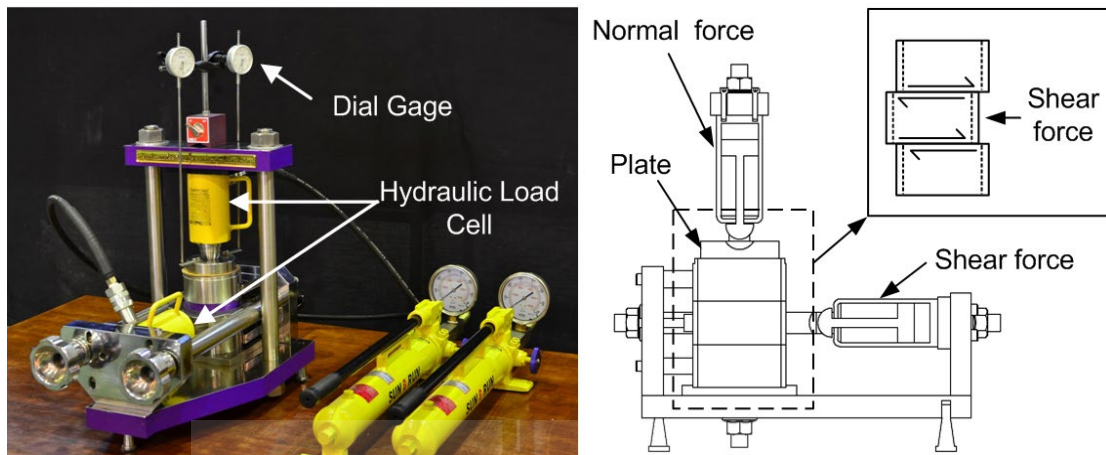


Figure 4.2 Direct shear test frame for three-ring mold (Sonsakul and Fuenkajorn, 2013).

4.3.2 Direct shear test results

The shear stresses in terms of shear displacement are shown in Figure 4.3. The shear stresses increase with shearing displacement, especially under high normal stresses. The test results are displayed in forms of the shear strength as an operation of normal stress. The cohesion and friction angle can be calculated by using the peak shear strength. Figure 4.4 exhibits peak shear stresses as an operation of normal stresses with varying shear stresses. The shear stresses increase with shearing displacement, particularly under high normal stresses. The normal displacement (d_n) tend to increase with the shearing displacement (d_s). Table 4.2 displays the cohesion and friction angle provided by the test of direct shear. The results imply that the cohesion and friction angle decrease with an increasing percentages of sludge mixtures. These data agree understandably with the results from Kaya and Durakan (2004), Charlermyanont and Arrykul (2005), Soltani-Jigheh and Jafari (2012) and Zhang et al. (2012).

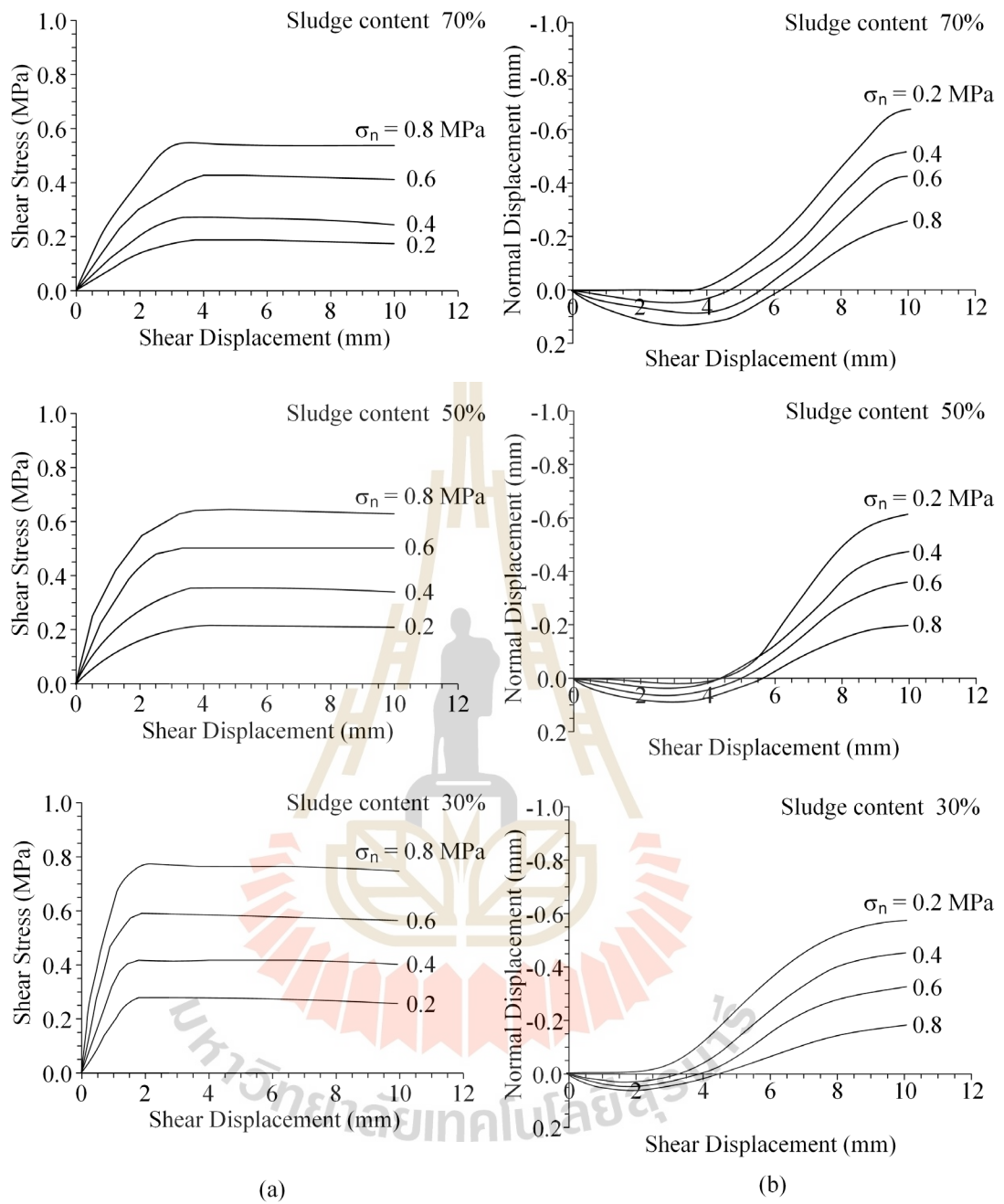


Figure 4.3 Shear stress (a) and normal displacement (b) for different shear displacement

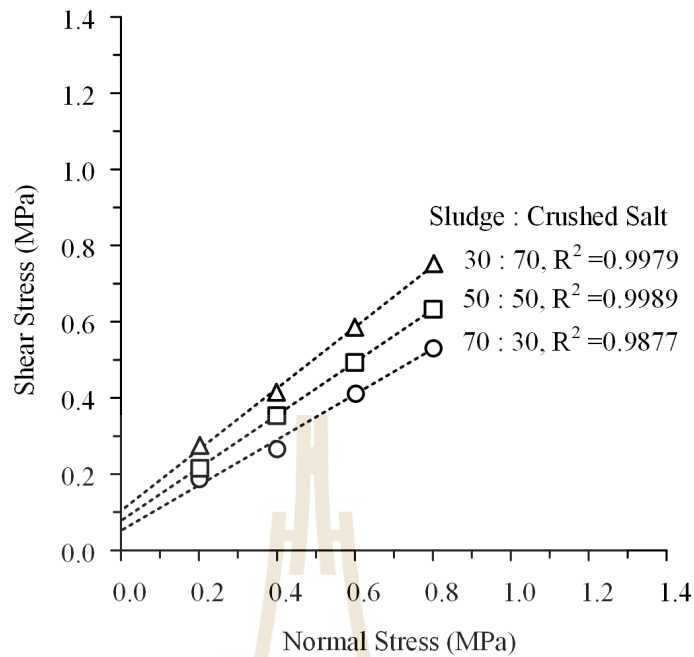


Figure 4.4 Shear strength as a function of normal stress

Table 4.2 Direct shear test results.

Sludge (S) : Crushed Salt (C)	c (kPa)	ϕ (degrees)	R ²
70:30	55	31	0.9877
50:50	80	35	0.9989
30:70	110	39	0.9979

4.4 Consolidation test

4.4.1 Test method

Consolidation tests are operated on the mixtures under previous obtained optimum brine content. An applying of constant axial stresses on loading steel piston to the mixtures set up in the three-ring mold (Figure 4.5) The constant axial stresses are ranging from 2.5, 5.0, 7.5 to 10.0 MPa for 0, 7, 15 and 30 days. All tests are performed under ambient temperature. The axial displacements are observed

using high precision dial gages ($\pm 0.001\text{mm}$). The axial displacements are applied to calculate the axial (consolidation) strains. The consolidation magnitude (axial strains, ϵ_{ax}) can be obtained using the equation as follows:

$$\epsilon_{ax} = \Delta L/L \quad (4.7)$$

which ϵ_{ax} is axial strain of consolidated sludge-crushed salt mixture (mm/mm), ΔL are length change overtime (mm), and L is initial length of the installed specimens.

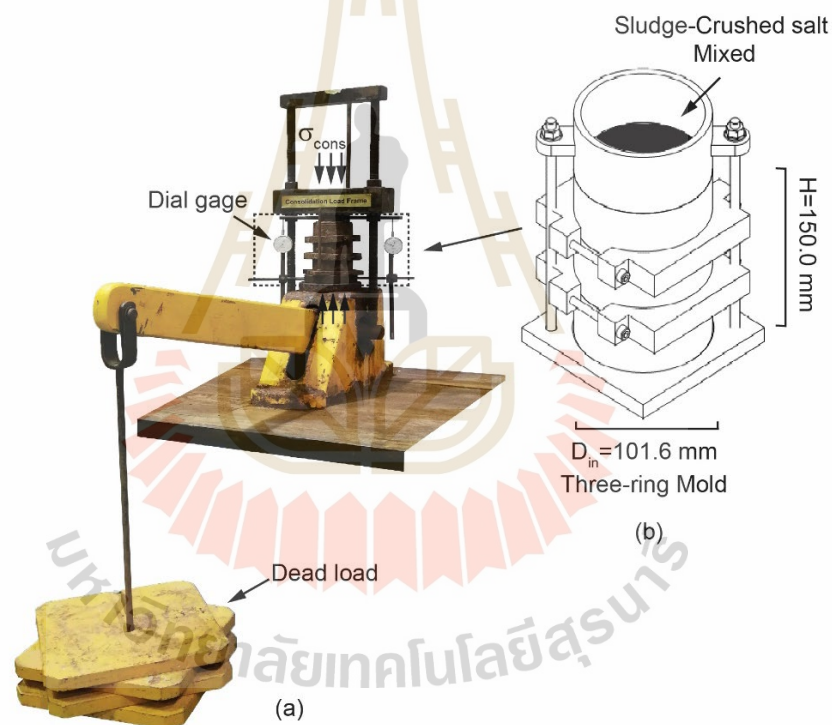


Figure 4.5 Test arrangement for consolidation testing.

4.4.2 Consolidation test and results

The axial displacements are applied to calculate the axial (consolidation) strains (ϵ_{axial}) with data up to 30 days as shown in Figure 4.6. The results indicate that ϵ_{cons} increase with sludge contents along with consolidation

stresses (σ_{cons}) and consolidation time. The increasing of ϵ_{cons} occurs rapidly after the application of axial stress with constant rate for all σ_{cons} . The ϵ_{axial} rates of 30% and 50% sludge content specimens decrease slowly with time and tend to remain constant after 15 days. The strain rates of 70% sludge mixtures have a tendency of time independent. This might attribute from an elastic silt and cohesionless properties of the sludge. Moreover, particle size of sludge is smaller than 0.047 mm that could fill and reduce void between crushed salt grains (Shor et al., 1981).

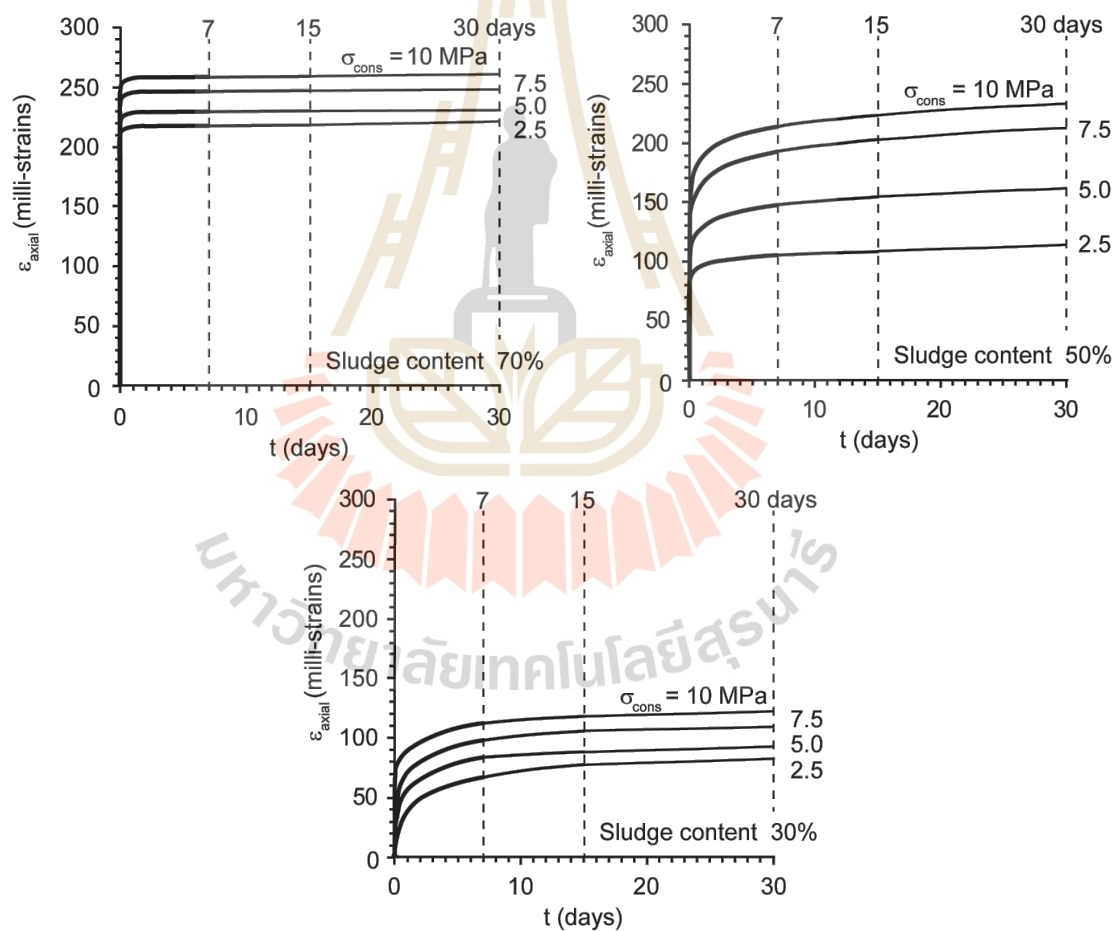


Figure 4.6 Axial (consolidation) strain (ϵ_{cons}) as a function of time (t) for different consolidation stresses (σ_{cons}). Dash lines indicate time at which each specimen is removed from three-ring mold.

4.5 Uniaxial compressive strength test

4.5.1 Test method

The compressive strength of the compacted mixtures under the optimum brine content before and after consolidation process can be investigated by the removing the specimen from the three-ring mold. The top and bottom ends of specimen are cut to provide flat and parallel surfaces. The specimens contain nominal diameter of 101.6 mm and the length-to-diameter ratios are approximately 2 to 3 (Figure 4.7). The density of specimen is determined before compression testing. Neoprene sheets are applied to reduce the friction at the interfaces between the loading platen and sample surface. Then, the compressive strengths are obtained by axially loading under constant rate of 0.5-1 MPa/second until the failure of specimens are occurred. The axial and lateral displacements are monitored through the dial gage (Figure 4.8). The compressive strength, the elastic modulus (E_{sec}) and Poisson's ratio are determined according to the ASTM (D7012-14e1) standard practice and the ISRM suggested method (Brown, 1981).



Figure 4.7 Sludge-crushed salt mixture specimens after consolidation.

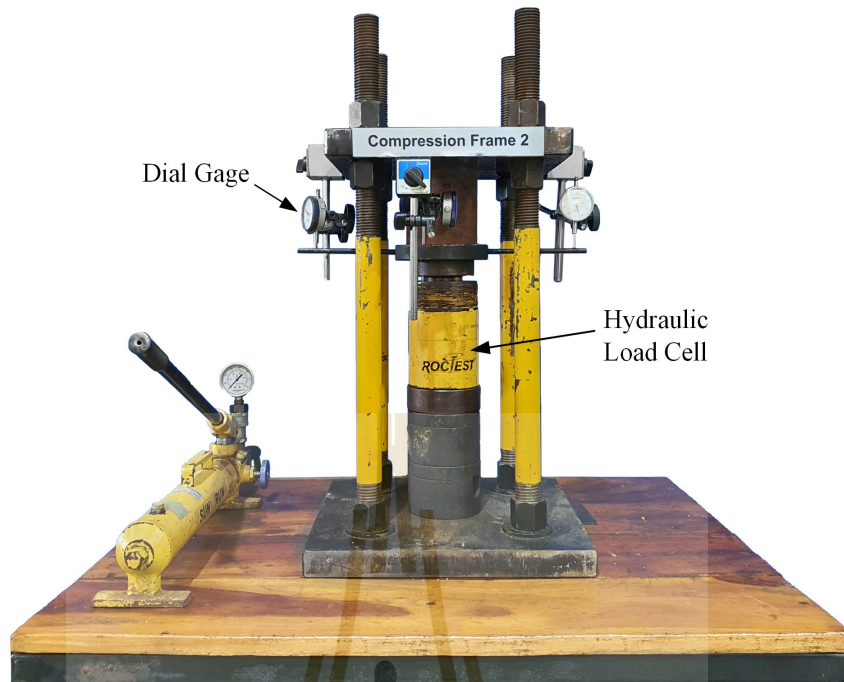


Figure 4.8 Uniaxial compressive strength device.

4.5.2 Uniaxial compression test results

Figure 4.9 shows some specimen of sludge-crushed salt mixture after the test of uniaxial compressive strength. The elastic modulus and Poisson's ratio are analyzed at around 50% of the failure stress (Figures 4.10 to 4.13) obtained by uniaxial stress-strain curves. The results from Figure 4.14 indicate that the density, strength and stiffness of the specimen decreases with an increasing of sludge content. Meanwhile, the density increases with increasing consolidation stresses and consolidation time. The results of Figures 4.15 through 4.17 imply that the compressive strength, elastic modulus and Poisson's ratios decrease with increasing of sludge content. While with an increasing of axial stress and consolidation time, the uniaxial compressive strength and elastic modulus values increase but the Poisson's ratios decrease. Table 4.3 presents the values of uniaxial test results including

consolidation stresses (σ_{cons}), consolidation time (t), Poisson's ratio (ν), Elastic modulus (E), uniaxial compressive strengths (σ_c) and density (ρ). The results suggest that longer consolidation time can make the specimen denser, stiffer and stronger. In general, this perform agrees with the conditions drawn by Wang et al. (1996) and Miao et al. (1995) who operated uniaxial compression test on compacted crushed salt specimens. Even though the increase of sludge content reduces the strengths and elastic modulus of the mixtures, it makes the mixtures less sensitive to consolidation time, i.e. the consolidation rate decreases with increasing sludge content.

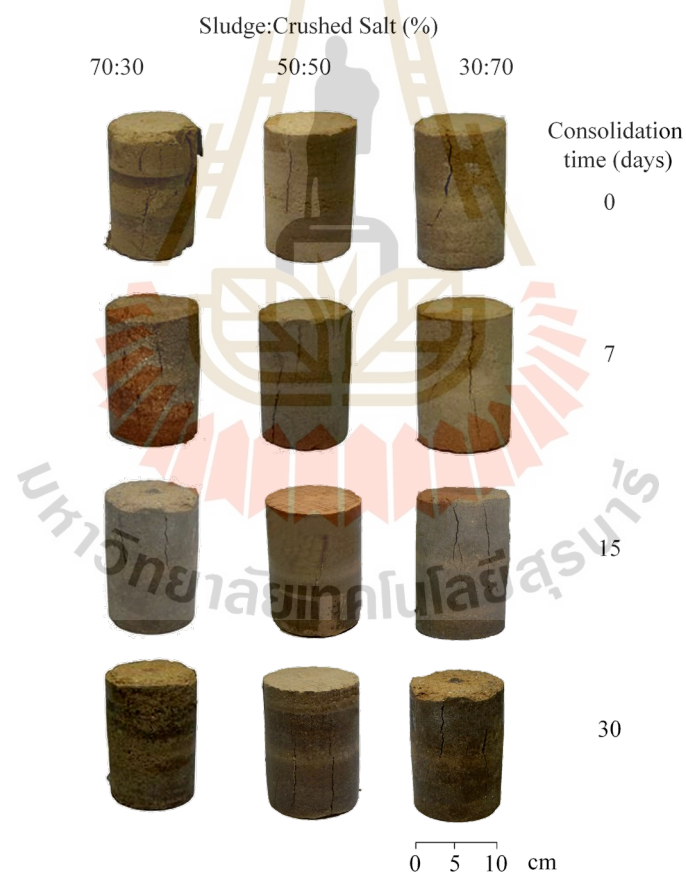


Figure 4.9 Some post-tested sludge-crushed salt mixture specimens after uniaxial compressive strength testing.

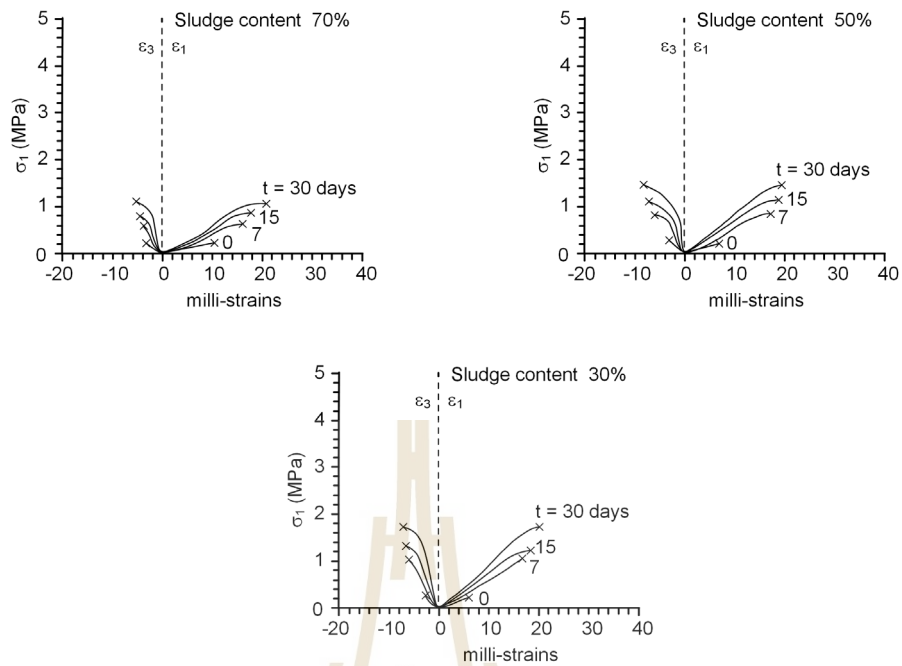


Figure 4.10 Uniaxial stress-strain curves of specimens after consolidation time (t) for consolidation stresses (σ_{cons}) 2.5 MPa.

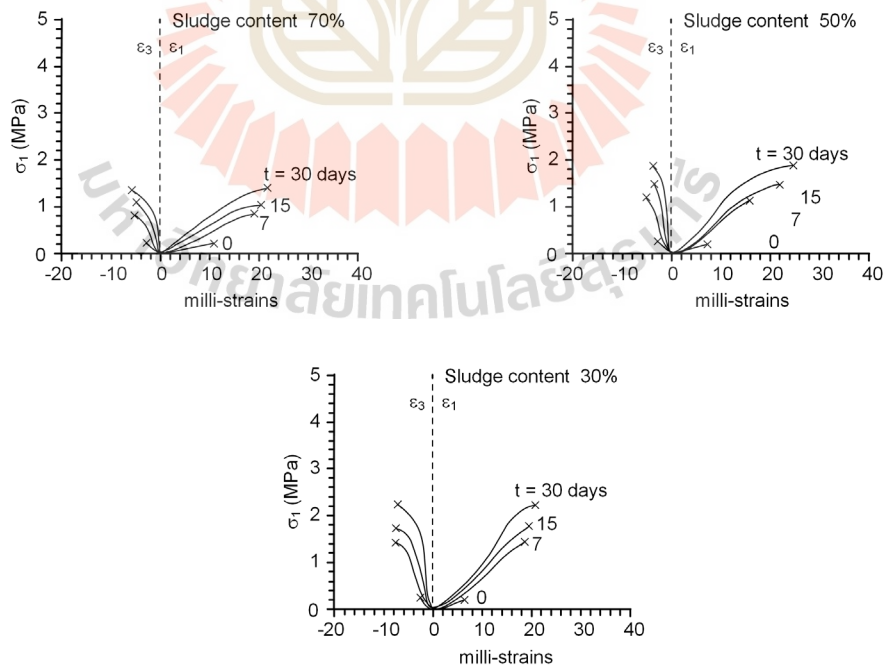


Figure 4.11 Uniaxial stress-strain curves of specimens after consolidation time (t) for consolidation stresses (σ_{cons}) 5.0 MPa.

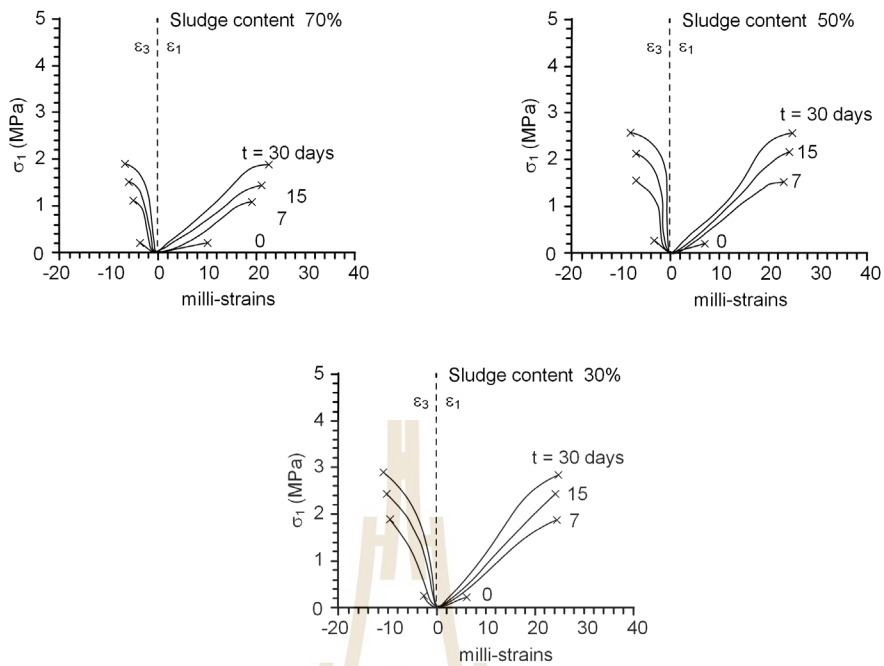


Figure 4.12 Uniaxial stress-strain curves of specimens after consolidation time (t) for consolidation stresses (σ_{cons}) 7.5 MPa.

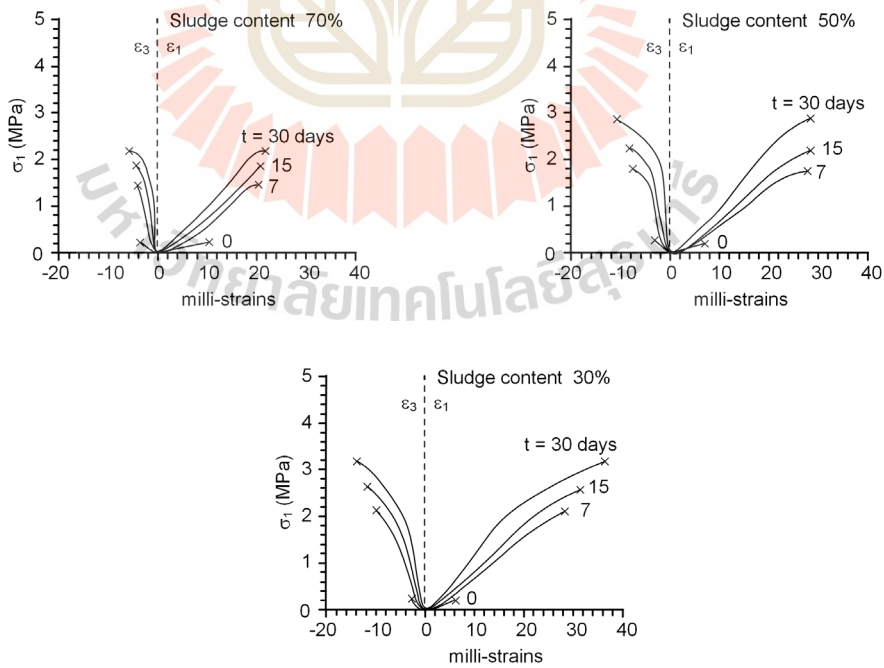


Figure 4.13 Uniaxial stress-strain curves of specimens after consolidation time (t) for consolidation stresses (σ_{cons}) 10.0 MPa.

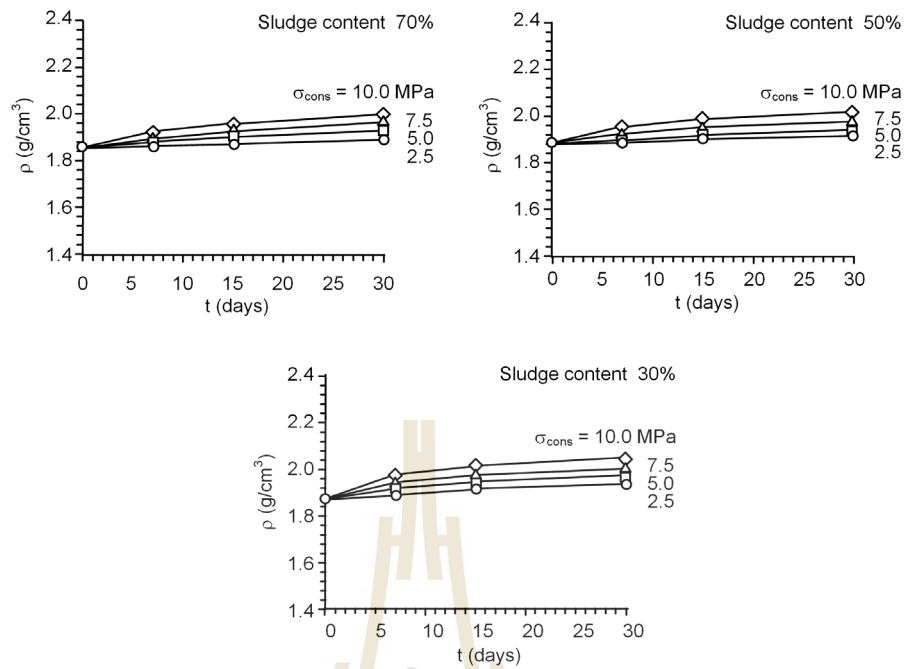


Figure 4.14 Density (ρ) as a function of consolidation time (t) for different consolidation stresses (σ_{cons}).

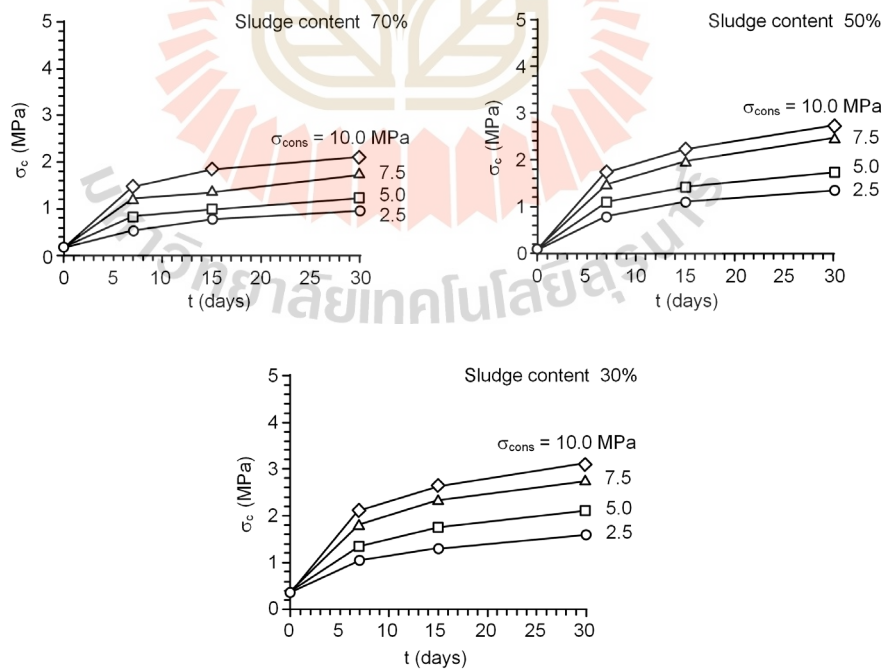


Figure 4.15 Uniaxial compressive strengths (σ_c) as a function of consolidation time (t) for different consolidation stresses (σ_{cons})

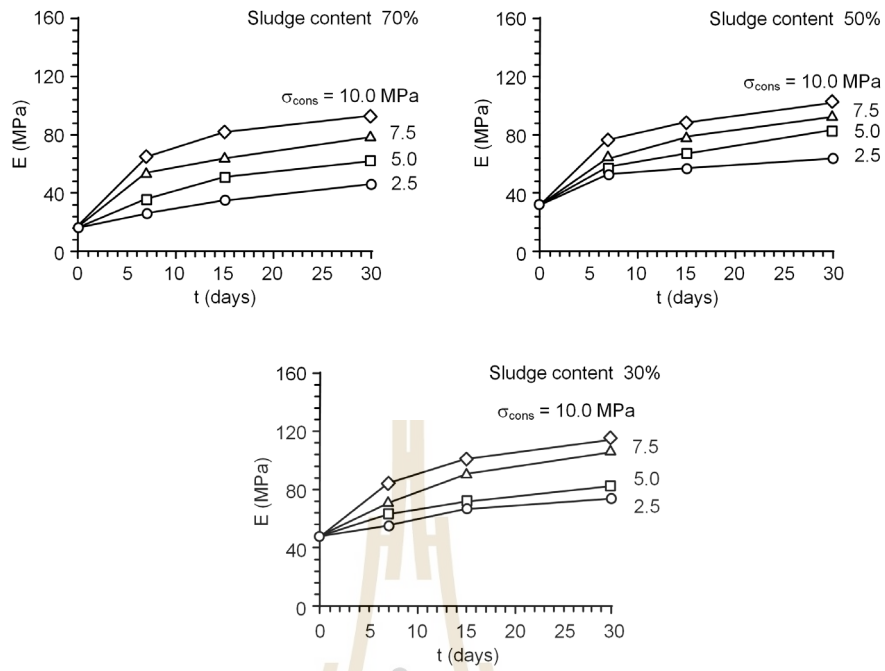


Figure 4.16 Elastic modulus (E) as a function of consolidation time (t) for different consolidation stresses (σ_{cons}).

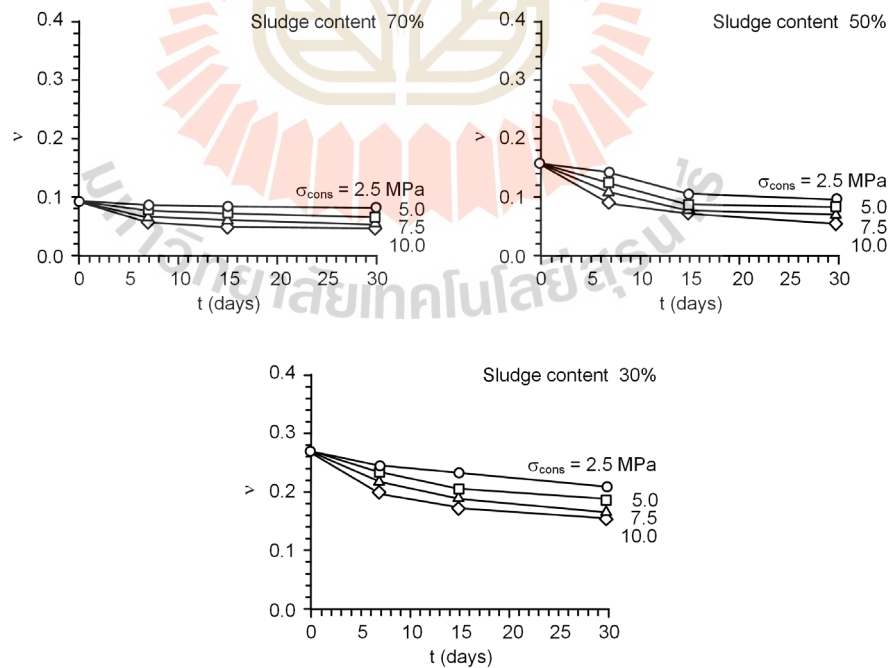


Figure 4.17 Poisson's ratio (ν) as a function of consolidation time (t) for different consolidation stresses (σ_{cons}).

Table 4.3 Uniaxial compressive test results.

Sludge (S) : crushed salt (C)	σ_{cons} (MPa)	t (days)	σ_c (MPa)	E (GPa)	ν	ρ (g/cm³)
70:30	0	0	0.09	0.017	0.09	1.86
	2.5	7	0.56	0.026	0.08	1.87
		15	0.81	0.035	0.08	1.91
		30	1.00	0.047	0.08	1.93
	5.0	7	0.87	0.036	0.08	1.88
		15	1.00	0.052	0.07	1.91
		30	1.25	0.062	0.06	1.93
	7.5	7	1.25	0.055	0.06	1.90
		15	1.37	0.064	0.06	1.93
		30	1.74	0.079	0.05	1.95
	10.0	7	1.49	0.065	0.06	1.92
		15	1.87	0.083	0.05	1.96
30		2.12	0.094	0.05	2.00	
50:50	0	0	0.19	0.032	0.16	1.87
	2.5	7	0.81	0.054	0.14	1.88
		15	1.12	0.058	0.11	1.90
		30	1.37	0.064	0.10	1.92
	5.0	7	1.12	0.059	0.13	1.90
		15	1.43	0.067	0.09	1.92
		30	1.74	0.084	0.08	1.94
	7.5	7	1.49	0.064	0.11	1.92
		15	1.99	0.080	0.08	1.95
		30	2.49	0.093	0.07	1.96
	10.0	7	1.74	0.077	0.09	1.95
		15	2.24	0.089	0.07	1.99
30		2.74	0.102	0.06	2.02	
30:70	0	0	0.31	0.047	0.27	1.88
	2.5	7	1.06	0.055	0.25	1.89
		15	1.31	0.067	0.23	1.92
		30	1.62	0.073	0.21	1.94
	5.0	7	1.37	0.063	0.24	1.90
		15	1.74	0.071	0.20	1.93
		30	2.12	0.082	0.19	1.95
	7.5	7	1.87	0.071	0.22	1.94
		15	2.37	0.091	0.19	1.97
		30	2.74	0.106	0.16	1.98
	10.0	7	2.12	0.085	0.20	1.98
		15	2.62	0.101	0.17	2.01
30		3.11	0.114	0.15	2.05	

4.6 Scanning Electron Microscopy Analysis

4.6.1 Test method

Scanning electron microscope (SEM) model, JEOL JSM-6010LV, is used to observe the microstructures of specimens before and after consolidation process. SEM technique provides a focused beam of electron that could interact and scan the material surface then produce images of a sample (Figure 4.18). The scanning electron beam is ordinarily a raster pattern, and position of the beam is combined with the detected signal to create a micrograph from various signals that carry information about the surface topography. SEM can achieve resolution greater than 1 nanometer

All specimens are prepared to have nominal dimensions of $1 \times 1 \times 1 \text{ cm}^3$ that is appropriate size to place on SEM sample holder (Figure 4.19). The specimens are oven dried at $105 \pm 5^\circ\text{C}$ for 24 hours. They are coated with the gold film for turning into an electrically conducting material. The samples are prepared to tolerate the vacuum circumstance and the high energy of electron beam.

Three sets of sludge: crushed salt mixtures: including 70:30, 50:50 and 30:70 by weight, are observed under SEM. All specimens are compacted to obtain maximum dry density and at optimum brine content. Each specimen is scanned in both before and after 30 days of consolidation. The different consolidation stress of 2.5MPa and 10.0 MPa are selected to study the recrystallization behavior microscopically through SEM analysis.



Figure 4.18 JEOL JSM-6010LV scanning electron microscope used in this study.

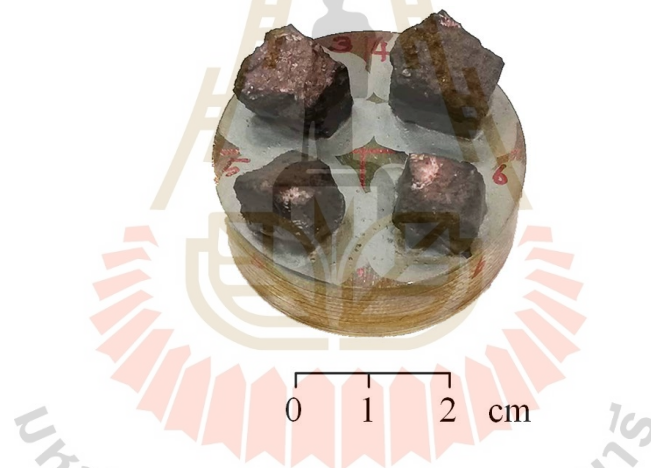


Figure 4.19 Some specimens prepared for scanning electron microscope (SEM).

4.6.2 Test Results

Table 4.4 shows the SEM images of the compacted specimens at 30 day-consolidated specimens of all ratios. Under consolidation pressure of 2.5 MPa, micrographs of all ratios reveal the crystal aggregation of salt. The increasing of crushed salt in the mixture under higher pressure of 10 MPa provides more aggregation with larger size of crystal that can be clearly seen from SEM observation.

However, the crystal shape cannot be identified in all cases due to the mixed morphology of the specimens.

The changes of properties in crushed salt might be attributed from two main mechanisms: consolidation and recrystallization. They govern the correlation between crushed salt properties and the applied mean strain energy density. The first mechanism concerns with the particle rearrangement, creep, cracking and sliding between grain boundaries of salt from volumetric reduction after applying stress (consolidation). The second mechanism is recrystallization between salt particles. This mechanism does not reduce the volume of crushed salt. However, it can stiffen and strengthen the specimen as the consolidation stress increases.

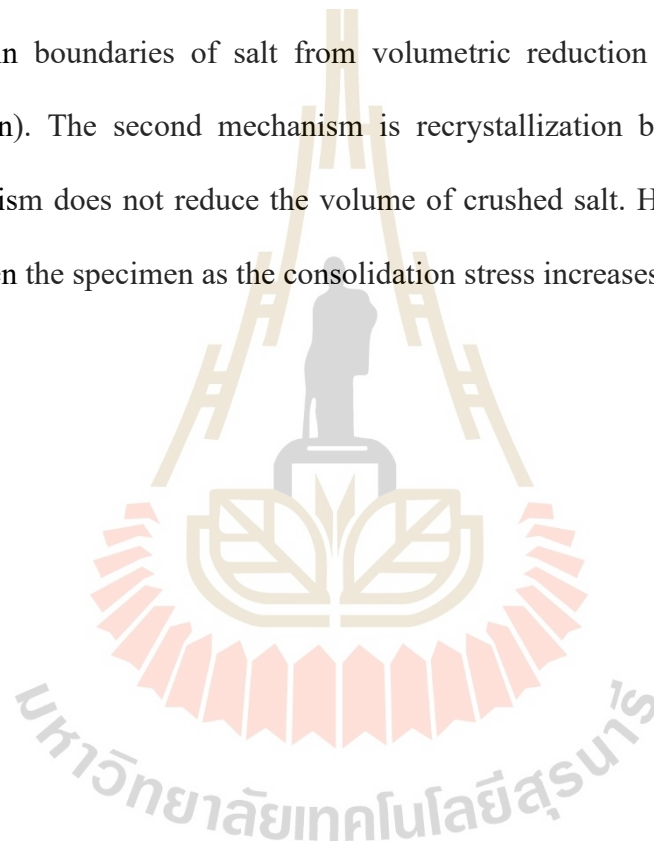
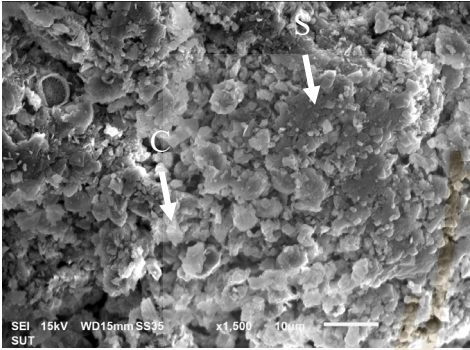
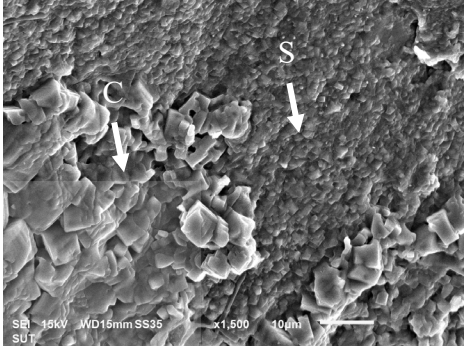
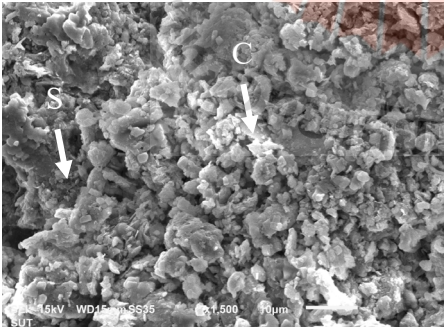
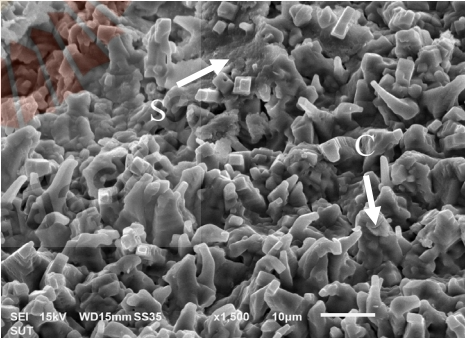
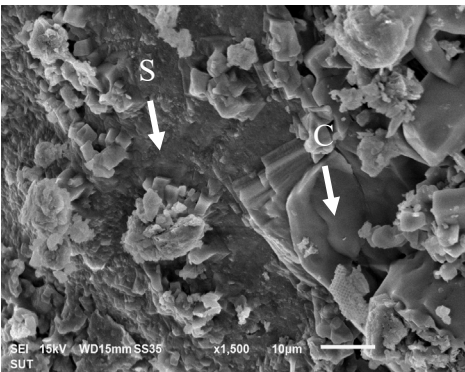
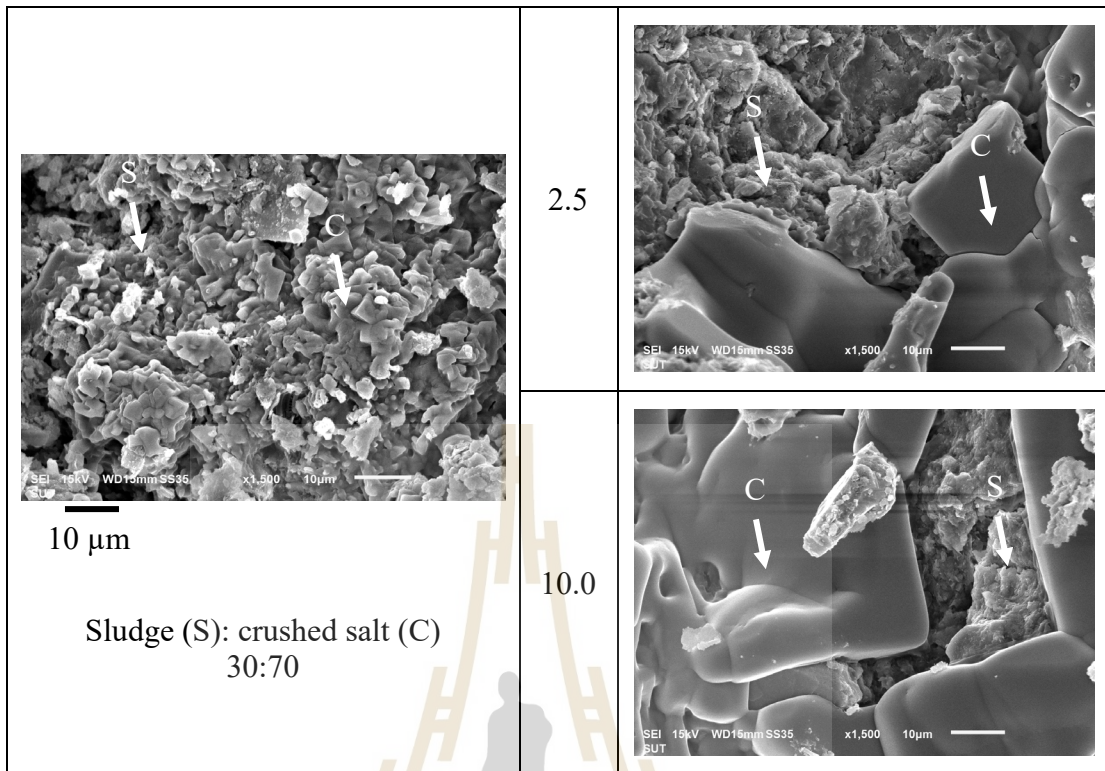


Table 4.4 SEM images of specimen under different consolidation stresses (σ_{cons}) at consolidation time (t) 30 days

After compaction with optimum brine contents	σ_{cons} (MPa)	t = 30 days
 <p data-bbox="331 1025 419 1066">10 μm</p> <p data-bbox="368 1111 727 1178">Sludge (S): crushed salt (C) 70:30</p>	2.5	
 <p data-bbox="344 1731 432 1771">10 μm</p> <p data-bbox="368 1816 727 1883">Sludge (S): crushed salt (C) 50:50</p>	10.0	 



CHAPTER V

DEVELOPMENT OF EMPIRICAL EQUATIONS

5.1 Introduction

A set of empirical equations are developed from test results to consider the mean strain energy and consolidation time. SPSS Statistics 19 software (Wendai, 2000) is used to determine the empirical constants. This allows predicting the sludge-crushed salt mixture behavior under various applied stress states.

5.2 Mean strain energy density of sludge-crushed salt mixtures

The sludge-crushed salt properties are correlated with the applied mean strain energy density during consolidation. It is first postulated that they are two main mechanisms controlling the changes of the properties of crushed salt: consolidation and recrystallization (Callahan et al., 1998). The first one relates to the volumetric decrease of the crushed salt by particle rearrangement, creep, cracking and sliding between crystal boundaries. It is shown as instantaneous and transient deformations which are governed by the energy. The second mechanism involves recrystallization and healing between salt particles (Hwang et al., 1993; Hansen, 1997). This mechanism does not reduce the crushed salt volume. It will stiffen and strengthen the specimens as increasing consolidation time.

5.2.1 Sludge-Crushed salt density

The empirical equations proposed in this section are based on the concept defined above. The change of sludge-crushed salt mixture density (ρ)

can be defined as:

$$\rho = \rho_{\text{initial}} + \Delta\rho_{\text{cons}} \quad (5.1)$$

where ρ_{initial} is the initial density and $\Delta\rho_{\text{cons}}$ is the reduction of density caused by the increase of strain energy and consolidation time. Regression analysis of the measurement results by SPSS software (Table 5.1) determines $\Delta\rho_{\text{cons}}$ as a function of mean strain energy and time as:

$$\Delta\rho_{\text{cons}} = a \cdot W_m^\alpha \cdot t^\beta \quad (5.2)$$

where W_m is mean strain energy density (MPa), t is consolidation time (days) and a , α and β are material constants. Density of the sludge-crushed salt samples increases with the axial stresses and consolidation time, and decreases with increasing sludge content. Table 5.1 shows constant parameters obtained from regression analysis. Good correlation is obtained ($R^2 > 0.9$). Regression curves are compared with the test results in Figure 5.1. Here, the sludge-crushed salt density does not depend on the recrystallization and healing mechanisms because these processes do not decrease the specimen volume.

Table 5.1 Parameters of density relationship ($S\%$ = Sludge content by weight)

Parameters	Values		
	$S\% = 70\%$	$S\% = 50\%$	$S\% = 30\%$
$\rho_{\text{initial}} \text{ (g/cm}^3\text{)}$	1.859	1.868	1.884
a	0.037	0.052	0.081
α	0.601	0.550	0.510
β	0.944	0.760	0.736
R^2	0.989	0.966	0.959

5.2.2 Sludge-Crushed salt strength

The strength of sludge-crushed salt mixtures (σ_c) is affected by both consolidation energy and time. The strengths resulting from the two factors can be superimposed as:

$$\sigma_c = \sigma_{\text{initial}} + \Delta\sigma_{\text{cons}} \quad (5.3)$$

where σ_{initial} is initial strength before applying the mean strain energy, and $\Delta\sigma_{\text{cons}}$ is the strength increase due to consolidation. They increase as increasing strain energy and time. The relationships can be described best by:

$$\Delta\sigma_{\text{cons}} = b \times W_m^\chi \times t^\delta \quad (\text{MPa}) \quad (5.4)$$

where W_m = mean strain energy (MPa), t is time for consolidation (days), b , χ and δ are material constants. The constants can be determined from regression analysis of the measurement results using equation (5.4). Unconfined compressive strength of the sludge-crushed salt samples increases with the decreasing sludge content, and increase with axial stresses and time. Regression analysis on the test results can determine these constants (Table 5.2). Good correlation ($R^2 > 0.9$) between the proposed equation and the test results is obtained. They are compared in Figure 5.2. It should be noted that under $W_m = 0$, the specimen strength continues to increase with time because of the processes of recrystallization and healing.

5.2.3 Elastic modulus of sludge-crushed salt

The elastic modulus of sludge-crushed salt mixtures (E) is governed by consolidation energy and time as well. Similar to the strength analysis, the elastic can

Table 5.2 Parameters of equation (5.4) ($S\%$ = Sludge content by weight)

Parameters	Values		
	$S\% = 70\%$	$S\% = 50\%$	$S\% = 30\%$
$\sigma_{c, \text{initial}}$ (MPa)	0.190	0.250	0.310
b	1.234	1.551	1.976
χ	0.283	0.300	0.30
δ	0.729	0.533	0.471
R^2	0.982	0.987	0.989

be separated into the parts:

$$E = E_{\text{initial}} + \Delta E_{\text{cons}} \quad (5.5)$$

where E_{initial} is initial elastic modulus (MPa) and ΔE_{cons} is the increase of elastic modulus during consolidation. The increase of elastic modulus can be defined as:

$$\Delta E_{\text{cons}} = c \times W_m^\phi \times t^\gamma \quad (5.6)$$

where W_m = mean strain energy (MPa), t is consolidation time (days), c , ϕ and γ are material constants. The constants can be calculated by the regression analysis on equation (5.5). Table 5.3 shows the numerical value of their constant parameters. Good correlation is obtained ($R^2 > 0.9$). Elastic modulus of the samples increases with decreasing sludge content and with increasing consolidation stresses and time. Regression curves are compared with the test results in Figure 5.3.

5.2.4 Sludge-Crushed salt Possion's ratio

The sludge-crushed salt Possion's ratio (ν) can also separated into two parts:

Table 5.3 Parameters of elastic modulus, time and energy relationship (S% = Sludge content by weight)

Parameters	Values		
	S% = 70%	S% = 50%	S% = 30%
E_{initial} (MPa)	16.687	31.587	47.306
c	40.365	38.871	37.237
φ	0.367	0.360	0.410
γ	0.798	0.550	0.561
R^2	0.981	0.976	0.972

$$v = v_{\text{initial}} + \Delta v_{\text{cons}} \quad (5.7)$$

where v_{initial} is initial Poisson's ratio before specimens subjected to mean strain energy and Δv_{cons} is the decrease of Poisson's ratio caused by the strain energy and consolidation time. The changes of the Poisson's ratio can be represented by:

$$\Delta v_{\text{cons}} = d \times W_m^v \times t^j \quad (5.8)$$

where W_m = mean strain energy (MPa), t is consolidation time (days), d , ϖ and ϑ are material constants. Table 5.4 shows the constant parameters from regression analysis. Good correlation ($R^2 > 0.9$) between the proposed equation and the tests is obtained. Poisson's ratio of the sludge-crushed salt samples increases with the sludge content, but decreases with increasing axial stresses and time. Figure 5.4 compares the regression curves with the test measurements.

Table 5.4 Parameters of Possion'ratio relationship ($S\%$ = Sludge content by weight)

Parameters	Values		
	$S\% = 70\%$	$S\% = 50\%$	$S\% = 30\%$
$V_{initial}$	0.091	0.160	0.271
d	0.037	0.050	0.113
ϖ	0.258	0.220	0.210
ϑ	0.891	0.272	0.482
R^2	0.980	0.904	0.923

The relationships between the mechanical properties of the sludge-crushed salt and its mean strain energy required during each consolidation time, as shown in Figures 5.1 - 5.4, can be used to predict the performance of sludge-crushed salt backfill under in-situ condition, as described in the following chapter. The properties of the compacted sludge-crushed salt after installation can be improved only if it is installed in the openings excavated in time-dependent rocks; such as salt and potash, where there is creep closure of the opening after excavation. The mechanical properties predictions are also sensitive to the creep parameters of the surrounding rock and the time at which the backfill is installed.

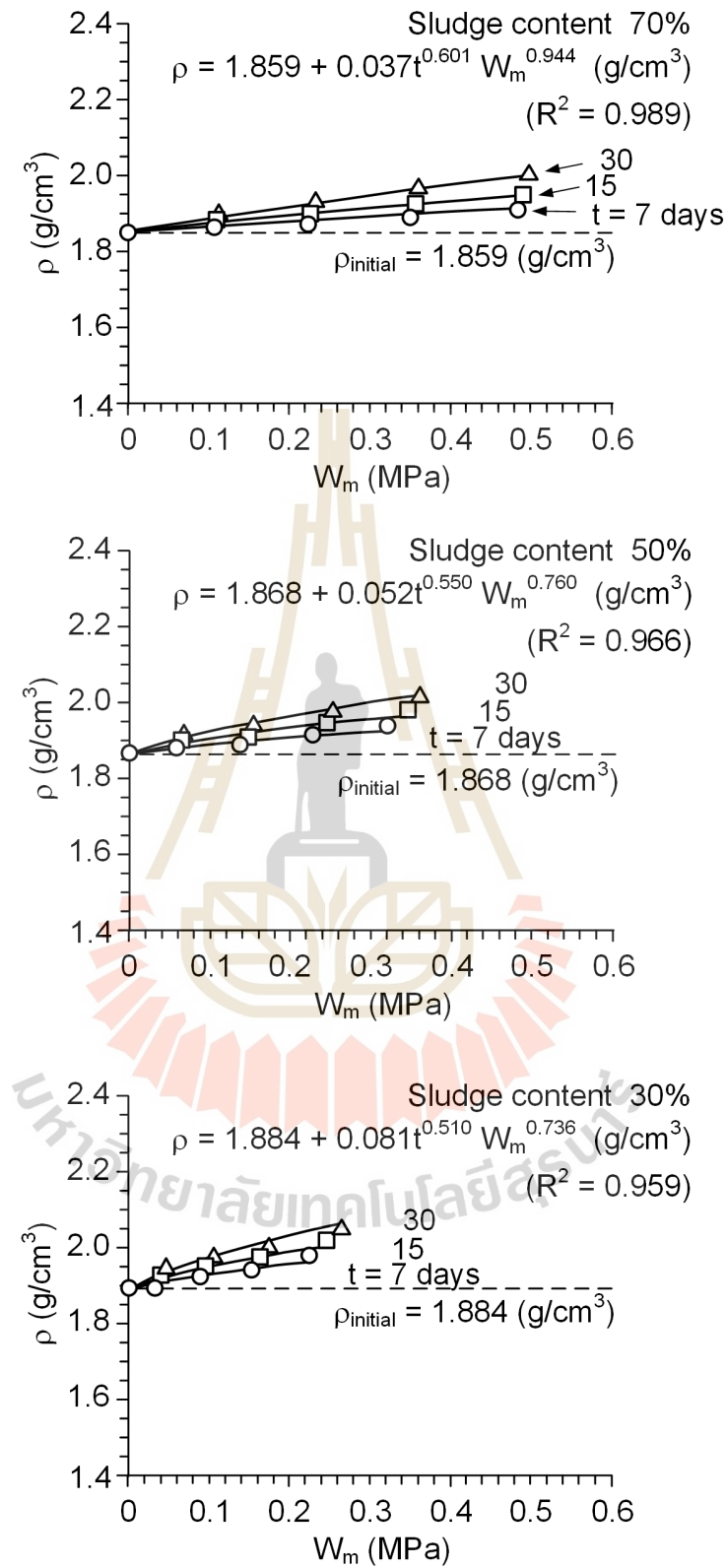


Figure 5.1 Density (ρ) in terms of mean strain energy (W_m) for different consolidation time (t)

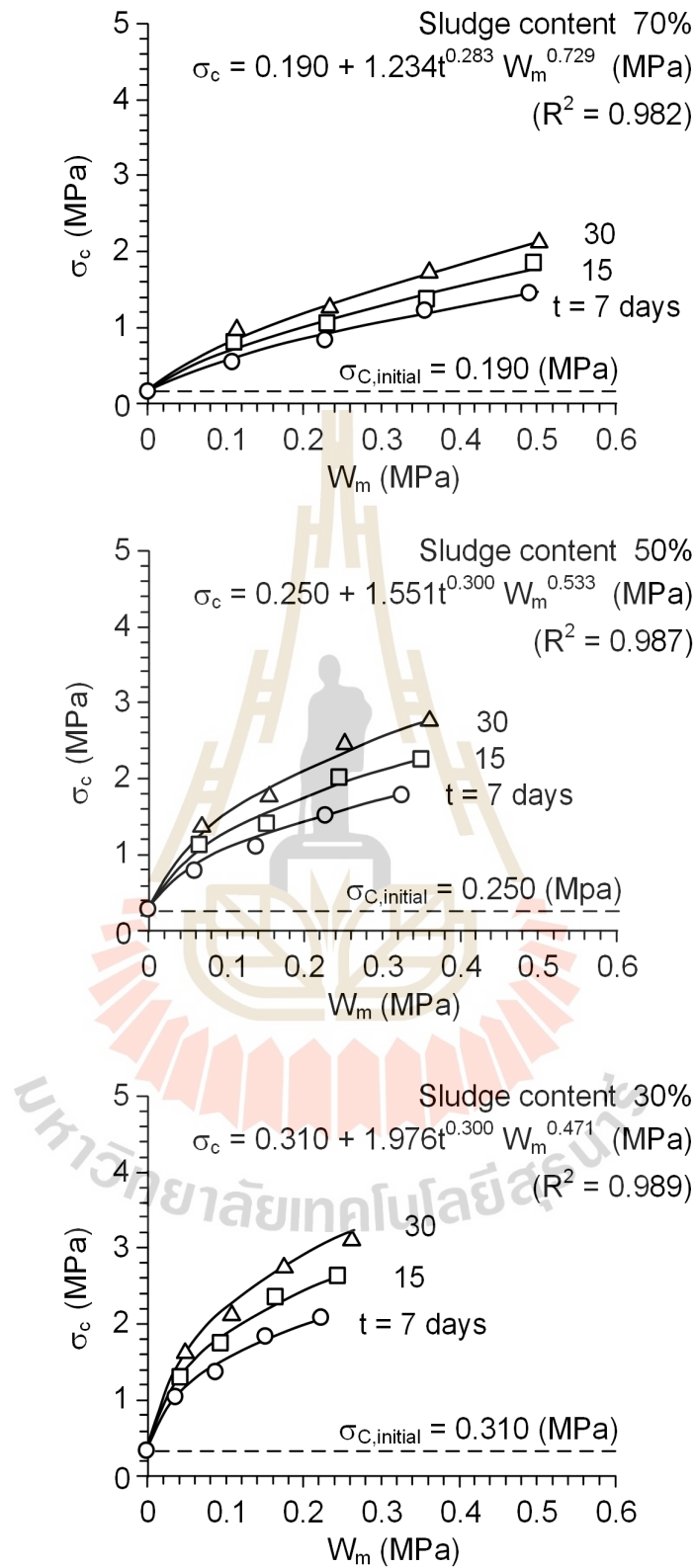


Figure 5.2 Uniaxial compressive strengths (σ_c) increases with increasing mean strain energy (W_m) for different consolidation time (t)

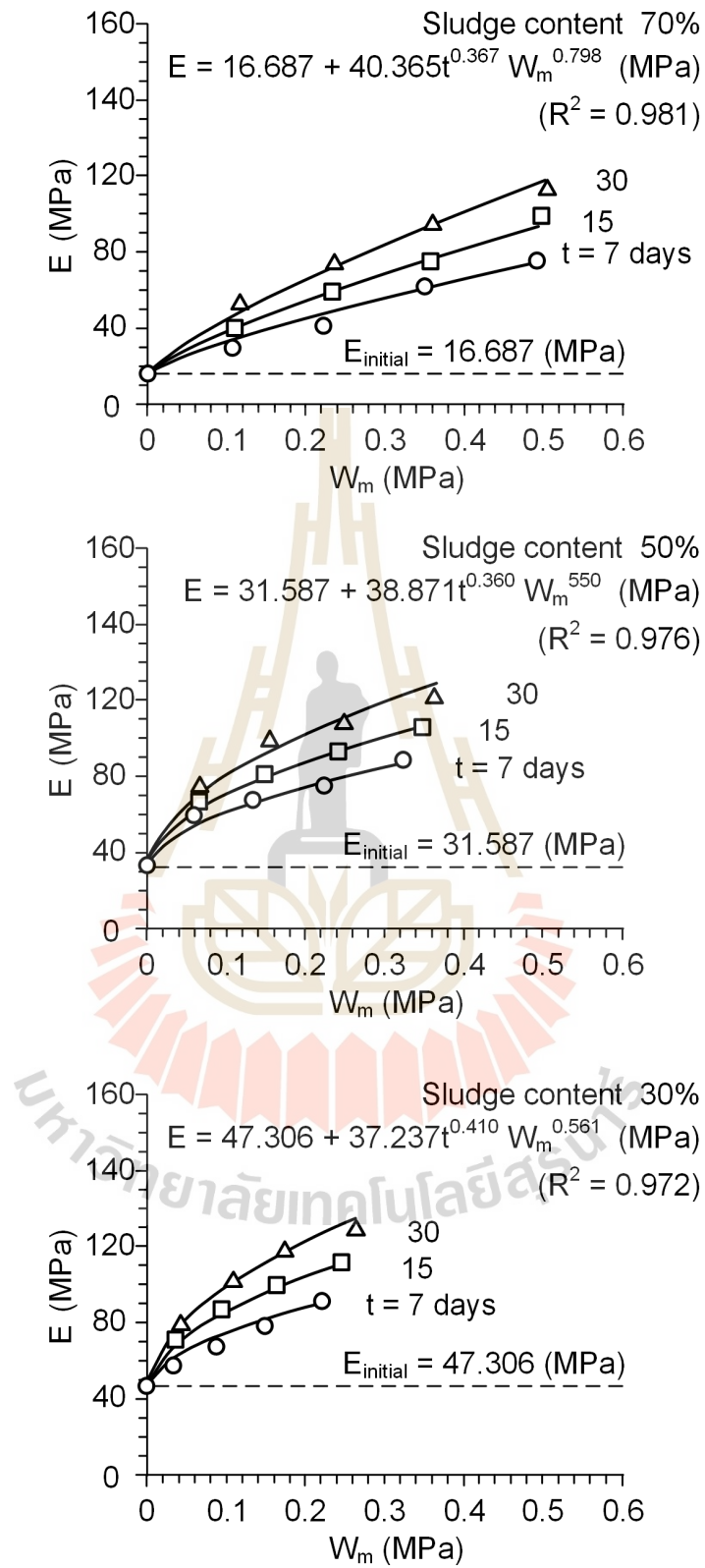


Figure 5.3 Elastic modulus (E) increases with increasing mean strain energy (W_m) for different consolidation periods (t)

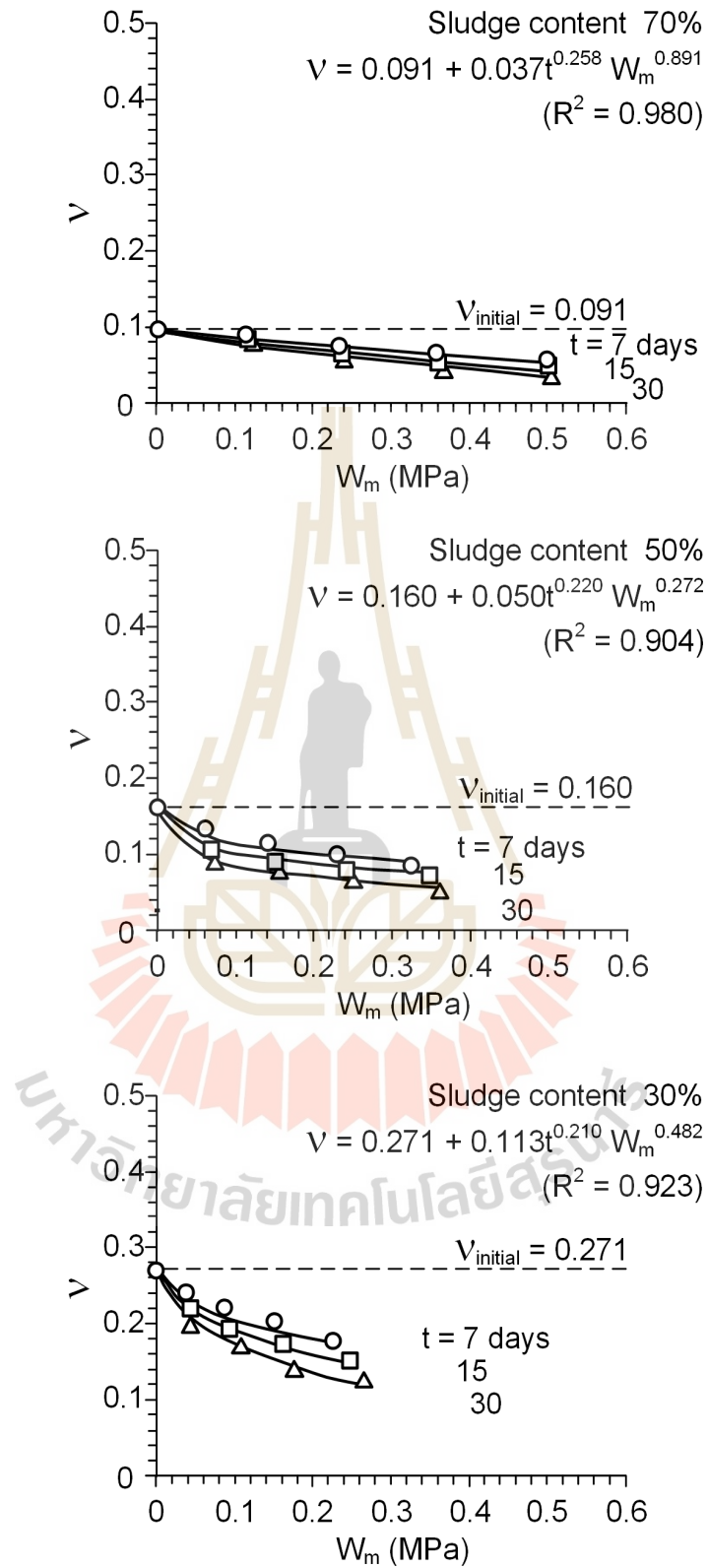


Figure 5.4 Poisson's ratio (ν) decreases with increasing mean strain energy (W_m) for different consolidation periods (t)

CHAPTER VI

PREDICTION OF BACKFILL PROPERTIES AFTER EMPLACEMENT

6.1 Introduction

The aim of this chapter is to demonstrate how to predict the mechanical behavior of sludge-crushed salt backfill after emplacing in salt or potash openings. The concept of mean strain energy is applied. To simplify the solutions, circular opening in infinite medium under uniform external stresses is assumed. The time-dependent deformation of salt and potash follows the potential creep law. Similar approach has been used by Khamrat et al. (2017).

6.2 Circular opening in salt and potash media under uniform external pressure

Mean strain energy induced by time-dependent deformation of circular opening in infinite medium under uniform in-situ stress is calculated to estimate the changes of sludge-crushed salt properties after installation. The strain energy released by the creep closure ($W_{m,s}$) can be determined from the stresses and strains at the opening boundary as (Jaeger et al., 2007):

$$W_{m,s} = \frac{3}{2} \left[\left\{ \frac{1}{3} (\sigma_r + \sigma_\theta + \sigma_z) \right\} \cdot \left\{ \frac{1}{3} (\varepsilon_r + \varepsilon_\theta + \varepsilon_z) \right\} \right] \quad (6.1)$$

where σ_r , σ_θ , and σ_z are radial, tangential and axial stresses, and ε_r , ε_θ and ε_z are radial, tangential and axial strains.

The stress distributions around opening wall can be calculated under plane strain condition by using the Kirsch's solution (Brady and Brown, 2006). Based on an elastic solution, the radial (σ_r) tangential (σ_θ) and axial (σ_z) stresses can be calculated by (Jaeger et al., 2007):

$$\sigma_r = \left(1 - \frac{a^2}{r^2}\right) P_o + P_i \left(\frac{a^2}{r^2}\right) \quad (6.2)$$

$$\sigma_\theta = \left(1 + \frac{a^2}{r^2}\right) P_o - P_i \left(\frac{a^2}{r^2}\right) \quad (6.3)$$

$$\sigma_z = \nu(\sigma_r + \sigma_\theta) \quad (6.4)$$

where a is radius, r is radial distance from the opening center, P_o and P_i are constant external and internal pressures. Here P_i is assumed to be zero (before backfill installation).

For a circular opening in time-dependent medium, the elastic and creep strains can be superimposed as:

$$\varepsilon_r = \varepsilon_r^e + \varepsilon_r^c \quad (6.5)$$

$$\varepsilon_z = \varepsilon_\theta = 0 \quad (6.6)$$

where ε_r^e is the radial strain in elastic mode and ε_r^c is the radial strain in creep mode caused by the time-dependent closure of the opening wall.

The elastic strain can be determined by (Jaeger et al., 2007):

$$\varepsilon_r^e = \frac{1}{E} \left[(1-\nu^2)\sigma_r - \nu(1+\nu)\sigma_\theta \right] \quad (6.7)$$

The radial creep strain around circular hole follows the potential creep law and under the associated flow rule as derived by Nair and Boresi (1970) and Fuenkajorn and Daemen (1988), as:

$$\varepsilon_r^c = \frac{3}{2} \kappa' (\sigma^*)^{(\beta'-1)} \cdot S_r (t_1^{\gamma'} - t_0^{\gamma'}) \quad (6.8)$$

where κ' , β' and γ' are material constants, S_r is the radial stress deviation, and σ^* is the equivalent (effective) stress, t_0 is time at which loading is applied and t_1 is time at which the strains are calculated. The stress deviation can be obtained from (Jaeger et al., 2007):

$$S_r = \sigma_r - \frac{1}{3}(\sigma_r + \sigma_\theta + \sigma_z) \quad (6.9)$$

From the von Mises flow rule, σ^* is determined as (Budynas et al., 2011):

$$\sigma^* = \frac{1}{\sqrt{2}} \left\{ (\sigma_r - \sigma_\theta)^2 + (\sigma_\theta - \sigma_z)^2 + (\sigma_z - \sigma_r)^2 \right\}^{\frac{1}{2}} \quad (6.10)$$

Substituting equations (6.2) through (6.10) into equation (6.1), the mean strain energy released at the opening boundary can be calculated.

To demonstrate the application of the mean strain energy from the circular opening in salt and carnallite, the mechanical and rheological parameters of the materials are needed (Table 6.1). They are obtained from Wilalak and Fuenkajorn (2016) as follows:

$$\kappa' = 0.0003 \cdot \exp(0.0255 \cdot C_{\%}) \quad 1/(\text{MPa} \cdot \text{day}) \quad (6.11)$$

$$\beta' = 1.3589 \cdot \exp(0.0005 \cdot C_{\%}) \quad (6.12)$$

$$\gamma' = 0.1941 \cdot \exp(0.003 \cdot C_{\%}) \quad (6.13)$$

where $C_{\%}$ is carnallite contents.

Table 6.1 Material parameters of Maha Sarakham salt with different carnallite contents (Wilalak and Fuenkajorn, 2016; Luangthip et al., 2016).

Parameters	Pure rock salt	Carnallite contents		
		10%	30%	50%
κ' ($\text{MPa}^{-1} \cdot \text{day}^{-1}$)	0.0003	0.0004	0.0006	0.0011
β'	1.43	1.37	1.38	1.39
γ'	0.601	0.200	0.212	0.226
E (GPa)	16.89	13.63	8.95	5.88
ν	0.27	0.28	0.32	0.36

The elastic parameters obtained from Luangthip et al. (2016), who derived the elastic modulus and Poisson's ratio as a function of carnallite contents, $C_{\%}$, as:

$$E = 16.81 \cdot \exp(-0.021 \cdot C_{\%}) \quad \text{GPa} \quad (6.14)$$

$$\nu = 0.002 \cdot C_{\%} + 0.26 \quad (6.15)$$

The released energy at the opening boundary is calculated for the external pressures of 6.5 and 12 MPa for rock salt (equivalent to the depths approximately of 240 and 450 m), and 8 and 9 MPa for potash (equivalent to the depths approximately of 300 and 350 m). Figures 6.1 and 6.2 plot the released strain energy ($W_{m,s}$) as a function of time after excavation. The released strain energy increases rapidly during the first year. The rate of releasing energy reduces with time. The higher external pressures lead to the larger released energy. Higher carnallite content yield higher released mean strain energy. This is principally caused by large creep strain owing to the low values of elastic and bulk moduli of the higher carnallite content salt. The diagrams indicate that the time at which the backfill is installed (t_B) is an important factor controlling the amount of released energy remaining for consolidating the sludge-crushed salt backfill. Quick installation leads to a larger amount of energy remaining for the backfill consolidation.

The strain energy principle allows incorporating both stress and strain to which the backfill is subjected after installation. This approach is considered more fundamental and simpler than those of complex creep and healing constitutive equations proposed elsewhere for the sealing of nuclear waste repository (Khamrat et al., 2017).

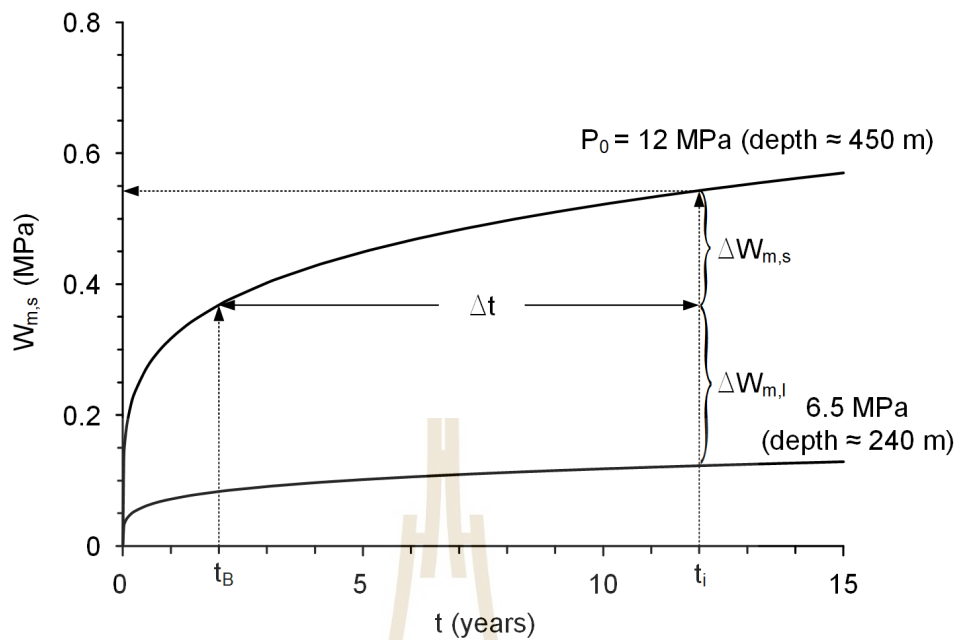


Figure 6.1 Mean strain energy density (W_m) released from time-dependent deformation of pure salt openings under different external pressures (P_0).

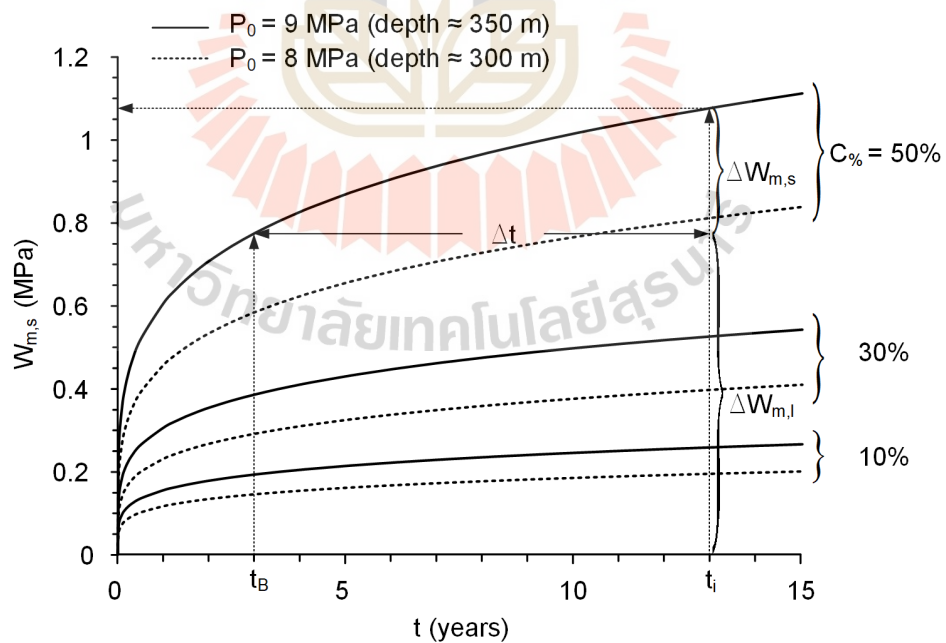


Figure 6.2 Mean strain energy density (W_m) released from time-dependent deformation of openings in potash with different carnallite contents ($C\%$).

6.3 Sludge-crushed salt properties after emplacement

The sludge-crushed salt properties after emplacement can be predicted by calculating the strain energy needed for consolidation. It can be obtained from:

$$\Delta W_{m,s} = W_{m,s} - W_{m,l} \quad (6.16)$$

where $W_{m,s}$ is the total released strain energy from excavation of any selected period (t_i) determined as if no backfill had been installed, and $W_{m,l}$ is the energy lost due to time-dependent deformation before backfill installation. For this demonstration, the $\Delta W_{m,s}$ at depths of 240 and 450 m are calculated for $t_B = 2$ and 4 years in salt mine. For potash, the $\Delta W_{m,s}$ at depths of 300 and 350 m are calculated for $t_B = 3$ years. The prediction period (Δt) is made up to 10 years. The time at which the backfill is emplaced is defined as t_B in Figures 6.1 and 6.2. The duration for consolidation (Δt) can be calculated from:

$$\Delta t = t_i - t_B \quad (6.17)$$

From equation (6.16), the remaining strain energy, $\Delta W_{m,s}$ can be determined as a function of Δt , as shown in Figure 6.3 for salt and potash openings. The results show that the $\Delta W_{m,s}$ increases with time (Δt). This is attributed from the fact that the released energy by time-dependent closure of the opening after backfill installation is contributed by the enhancement of the radial stresses and the reduction of the radial strain at the opening wall. This is generated from the mechanical interaction between the opening wall and the sludge-crushed salt backfill. The influence of t_B pronounces more under higher external pressure than under lower one. This suggests that the time

at which the backfill is installed is more critical for deep openings than for the shallow ones.

Substituting $\Delta W_{m,s}$ and Δt values from Figures 6.3 into W_m and t values in equations (5.1), the density, compressive strength elastic modulus and Poisson's ratio can be predicted, as shown in Figures 6.4 to 6.11. The predictions are made up to 10 years. The results show that the sludge-crushed salt density increases with time (Δt), and slightly increases with the increasing of sludge content from its initial value (Figures 6.4 to 6.5). The higher sludge content reduces the changes in properties of the mixtures. This is because the particle sizes of sludge are smaller than that of crushed salt. It can fill and reduce void between crushed salt grains. Hence, the mixture is compacted better than those in the pure crushed salt. The results agree with Shor et al. (1981), who studied the relationship between permeability, porosity with the initial grain size by consolidation mixture of crushed salt and brine. They found that the fine grains (0.02 cm) can reduce porosity and permeability better than the coarse grains (0.34 cm). These observations agree well with Akgün and Koçkar (2018) and Sonsakul et al. (2013), who investigated the mechanical and hydraulic performance of compacted bentonite-sand for using in underground waste disposal repositories. Their results show that the permeability decreases with the increasing of bentonite content.

Both σ_c and E increase, while ν decreases with increasing P_o and Δt (Figures 6.6 through 6.11). The sludge content reduces the strength and elasticity of the mixtures. In addition, higher sludge content backfill tends to be independent of time. Since the sludge is classified as elastic silt with over 90% of silica with grain size smaller than 0.047 mm and it is cohesionless material. While crushed salt is highly

sensitive to loading and is time-dependent material, which agrees with the results of Fuenkajorn and Daemen (1988), Wang et al. (1996), Miao et al. (1995), Fuenkajorn and Pueakphum (2010) and Samsri et al. (2010). The backfill Poisson's ratios decrease with time and sludge content. Large reduction of its Poisson's ratio is observed for low sludge content backfill, particularly those installed in potash mine (Figures 6.11). The application of the strain energy principle allows the considering of both stress and strain to the subjected sludge-crushed salt specimens. Two main mechanisms that simultaneously take place in the changes of crushed salt properties are consolidation and recrystallization. The crushed salt density is dependent on the consolidation which governed by the energy. The increasing of σ_c and E with the decreasing of ν from the applied mean strain energy and time are the results of the recrystallization and healing.

Under no W_m application, there values will remain unchanged. The property of sludge-crushed salt backfill can improve more for opening in rock salt with high carnallite contents than those in lower carnallite contents. This is because carnallite makes rock salt softer and results in a larger creep rate. The effects of t_B on the strength and elasticity act more for the backfill emplaced in deep openings than in the shallow ones.

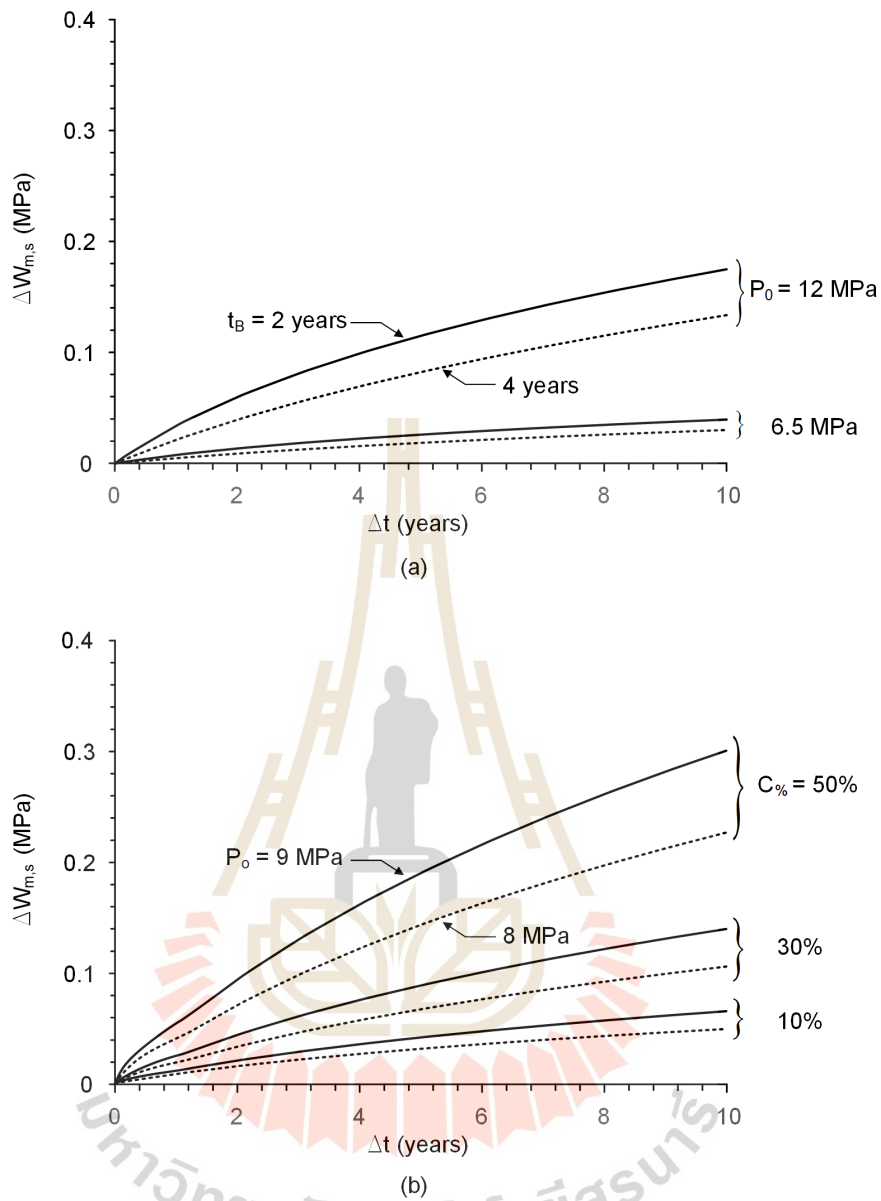


Figure 6.3 Remaining strain energy density (ΔW_m) as a function of time after backfill emplacement in salt (a) and potash (b) at year 3.

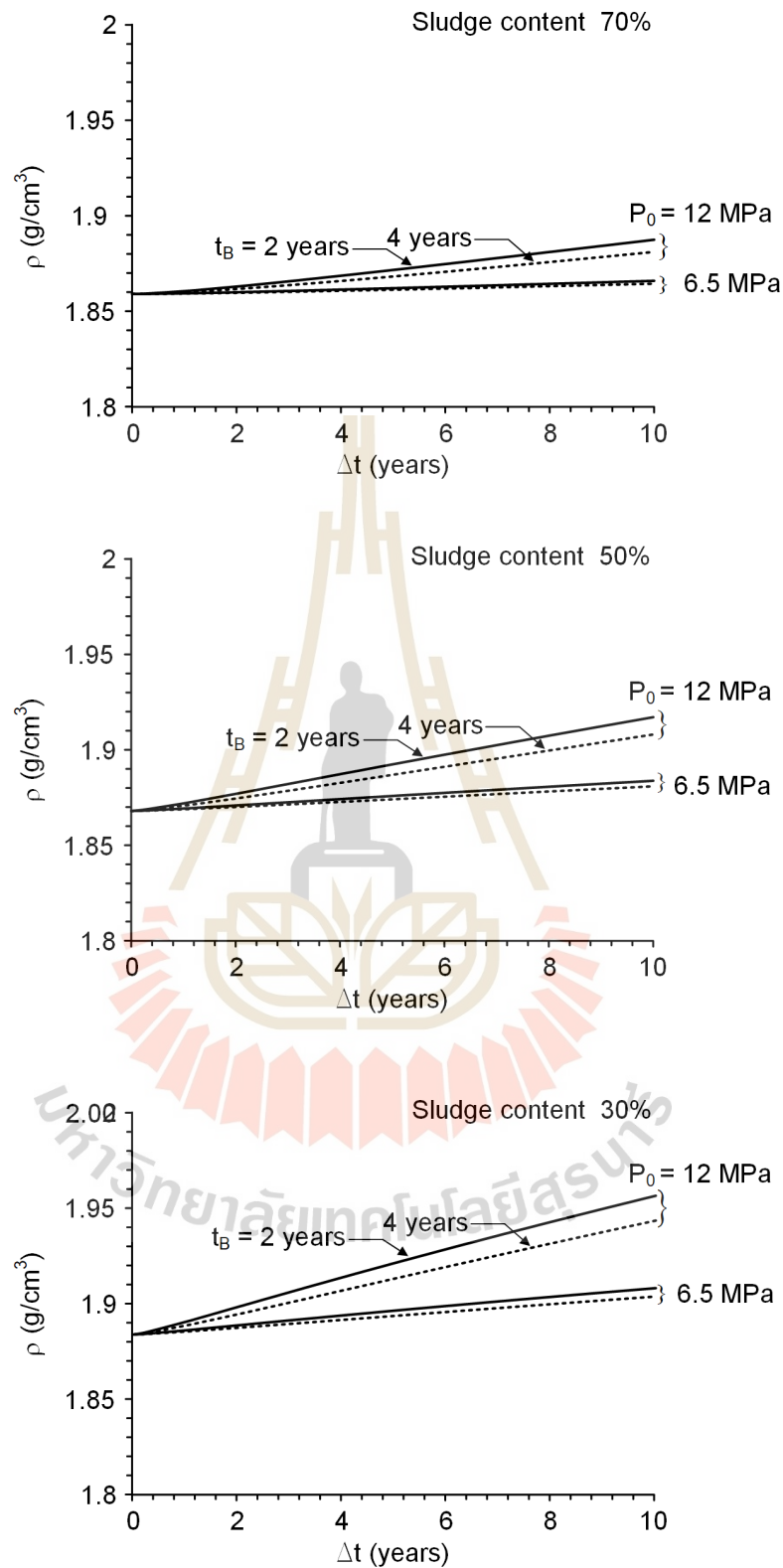


Figure 6.4 Density of different sludge content backfill as a function of time after emplacement.

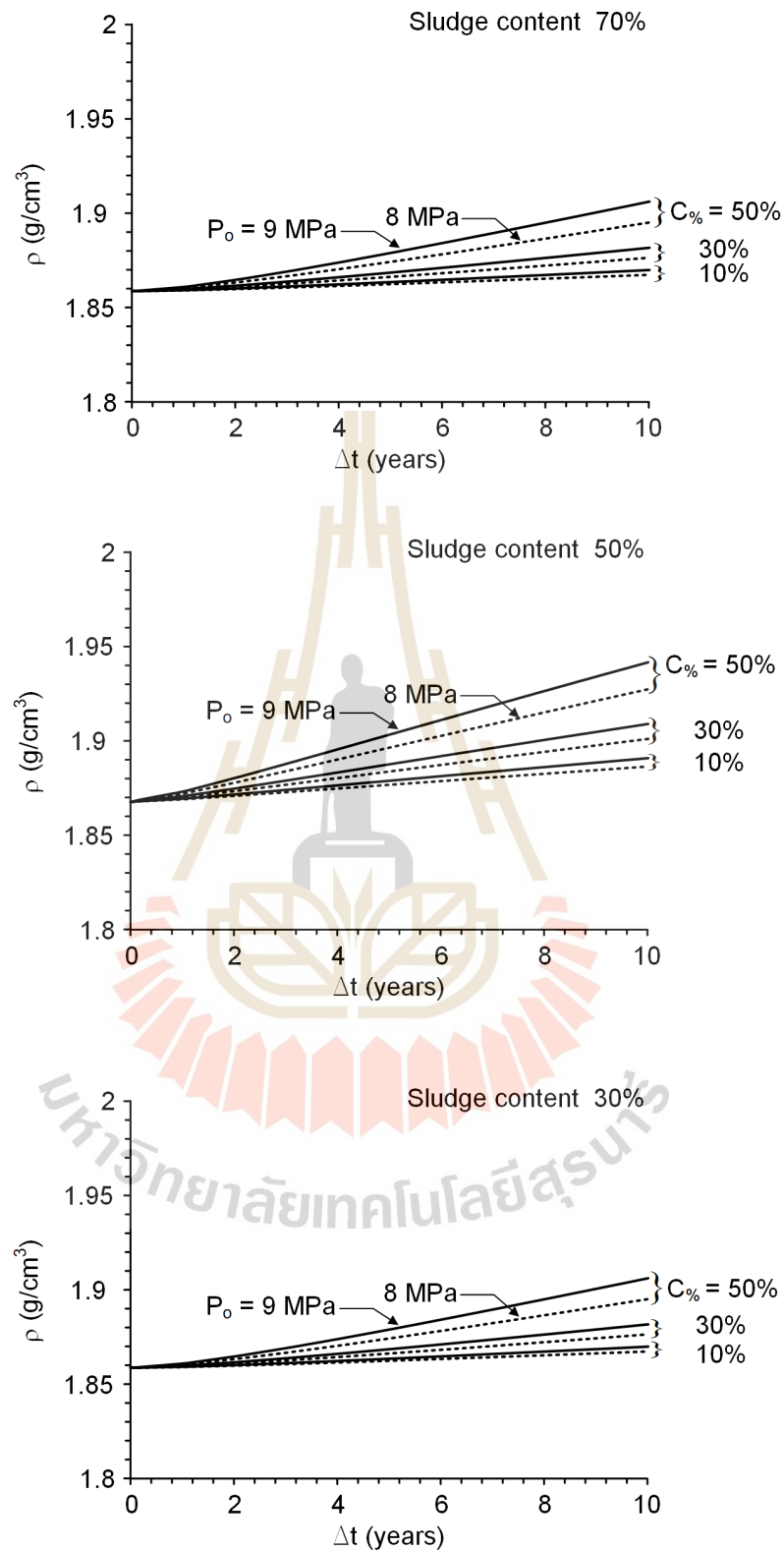


Figure 6.5 Density of different sludge content backfill as a function of time after emplacement in salt mass with different carnallite contents.

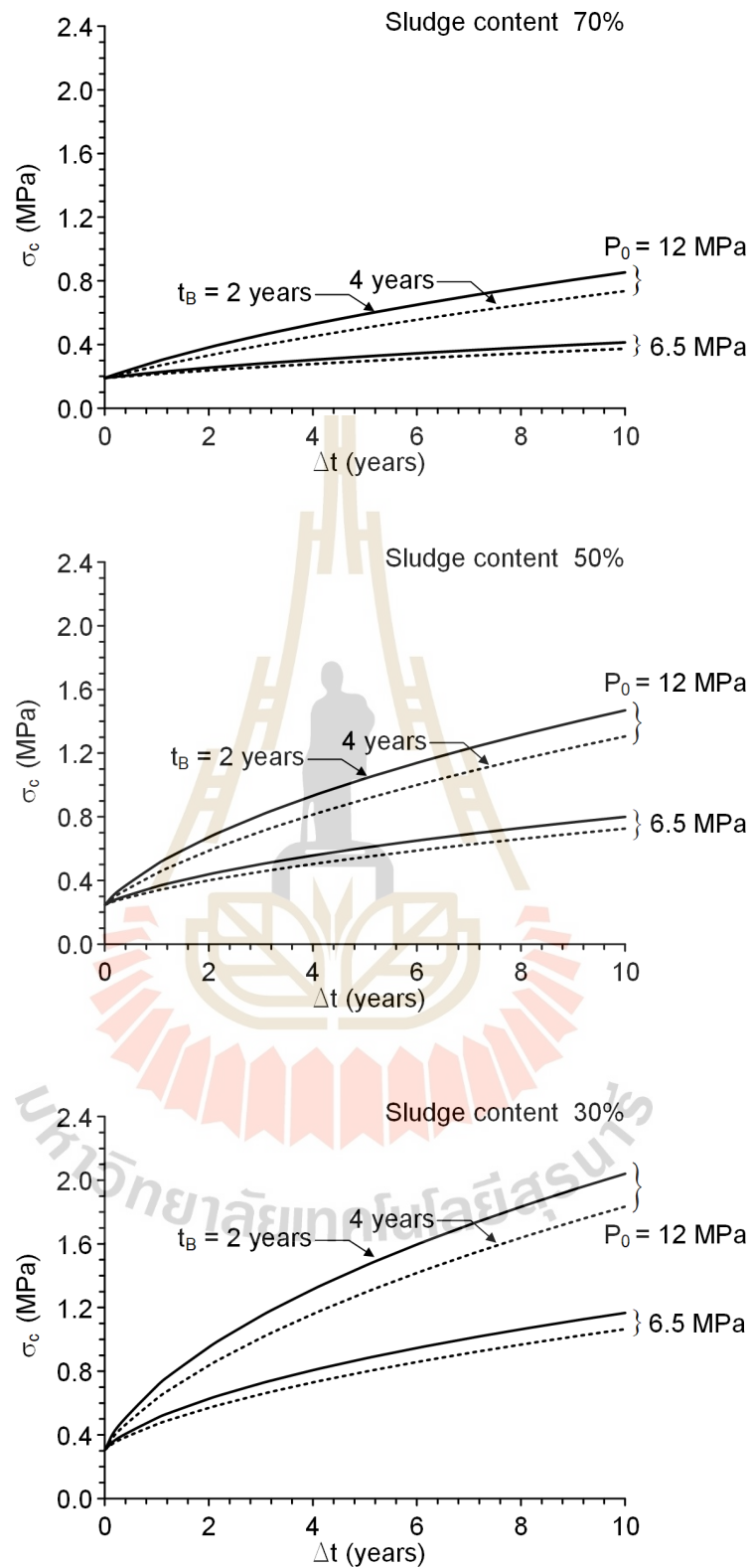


Figure 6.6 Uniaxial compressive strength of different sludge content backfill as a function of time after emplacement in salt opening.

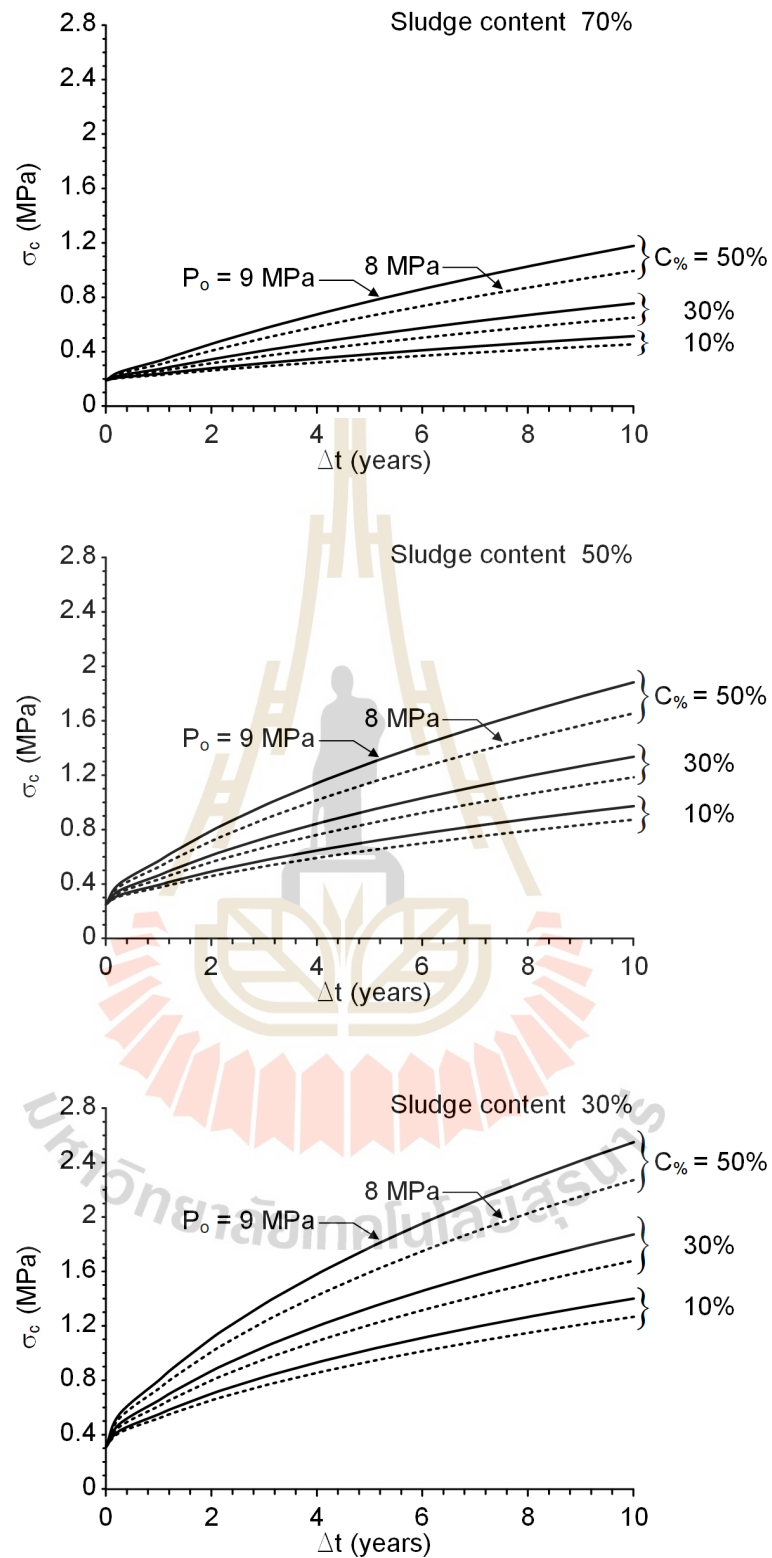


Figure 6.7 Uniaxial compressive strength of different sludge content backfill as a function of time after emplacement in salt with different carnallite contents.

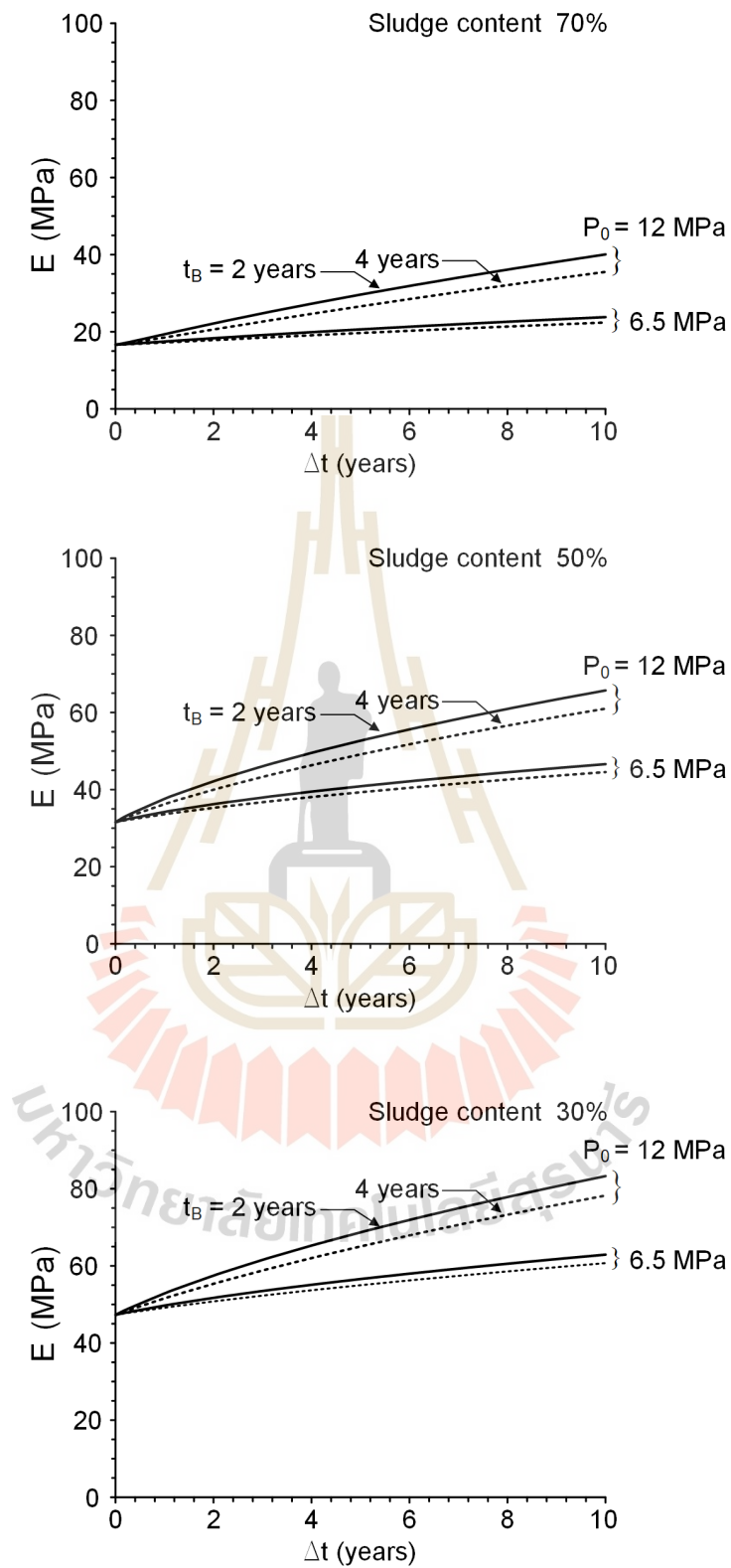


Figure 6.8 Elastic modulus of different sludge content backfill as a function of time after emplacement in salt openings.

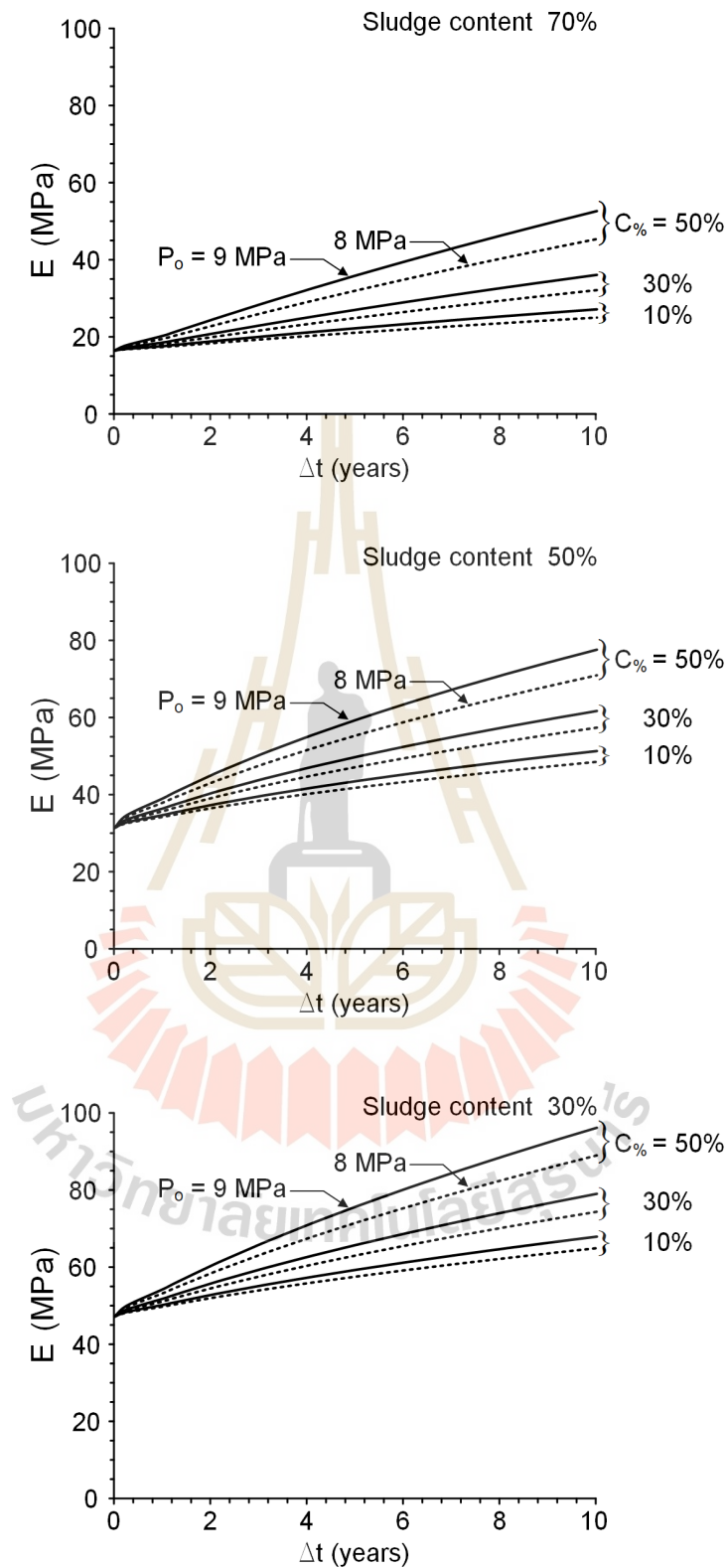


Figure 6.9 Elastic modulus of different sludge content backfill as a function of time after emplacement in salt with for different carnallite contents.

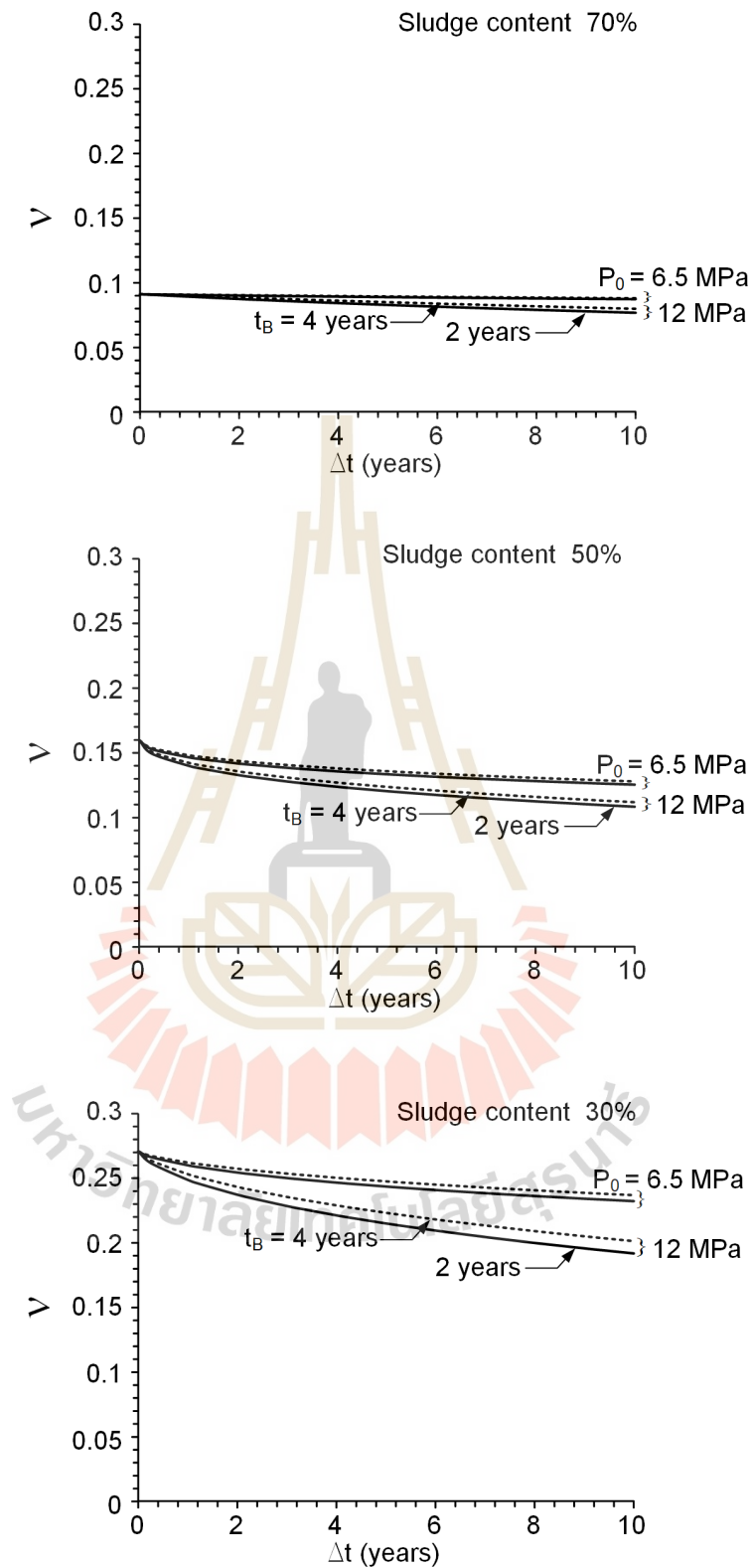


Figure 6.10 Poisson's ratios of different sludge content backfill in terms of time which install after emplacement in salt openings.

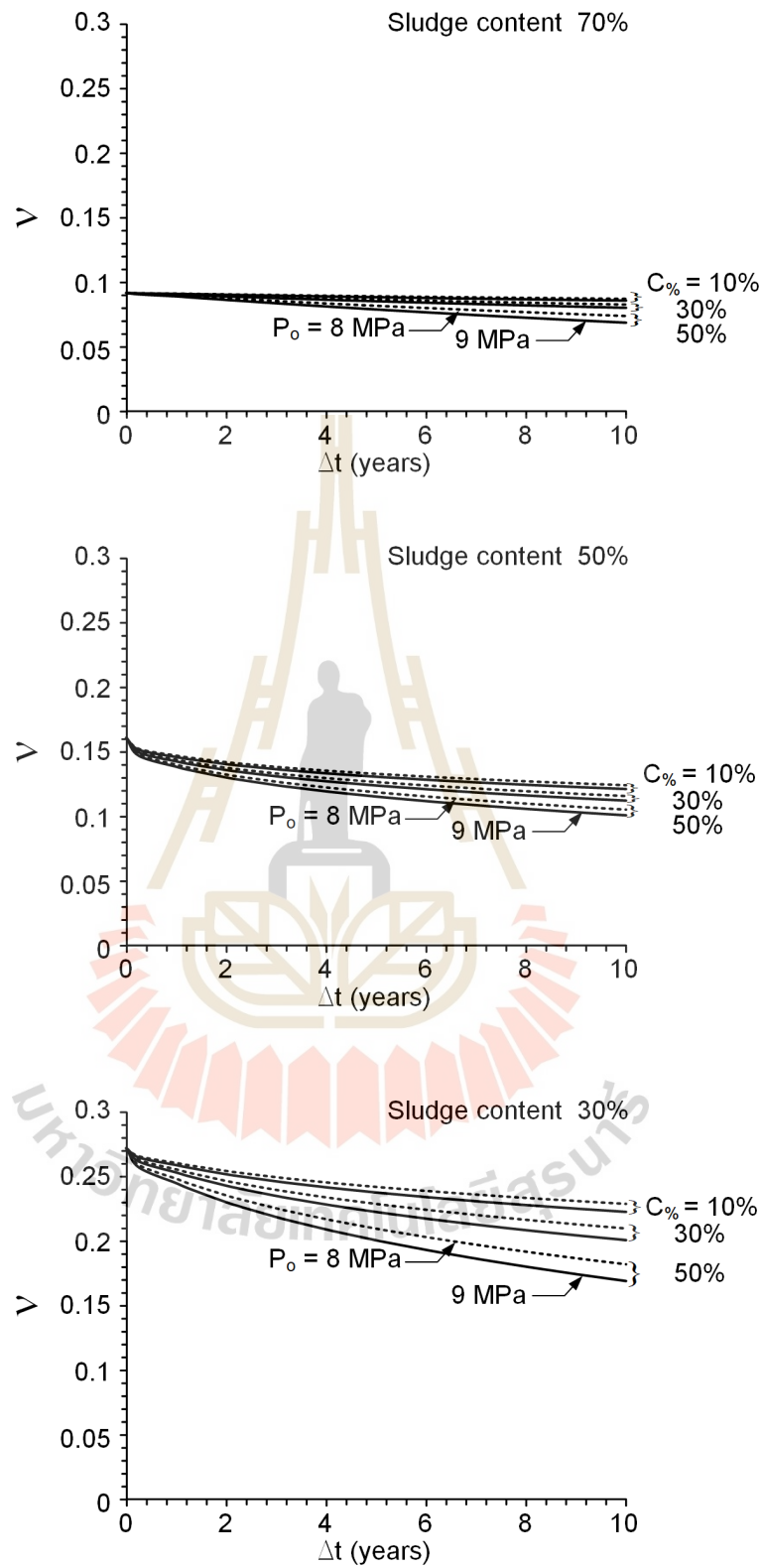


Figure 6.11 Poisson's ratios of different sludge content backfill as a function of time after emplacement in salt with different carnallite contents.

CHAPTER VII

DISCUSSIONS AND CONCLUSIONS

7.1 Discussions

The section discusses the effects of compacted sludge-crushed salt mixed with saturated NaCl solution on the physical and mechanical properties for using as backfill material in salt and potash mines. Comparisons of the results and findings from this study with related researches obtained elsewhere under similar test conditions have been discussed.

The applications of sewage sludge in different alternative fields of geotechnical work indicate the significant improvement of soil properties from the obtained shear strength and settlement. (Tay and Goh, 1991). The use of industrial wastewater sludge as soil stabilizer can enhance soil characteristics. In addition, the utilization of waste materials contributes an important benefit for environmental issues. (Laothong, 2003; Lin et al., 2007; Kim et al., 2009, 2012; Ohm et al., 2009; Soriano-Disla et al., 2010; Ma et al., 2012). Besides, the stabilized enhancement of subgrade soil can be obtained from the application of urban sewage wastewater sludge (Tay and Goh, 1991; Lin et al., 2005, 2007, b; Chen and Lin, 2009).

The compaction test results of sludge-crushed salt mixtures (particle size of sludge and crushed salt are 0.001 to 0.475 mm and 0.075-2.35 mm) with higher maximum dry densities and the lower optimum NaCl brine contents significantly depend on the mentioned particle sizes for the increases crushed salt contents. The results agree reasonably well with the reports presented by Kaya and Durakan

(2004) and Sitthimongkol et al. (2020). They find that the decrease of the bentonite weight ratio increased the dry density and decreased the optimum MgCl_2 brine content. Soltani-Jigheh and Jafari (2012) also improved the properties of mixed clay soils with coarse by using 30% bentonite and 70% aggregates. Their result exhibited relatively high maximum dry density. Similar to the experiment of Johannesson and Nilsson (2006), who conducted the compaction test on bentonite-crushed rock and obtained the maximum dry density and optimum MgCl_2 brine content of 30:70 mixture. The higher maximum dry density and lower optimum brine contents are contributed from coarser particles containing as supported by Srikanth and Mishra (2016).

The shear strength of the mixtures increases with decreasing of sludge contents (Sattra and Fuenkajorn, 2015). This attributed from the effect of crushed salt particles with large grain sizes exhibits greater interlocking character between the particles (Lambe and Whitman, 1969). The result obtained here relates well with those from Sonsakul and Fuenkajorn (2013), Neiwphueng and Fuenkajorn (2015) and Sitthimongkol et al. (2020) who studied the shear strength of compacted bentonite-crushed salt mixtures and found that higher amounts and larger particle sizes of crushed salt provided the larger shear strengths. This also agrees well to the report of Bagherzadeh-Khalkhali and Mirghasemi (2009) who studied the direct shear test for coarse-grained soils. In addition, Sonsakul et al. (2013) reported that the shear strength parameters and permeability properties are the key factors for designing in brine leakage sealing of salt mine.

The shear behavior of the sludge-crushed salt mixtures from the using of normal stresses ranging from 0.2 to 0.8 MPa can be explained by Coulomb criterion.

The higher friction angles and lower cohesion were obtained from the higher content of crushed salt (coarser particles) in the mixture. In addition, many researchers revealed that an increasing of crushed salt contents increased the shear properties that identified as Angular-sub-Angular. That attributed from an effective filling of sludge or fine particle in the small void spaces that existed between the coarse particles in the mixture. Many researchers also related that behavior with their works. For instance, Yanrong (2013) investigated the constitutive properties of composite soils from the varying of the particle shape and size distribution of crushed salt. Kim and Ha (2014), Soltani-Jigheh and Jafari (2012) and Zhang et al. (2016) investigated the consequences of using different particle size of coarse-grained soils to the shear properties.

The consolidation time in periods of 0 to 30 days of compacted sludge-crushed salt specimens have been used here. These periods were longer comparing to other research that performed similar studies on crushed salt (Case and Kelsall, 1987; Pfeifle, 1991; Miao et al., 1995; Khamrat et al., 2017; Suwannabut et al., 2020). However, the study of effect in consolidation time of sludge-crushed salt should be investigated as long-term testing (month or years). As Miao et al. (1995), Somtong et al. (2015) and Bumrungsuk and Fuenkajorn (2015) pointed out that the mechanical characteristics of crushed salt is complicated and greatly time-dependent deconstruction. In addition, Kelsall et al. (1984) also stated that low porosity and fracture healing of crushed salt take a long time as tens to hundreds of years to arise distinctly. In order to clarify the reliable of this study, the results of consolidation periods and stresses as exhibited in Figure 4.2 indicated that the rates of axial strain decrease with time and tend toward unchanged after 15 days. The evidence of an

overlapping (repeating) of the measured axial strains under different periods with the same σ_{cons} suggest sufficient reliability of the consolidation performed in this study.

The dynamic compaction is applied here as construction technique since it contributes the greater energy that is suitable to produce an effective compactive depth than lift thickness (around 2 m) for the sludge-crushed salt mixtures. In addition, it is an easily available technique to use in laboratory test. A large-scale dynamic compaction in this study demonstrated that sludge-crushed salt produced a high initial density. Hence, it leads to the high density after subjecting to the consolidation in a short period of time.

The results of consolidation tests by using three-ring mold in this study provides higher axial strain, void ratio and suitable brine comparing to standard test. Since the size of the three-ring mold is relatively larger than that of the standard. The obtained results agree well with the study of Aydilek et al. (1999). They compared the consolidation tests (ASTM D2435) of wastewater sludge using small-scale (50 mm inside diameter and 12 mm height of specimen) with the large-scale (50 mm inside diameter and 48 mm height of specimen). The results show that a much higher of volumetric strains are generated from large-scale testing owing to the high initial water contents and void ratio containing. This results in a denser compacted specimens.

The increment of sludge content provides the increasing of volumetric strain of the mixtures. Then it tends to be time-independent afterward. Since the sludge is clarified as elastic silt or cohesionless material along with the grain size smaller than 0.047 mm, it can be compacted more efficient than that of the pure crushed salt. The similar phenomenon is obtained from the study of Shor et al. (1981). They find that

the fine grains (0.02 cm) enhanced the reduction of porosity better than coarse grains (0.34 cm). The volumetric of crushed salt increase with consolidation time. This attributes from the grain size of crushed salt which is ranged from 0.075 to 2.35 mm with the time-dependent character as reported by Fuenkajorn and Daemen (1988), Fuenkajorn and Pueakphum (2010) and Samsri et al. (2010).

The microstructures of compacted sludge-crushed salt may exhibit recrystallization behavior under the conditioned with the NaCl brine. The salt crystals on the mixture may show contacts between the coarse particles. In addition, the increasing of salt concentration could change the surface roughness and specific surface area of the mixture. Then the higher interaction between the salt aggregates may be produced. This reasonably related to the sludge obtained by Zhang et al. (2016) and Proia et al. (2016).

The calculation for the prediction of the sludge-crushed salt behavior after emplacement in mine might be conservative since the axial load with seal gravity does not involved in the estimation. The calibrated creep parameters are important for the predictions of mechanical properties. The different constitutive creep models may provide different predictions of crushed salt properties. Nevertheless, the proposed empirical equation provides the good correlation coefficients ($R^2 > 0.9$). However, it cannot be claimed that the proposed empirical equation can be applied universally for all grain size distributions and particle shapes. Nevertheless, the advantage of proposed equation is it can exhibit the representation of consolidation behavior of crushed salt with the size ranges equal to those expected from the potash mines as waste product.

The use of sludge-crushed salt mixed with NaCl brine as backfill material may not suitable to high carnallite content openings. This is because the carnallite can be

dissolved by NaCl brine (Theerapun et al., 2017).

The optimum brine content is used in this study for reducing humidity condition that might be obtained from mine opening. The optimum brine content of mixtures used in this study, which is the brine content at which a maximum dry unit weight can be achieved after a given compaction effort. A maximum dry unit weight would have no voids in the mixtures. The determination of the optimum brine content is important. The determination of the optimum brine content is important. If the tillage is carried out on fields that are wetter or drier than the optimum brine content, many problems can be caused, including mixtures structural damage through the production of large clods, and an increased content of readily dispersible clay which is indicative of the backfill material stability.

7.2 Conclusions

Conclusions drawn from this study can be summarized as follows.

The proportion of saturated brine to sludge-crushed salt mixture in this study is determined as compaction are optimum brine content increases with sludge increases. The maximum dry density and optimum brine content of 30% sludge by weight, is 1.73 ton/m³, 9.1%. and increasing of sludge percentages provide the decreasing of maximum dry density the increasing of optimum brine content. The higher cohesion and friction angle of sludge-crushed salt mixture is 110 kPa and 39 for 30% sludge by weight, and decreases with increasing of sludge content. The lowest shear strength is observed for sludge content of 70% by weight with the friction angle = 31 degrees and the cohesion = 55 kPa. The cohesion and friction angle provided by the test of direct shear. The results imply that the cohesion and friction angle decrease with an increasing percentages of sludge mixtures.

Reduction of Sludge content results in higher dry densities and shear strength of the mixtures. This is because the crushed salt densities are higher than the sludge densities. Since sludge does not densify the mixtures, high sludge content results in lower compressive strength. The coarser particles have higher density than the finer particles. The mixtures with coarser particles show higher friction angles and lower cohesions.

The consolidation strain (ϵ_{cons}) increases with sludge contents along with consolidation stresses (σ_{cons}) and consolidation time. The increasing of ϵ_{cons} occurs rapidly after the application of axial stress with constant rate for all σ_{cons} . The ϵ_{cons} values of 30% and 50% sludge content specimens decrease slowly with time and tend to remain constant after 15 days. The strain rates of 70% sludge mixtures have a tendency of time independent. This might attribute from an elastic silt and cohesionless properties of the sludge. The particle size of sludge is smaller than 0.047 mm which could fill and reduce voids between crushed salt grains. While crushed salt is highly sensitive to loading and is time-dependent material.

The results of Figures 4.15 through 4.17 imply that the compressive strength, elastic modulus and Poisson's ratios decrease with increasing sludge content. A increasing of axial stress and consolidation time increases, the uniaxial compressive strength and elastic modulus values, but decreases the Poisson's ratios. The lowest compressive strength is observed for sludge content of 70% with consolidation stress = 2.5 MPa at 7 days, which equal to 0.56 MPa. The highest compressive strength is observed for 10 MPa consolidation stress of 30% sludge content which equals 3.11 MPa. The elastic modulus, Poisson's ratios and density are 0.114 GPa, 0.15 and 2.05 g/cm³ after 30 days of consolidation.

Even though the increase of sludge content reduces the mechanical properties of the mixtures, it makes the mixtures less sensitive to consolidation time, i.e. the consolidation rate decreases with increasing sludge content. Poisson's ratios however tend to decrease with consolidation period. The relationships between compressive strength, elastic modulus and Poisson' ratio as a function of consolidation stress and consolidation period which can be represented by an exponential equation.

The SEM images of the compacted specimens reveal the crystal aggregation of salt. The increasing of crushed salt in the mixtures under pressure of 10 MPa provides more aggregation with larger size of crystal that can be clearly seen from SEM observation. However, the crystal shape cannot be identified in all cases due to the mixed morphology of the images. This implies the bridging that can develop between aggregate particles. The results may be attributed to the recrystallization process of crushed salt.

The empirical equations relating the sludge-crushed salt properties with the applied mean strain energy density can be used to predict the mechanical properties of sludge-crushed salt mixture after installation as backfill material in the salt and potash mines. The application of the strain energy principle allows considering both stress and strain to which the backfill specimens are subjected. This approach is considered more fundamental and simpler than those of the complex creep and healing constitutive equations proposed elsewhere for the sealing of nuclear waste repository. The prediction indicated that the density, uniaxial compressive strength and elastic modulus of consolidated compacted sludge-crushed salt mixture increase but Poisson's ratio decreases with increasing consolidation time and installation depth.

The timing of backfill installation in salt and potash mines is a major factor in improving the mechanical performance of the sludge-crushed salt backfill, particularly at great depths. The available mean strain energy at the opening boundary is limited at shallow depths, the strength and elastic properties can be slightly improved under low mean strain energy. Both consolidation and recrystallization affect these mechanical characteristics. Without applying mean strain energy, the processes do not reduce the bulk volume of specimens.

7.3 Recommendations for futures studies

The performance assessment of compacted sludge-crushed salt mixtures could be further improved as the following lists:

- The effect of environment factors including temperature, porosity, and permeability that lead to accelerate the reconsolidation of backfill behavior of sludge-crushed salts mixture should be performed.
- The concentration influence of saturated brine at high temperature and unsaturated brine in mixtures should be studied and compared.
- The collection of sludge should be varied from different sources and conditions, for instance the sludge from a lagoon in various seasons, the sludge from the plants with and without treatment or sewage sludge. The effect of mineral compositions of various sludges should be investigated.
- The deformation of surface subsidence after the installation should be studied since the variables types of overburden thickness could produce an external stress to the backfill material.

REFERENCES

- Akgün, H. and Koçkar, M. K. (2018). Evaluation of a sand bentonite mixture as a shaft/borehole sealing material. **Applied Clay Science**. 164: 34-43.
- ASTM D2435. (2020). Standard test methods for one-dimensional consolidation properties of soils using incremental loading. In **Annual Book of ASTM Standards**. Philadelphia: American Society for Testing and Materials.
- ASTM D2487-17e1. (2017). Standard practice for classification of soils for engineering purposes (Unified Soil Classification System). In **Annual Book of ASTM Standards**. Philadelphia: American Society for Testing and Materials.
- ASTM D3080-11. (2011). Standard test method for direct shear test of soils under consolidated drained conditions. In **Annual Book of ASTM Standards**. Philadelphia: American Society for Testing and Materials.
- ASTM D4543-19. (2019). Standard practices for preparing rock core as cylindrical test specimens and verifying conformance to dimensional and shape tolerances. In **Annual Book of ASTM Standards**. Philadelphia: American Society for Testing and Materials.
- ASTM D7012-14e1. (2014). Standard test methods for compressive strength and elastic moduli of intact rock core specimens under varying states of stress and temperatures. In **Annual Book of ASTM Standards**. Philadelphia: American Society for Testing and Materials.
- Aubertin, M., Bussiere, B., and Bernier, L. (2002). **Environnement et gestion des**

- rejets miniers**. manual on CD-Rom, Presses Internationales Polytechnique. Montreal., QC, Canada.
- Aydilek, A.H., Edil, T.B., and Fox, P.J. (1999). Consolidation characteristic of wastewater sludge. **American society for testing and materials**. pp.15.
- Ayininuola, G.M. and Ayodeji, I.O. (2016). Influence of sludge ash on soil shear strength. **Journal of Civil Engineering Research**. 6(3): 72-77.
- Ayodele, A.L., Adebisi, A.O., and Kareem, M.A. (2016). Use of sludge ash in stabilising two tropical laterite. **International Journal of Scientific and Engineering Research**. 7(8): 104-108.
- Bagherzadeh-Khalkhali, A. and Mirghasemi, A.A. (2009). Numerical and experimental direct shear tests for coarse-grained soils. **Particuology**. 7(1): 83-91.
- Brady, B. H. G. and Brown, E. T. (2006). **Rock Mechanics for Underground Mining**. 3rd ed. Dordrecht: Springer, Netherlands.
- Brown, E.T. (1981). Rock Characterization testing and monitoring: ISRM Suggested methods. The Commission on Rock Testing Methods, **International Society for Rock Mechanics**, Pergamon Press, New York, 211 pp.
- Budynas, R.G., Nisbett, J.K., and Shigley, J.E. (2011). **Mechanical Engineering Design**. McGraw-Hill. New York.
- Bumrungsuk, A. and Fuenkajorn, K. (2015). Mechanical and hydraulic properties of sludge-crushed salt mixture as applied for backfill material in salt and potash mines. In **Proceedings of the Ninth South East Asian Technical University Consortium (SEATUC)**, Suranaree University of Technology, Nakhon Ratchasima, Thailand.

- Bunjongsiri, K. and Bunjongsiri, J. (2005). A study of quantity of heavy metal in bricks produce by clay mix with sludge from community wastewater treatment. In **Proceedings of the Eleventh Conference on International Convention on Civil Engineering**. Chonburi, Thailand.
- Butcher, B.M. (1991). **The Advantages of a Salt/Bentonite Backfill for Waste Isolation Pilot Plant Disposal Rooms**. Technical Report No.SAND90-3074, Sandia National Laboratories, Albuquerque, NM.
- Callahan, G.D., Mellegard, K.D., and Hansen, F.D. (1998). **Constitutive Behavior of Reconsolidating Crushed Salt**. Technical Report. No. SAND98-0179, Sandia National Laboratories, Albuquerque, NM.
- Case, J.B. and Kelsall, P. (1987). Laboratory investigation of crushed salt consolidation. **International Journal of Rock Mechanics and Mining Science and Geomechanics Abstracts**. 25 (5): 216-223.
- Chapuis, R.P. (1990). Sand–bentonite liners: predicting permeability from laboratory tests. **Canadian Geotechnical Journal**. 27: 47-57.
- Chapuis, R.P. (2002). The 2000 R.M. Hardy Lecture: Full-scale hydraulic performance of soil-bentonite and compacted clay liners. **Canadian Geotechnical Journal**. 39(2): 417-439.
- Charlermyanont, T. and Arrykul, S. (2005). Compacted sand-bentonite mixtures for hydraulic containment liners. **Songklanakarin Journal of Science and Technology**. 27(2): 313-323.
- Chen, L. and Lin, D.F. (2009). Stabilization treatment of soft subgrade soil by sewage sludge ash and cement. **Journal of Hazardous Materials**. 162(1): 321-327.
- Crosby, K. (2007). Integration of rock mechanics and geology when designing the

- Udon South sylvinitic mine. In **Proceedings of the First Thailand Symposium on Rock Mechanics** (pp. 3-22). Nakhon Patchasima, Thailand.
- de Figueirêdo Lopes Lucena, L.C., Thomé Juca, J.F., Soares, J.B., and Portela, M.G. (2013). Potential uses of sewage sludge in highway construction. **Journal of Materials in Civil Engineering**. 26(9): 04014051.
- Fuenkajorn, K. and Daemen, J. J. K. (1988). **Boreholes Closure in Salt**. Technical Report Prepared for The U.S. Nuclear Regulatory Commission, Washington, D.C. by the University of Arizona.
- Fuenkajorn, K. and Phueakphum, D. (2010). Effects of cyclic loading on mechanical properties of Maha Sarakham salt. **Engineering Geology**. 112 (1-4) 43-52.
- Gullu, H. and Giriskan, S., (2013). Performance of fine-grained soil treated with industrial wastewater sludge. **Environmental Earth Sciences**. 70:777-788.
- Hansen, F. D. (1997). Reconsolidating salt: compaction constitutive modeling, and physical processes. **International Journal of Rock Mechanics and Mining Sciences**. 34(3-4): 119.e1-119.e12.
- Hansen, F.D. and Mellegard, K.D. (2002). Mechanical and permeability properties of dynamically compacted crushed salt. In **Proceedings of the Basic and Applied Salt Mechanics** (pp. 253-256).
- Hansen, F.D., Callahan, G.D., and Van Sambeek, L.L. (1993). Reconsolidation of salt as applied to permanent seals for the waste isolation pilot plant. In **Proceedings of the Third on the Mechanical Behavior of Salt** (pp. 323-335). Transtech Publications, Palaiseau, France.
- Hashimoto, L., Iqbal, M.R., Kawamoto, K., Saito, T., and Tachibana, S. (2016). Compaction and consolidation characteristics for waste materials (sludge,

- crushed concrete and incineration ash). In **Proceedings of the Fourth International Symposium on Advances in Civil and Environmental Engineering Practices for Sustainable Development** (pp. 31-36). Sri Lanka.
- Holcomb, D.J. and Hannum, D.W. (1982). **Consolidation of Crushed-Salt Backfill Under Conditions Appropriate to the WIPP Facility**. Technical Report. No. SAND82-0630, Sandia National Laboratories, Albuquerque, NM.
- Holcomb, D.J. and Shields, M. (1987). **Hydrostatic Creep Consolidation of Crushed Salt with Added Water**. Technical Report. No. SAND87-1990, Sandia National Laboratories, Albuquerque, NM.
- Hwang, C.L., Wang, M.L., and Miao, S. (1993). Proposed healing and consolidation mechanisms of rock salt revealed by ESEM. **Microscopy Research and Technique**. 25(5-6): 456-464.
- Iqbal, M. R., Hashimoto, K., Tachibana, S., and Kawamoto, K. (2019). Geotechnical Properties of Sludge Blended with Crushed Concrete and Incineration Ash. **International Journal of GEOMATE**. 16(57): 116-123.
- Jaeger, J.C, Cook, N.G.W., and Zimmerman, R.W. (2007). **Fundamental of Rock Mechanics**. 4th ed. Blackwell, Australia. pp. 475.
- Johannesson, L.E. and Nilsson, U. (2006). **Geotechnical Properties of Candidate Backfill Material for Deep Repository**, Technical Report, Svensk Kärnbränslehantering AB.
- Kang, Y., Fan, J., Jiang, D., and Li, Z. (2021). Influence of geological and environmental factors on the reconsolidation behavior of fine granular salt. **Natural Resources Research**. 30(1): 805-826.
- Kaoser, S., Barrington, S., Elektorowicz, M., and Ayadat, T. (2006). The influence of

- hydraulic gradient and rate of erosion on hydraulic conductivity of sand-bentonite mixtures. **Soil and Sediment Contamination**. 15(5): 481-496.
- Kaya, A. and Durukan, S. (2004). Utilization of bentonite-embedded zeolite as clay liner. **Applied Clay Science**. 25(1-2): 83-91.
- Kelsall, P.C., Case, J.B., Coons, W.E., Franzone, J.G., and Meyer, D. (1984). **Assessment of Crushed Salt Consolidation and Fracture Healing in a Nuclear Waste Repository in Salt**. D'Appolonia Waste Mangement Services.
- Kenney, T.C., Van veen, W.A., Swallow, M.A., and Sungaila, M.A. (1992). Hydraulic conductivity of compacted bentonite-sand mixture. **Canadian Geotechnical Journal**. 29: 364-374.
- Khamrat, S., Tepnarong, P., Artkhonghan, K., and Fuenkajorn, K. (2017). Crushed Salt Consolidation for Borehole Sealing in Potash Mines. **Geotechnical and Geological Engineering**. 36(1): 49-62.
- Kim, D. and Ha, S. (2014). Effects of particle size on the shear behavior of coarse grained soils reinforced with geogrid. **Materials**. 7(2): 963-979.
- Kim, D., Park, J.S., and Yen, T.F. (2012). Feasibility study on cross-linked biopolymeric concrete encapsulating selenium glass wastes. **Journal of the Air and Waste Management Association**. 62(8): 898-904.
- Kim, D., Quinlan, M., and Yen, T.F. (2009). Encapsulation of lead from hazardous CRT glass wastes using biopolymer cross-linked concrete systems. **Waste Management**. 29(1): 321-328.
- Komine, H. (2004). Simplified evaluation on hydraulic conductivities of sand-bentonite mixture backfill. **Applied Clay Science**. 26: 13-19.

- Komine, H. (2010). Predicting hydraulic conductivity of sand-bentonite mixture backfill before and after swelling deformation for underground disposal of radioactive wastes. **Engineering Geology**. 114: 123-134.
- Kongthong, R. and Lertpocasombut, K. (2006). A study of sludge from water treatment plant on dye adsorption. In **Proceedings of the Eleventh Conference on International Convention on Civil Engineering**. Phuket.
- Lambe, T.W. and Whitman, R.V. (1969). **Soil Mechanics**. Wiley, New York. pp. 553.
- Laothong, K. (2003). **The Utilization of Sludge Cake from Water Treatment Processes of Wang Noi Power Plant**. Master Thesis, Department of Environmental Engineering, Kasetsart University.
- Lim, S.C., Gomes, C., and Kadir, M.Z.A.A. (2013). Characterizing of bentonite with chemical, physical and electrical perspectives for improvement of electrical grounding systems. **International Journal of Electrochemical Science**. 8: 11429-11447.
- Lin, D.F., Lin, K.L., and Luo, H.L. (2007). A comparison between sludge ash and fly ash on the improvement in soft soil. **Journal of the Air and Waste Management Association**. 57(1): 59-64.
- Lin, D.F., Luo, H.L., Hsiao, D.H., and Yang, C.C. (2005). The effects of sludge ash on the strength of soft subgrade soil. **Journal of the Chinese Institute of Environmental Engineering**. 15: 1-10.
- Luangthip, A., Khamrat, S., and Fuenkajorn, K. (2016). Effects of carnallite contents on stability and extraction ratio of potash mine. In **Proceedings of the ninth Asian Rock Mechanics Symposium**. Bali, Indonesia.
- Ma, X.W., Weng, H.X., Su, M.H., and Pan, L. (2012). Drying sewage sludge using

- flue gas from power plants in China. **Environmental Earth Sciences**. 65(6): 1841-1846.
- Miao, S., Wang, M.L., and Schreyer, H.L. (1995). Constitutive models for healing of materials with application to compaction of crushed rock salt. **Engineering mechanics**. 121 (10): 1122-1129.
- Mills, M. M., Stormont, J. C., and Bauer, S. J. (2018). Micromechanical processes in consolidated granular salt. **Engineering Geology**. 239: 206-213.
- Nair, K. and Boresi, A.P. (1970). Stress analysis for time dependent problems in rock mechanics. In **Proceedings of the second Congress of the International Society for Rock Mechanics** (pp. 531-536). Belgrade.
- Neiwphueng, U. and Fuenkajorn, K. (2015). Compacted bentonite-crushed salt mixtures as sealants in rock salt and potash openings. In **Proceedings of the Ninth South East Asean Technical University Consortium Symposium** (pp. 326-329). Thailand.
- O'Kelly (2004). Mechanical properties of dewatered sewage sludge. **Waste management**. 24: 47-52.
- Ohm, T.I., Chae, J.S., Kim, J.E., Kim, H.K., and Moon, S.H. (2009). A study on the dewatering of industrial waste sludge by fry-drying technology. **Journal of hazardous materials**. 168(1): 445-450.
- Pfeifle, T.W. (1991). **Consolidation, Permeability, and Strength of Crushed Salt/Bentonite Mixtures with Application to the WIPP**. Technical Report. No. SAND90-7009, Sandia National Laboratories, Albuquerque, NM.
- Pongpeng, K., Tepnarong, P., Artkhonghan, K., and Fuenkajorn, K. (2017). Performance assessment of three-ring compaction and direct shear mold for

- testing granular and clayey mixtures. In **Proceedings of the Eleventh South East Asean Technical University Consortium Symposium**. Viet Nam.
- Poonsawat, C. and Lertpocasombut, K. (2006). Study on the properties of sludge from water supply plant as raw material for clay plan roofing tile. In **Proceedings of the Eleventh Conference on International Convention on Civil Engineering**. Phuket, Thailand.
- Power, M.C. (1982). **Comparison Charts for Estimating Roughness and Sphericity**. AGI Data Sheets, American Geological Institute, Alexandria, VA.
- Proctor, R. (1933). **Fundamental Principles of Soil Compaction**. Engineering News-Record. 111(13).
- Proia, R., Croce, P., and Modoni, G. (2016). Experimental investigation of compacted sand-bentonite mixtures. **Procedia Engineering**. 158: 51-56.
- Ran, C. and Daemen, J.J.K. (1995). The influence of crushed salt particle gradation on compaction. In **Proceedings of The Thirty-fifth U.S. Symposium on Rock Mechanics** (pp.761-766). Reno, NV, A.A. Balkema, Rotterdam.
- Salzer, K., Popp, T., and Böhnell, H. (2007). Mechanical and permeability properties of highly pre-compacted granular salt bricks. In **Proceedings of the sixth Conference on the Mechanical Behavior of Salt** (pp. 239-248). Hannover, Germany.
- Samsri, P., Sriapai, T., Walsri, C., and Fuenkajorn, K. (2010). Polyaxial creep testing of rock salt. In **Proceedings of the Third Thailand Symposium on Rock Mechanics** (pp. 125-132). Thailand.
- Sangiumsak, N. and Cheerarot, R. (2008). The study of properties of artificial aggregates made from water supply sludge. In **Proceedings of the Eleventh**

Conference on International Convention on Civil Engineering. Pattaya, Chonburi. Thailand.

Sattra, P. and Fuenkajorn, K. (2015). Shear strength of compacted sludge-crushed salt mixtures. In **Proceedings of the Ninth South East Asean Technical University Consortium Symposium** (pp. 322-325). Thailand.

Shariatmadari, N., Salami, M., and Karimpour Fard, M. (2011). Effect of inorganic salt solutions on some geotechnical properties of soil-bentonite mixtures as barriers. **International Journal of Civil Engineering.** 9(2): 103-110.

Shor, A.J., Baes, C.F., and Canonico, C.M. (1981). **Consolidation and Permeability of Salt in Brine.** Technical Report. No. ORNL-5774, Oak Ridge National Laboratory, Oak Ridge, TN.

Sitthimongkol, L., Thongprapha, T., and Fuenkajorn, K. (2020). Properties of compacted bentonite-aggregate mixtures as backfill in salt and potash mines. **Engineering Journal of Research and Development.** 30(1): 45-53.

Siyuan, H., Yao, C., Xiaojun, C., Wen-an, D., and Li, L. (2020). Experimental study on characteristics of consolidation of sludge. In **Proceeding of sixth International Conference on Energy, Environment and Materials Science.** USA.

Soltani-Jigheh, H. and Jafari, K. (2012). Volume change and shear behavior of compacted clay-sand/gravel mixtures. **International Journal of Engineering and Applied Sciences.** 4: 52-66.

Somtong, S., Khamrat, S., and Fuenkajorn, K. (2015). Laboratory performance assessment of consolidated crushed salt for backfill material in potash mine openings. **Research and Development Journal of the Engineering**

Institute of Thailand under H.M. the King's Patronage. 26(1): 15-22.

Sonsakul, P. and Fuenkajorn, K. (2013). Development of three-ring compaction and direct shear test mold for soil with oversized particles. **Research and Development Journal of the Engineering Institute of Thailand under H.M. the King's Patronage.** 24(2): 1-7.

Sonsakul, P., Walsri, C., Horvibolsuk, S., and Fuenkajorn, K. (2013). Shear strength and permeability of compacted bentonite-crushed salt seal. In **Proceedings of the Fourth Thailand Symposium on Rock Mechanics.** Thailand.

Soriano-Disla, J.M., Navarro-Pedreño, J., and Gómez, I. (2010). Contribution of a sewage sludge application to the short-term carbon sequestration across a wide range of agricultural soils. **Environmental earth sciences.** 61(8): 1613-1619.

Srikanth, V. and Mishra, A. K. (2016). A laboratory study on the geotechnical characteristics of sand–bentonite mixtures and the role of particle size of sand. **International Journal of Geosynthetics and Ground Engineering.** 2(3): 1-10.

Stormont, J.C. and Finley, R.E. (1996). Sealing borehole in rock salt. **Sealing of Boreholes and Underground Excavations in Rock** (K. Fuenkajorn and J.J.K. Daemen eds) (pp.184-224). Chapman and Hall, London.

Suriyachat, D., Vichitamornpun, P., and Ruengsumrej, W. (2004). **Water treatment sludge utilization.** Technical Report. No. 16/2547, Department of primary industries and mines, Bangkok.

Suwannabut, W., Thongprapha, T., and Fuenkajorn, K. (2020). Mechanical performance of consolidated crushed salt mixed with MgCl₂ brine for carnalite mine backfill. **Engineering Journal of Research and Development.** 31(1):

33-43.

- Taki, K., Choudhary, S., Gupta, S., and Kumar, M. (2020). Enhancement of geotechnical properties of municipal sewage sludge for sustainable utilization as engineering construction material. **Cleaner Production**. 251: 119723-119759
- Tashiro, S., Fujiwara, A., and Senoo, M. (1998). Study on the permeability of engineered barriers for the enhancement of a radioactive waste repository system. **Nuclear Technology**. 121(1): 14-23.
- Tay, J.H. and Goh, A.T.C. (1991). Clay-blended sludge as lightweight aggregate concrete material. **Journal of Environmental Engineering**. 117(6): 834-844.
- Theerapun, C., Khamrat, S., Sartkeaw, S., and Fuenkajorn, K. (2017). Effects of backfill compositions on integrity of underground salt and potash mines. **Engineering Journal of Research and Development**. 28(2): 15-22.
- Valls, S., Yague, A., Vazque, E., and Mariscal, C. (2004). Physical and mechanical properties of concrete with added dry sludge from a sewage treatment plant. **Cement and Concrete Research**. 34: 2203-2208.
- Wang, M. L., Miao, S., and Maji, A. K. (1996). Deformation mechanisms of WIPP backfill. **Radioactive Waste Management and Environmental Restoration**. 20(2-3): 191-211.
- Wendai, L. (2000). **Regression Analysis, Linear Regression and Probit Regression in 13 Chapter**. SPSS for Windows: statistical analysis, Publishing House of Electronics Industry, Beijing.
- Wetchasat, K. and Fuenkajorn, K., (2013). Laboratory Assessment of Mechanical and Hydraulic Performance of Sludge-Mixed Cement Grout in Rock Fractures. In

Proceedings of the Fourth Thailand Symposium on Rock Mechanics.

Wang Nam Keaw, Nakhon Ratchasima, Thailand.

- Wilalak, N. and Fuenkajorn, K. (2016). Constitutive equation for creep closure of shaft and borehole in potash layers with varying carnallite contents. In **Proceedings of the ninth Asian Rock Mechanics Symposium**. Bali, Indonesia.
- Yanrong, L. (2013). Effects of particle shape and size distribution on the shear strength behavior of composite soils. **Bulletin of Engineering Geology and the Environment**. 72(3-4): 371-381.
- Zbar, B.S., Khan, M.A., and Jawad, A. (2013). Geotechnical properties of compacted silty clay mixed with different sludge contents. **Engineering and Technology Journal**. 31: 263-279.
- Zhang, L., Sun, D. A., and Jia, D. (2016). Shear strength of GMZ07 bentonite and its mixture with sand saturated with saline solution. **Applied Clay Science**. 132: 24-32.
- Zhang, M., Zhang, H., Jia, L., and Cui, S. (2012). Salt content impact on the unsaturated property of bentonite-sand buffer backfilling materials. **Nuclear Engineering and Design**. 250: 35-41.

BIOGRAPHY

Mr. Nateenon Pokhee was born on October 22, 1993 in Maha Sarakham Province, Thailand. He received his Bachelor's Degree in Engineering (Geological Engineering) from Suranaree University of Technology in 2016. For his post-graduate, he continued to study with a Doctor of Philosophy Program in the Geological Engineering Program, Institute of Engineering, Suranaree university of Technology. During graduation, 2016-2021, he was a part time worker in position of research assistant at the Geomechanics Research Unit, Institute of Engineering, Suranaree University of Technology.

